Evaluation of the effects of selected disintegrants on drug membrane permeation

W Gerber

22117040

Dissertation submitted in partial fulfilment of the requirements for the degree *Master* in Pharmaceutics at the Potchefstroom Campus of the North-West University

Supervisor: Dr D Steyn

Co-Supervisor: Prof JH Hamman

November 2016

ACKNOWLEDGEMENTS

I was once told to never despise humble beginnings.

So on finishing the biggest endeavor of my life so far the largest possible amount of love and gratitude goes out to my mom, Alta and to my brother and sister, Deji and Elzanne for teaching me that through hard work and the favour and the glory of God on one's side, that one will always rise above and beyond even the most humble of beginnings.

To my mates, you lot are way too many to mention!

But Jacques and "Rooi" Ruan, during these two years you guys helped and supported me through more than you will ever believe. Through the hard work and through the parties, I will always remember and always appreciate you. And the rest of you, Reeves, Mandi, Uncle Roux, "Net" Ruan and the many many more, your constant support and help is second to none!

A special thanks goes to the NWU, the NRF and Imperial for funding received during these two years. You may never understand what amazing differences you make in people's lives and without you, no knowledge, science or research...absolutely none of this would be possible.

And last, but by far not the least, Doc Steyn, Prof Sias, your infinite patience, wisdom, help and support could not have been any more or any better. I want to thank you two from the bottom of my heart for everything...I look forward to the next three years.

ABSTRACT

Virtually all solid dosage forms contain a disintegrating agent to help facilitate breakup, dissolution and absorption. Traditionally, excipients were thought to be pharmacologically inert, but recently, an increasing number of studies have shown that they may play a part in either increasing or decreasing drug membrane permeation. This study focused on investigating the effects of selected disintegrants on intestinal epithelial drug permeation. Five different disintegrants were selected and tested together with a model compound which is a known P-glycoprotein (P-gp) substrate, namely Rhodamine 123 (R123).

Bi-directional transport studies were conducted across excised pig jejunum tissue using a Sweetana-Grass diffusion apparatus. Samples of 180 µl were taken at 20 min intervals over a 2 h period and analyzed for R123 by means of a validated fluorescence spectroscopic method using a Spectramax Paradigm® plate reader. All transport studies were conducted in triplicate at four different concentrations of each selected disintegrant. The percentage transport, apparent permeability coefficient (P_{app}) values as well as efflux ratio (ER) values were calculated from the transport data. Trans-epithelial electrical resistance (TEER) was measured every 20 min using a Warner Instruments® EC-825A epithelial voltage clamp and changes were calculated to ensure membrane integrity was maintained and/or to register any effects on tight junctions by the disintegrants.

Croscarmellose sodium (Ac-di-sol®) mediated pronounced increases in R123 transport in the absorptive (i.e. apical-to-basolateral) direction and decreased R123 transport in the secretory (i.e. basolateral-to-apical) direction when compared to the control group (R123 alone). This proved that Ac-di-sol® is capable of inhibiting P-gp-mediated efflux in a concentration dependent manner. Microcrystalline cellulose (Avicel® PH-200) caused less R123 transport at higher concentrations in both directions when compared to the control but also seemingly inhibited P-gp at lower concentrations. However, results were inconclusive, due multi-molecular complexes that may have formed and led to inconsistent R123 transport at higher concentrations. Sodium starch glycolate (Explotab®) exhibited an inhibitory effect on R123 transport at all concentrations and in both directions when compared to R123 alone, possibly indicating inhibition of transport by an increase in the diffusion distance. Crospovidone (Kollidon® CL-M) exhibited a concentration dependent inhibition of efflux, but to a lesser extent than Ac-di-sol®. Sodium alginate had no direct effect on P-gp, but did concentration dependently increase TEER in both transport directions. Increased TEER values indicate a closing of tight junctions, resulting in an apparent increase in efflux as paracellular transport is inhibited.

The results of this study confirmed that some excipients, such as certain disintegrants, influence drug absorption by means of efflux inhibition or other mechanisms, which may result in changes in the bioavailability of certain drugs.

Key words: P-glycoprotein, Rhodamine 123, *ex vivo*, Sweetana-Grass diffusion apparatus, pharmacokinetic interactions, excipient-drug interactions, disintegrants, croscarmellose sodium, microcrystalline cellulose, sodium starch glycolate, crospovidone, sodium alginate.

UITTREKSEL

Bykans alle soliede doseervorme bevat een of meer disintegreermiddels om disintegrasie, dissolusie en absorpsie te bemiddel. Histories was vulstowwe as farmakologies onaktief beskou, maar meer onlangs het 'n toenemende aantal studies bevind dat vulstowwe wel 'n rol mag speel in die toename of afname van geneesmiddel absorpsie deur biologiese membrane. Hierdie studie het ten doel gehad om die absorpsie van rhodamien 123 (R123), wat 'n P-glikoproteïen (P-gp) substraat is, in die teenwoordigheid van vyf gekose disintegrante te ondersoek.

Rhodamien 123 transport studies oor gedissekteerde vark jejenum segmente was in twee rigtings met behulp van 'n Sweetana-Grass diffusie apparaat uitgevoer. Monsters van 180 µl was elke 20 min oor 'n tydperk van 2 ure onttrek en daarna vir die teenwoordigheid van R123 met behulp van 'n gevalideerde fluoressensie spektroskopiese metode op 'n Spectramax Paradigm® plaatleser ontleed. Alle transport studies was in triplikaat uitgevoer en 4 verskillende konsentrasies van elke disintegrant was getoets. Die persentasie transport, die skynbare permeabiliteitskoëffisiënt (P_{app}) sowel as die effluks verhouding (EV) is vanuit die transport data bereken. Die trans-epiteliale elektriese weerstand (TEEW) was elke 20 min met behulp van 'n Warner Instruments® EC-825A trans-epiteliale spanningsklamp gemeet om membraanintegriteit te monitor en om enige effekte van die disintegrante op intersellulêre-aansluitings te ondersoek.

Natrium-kruiskarmellose (Ac-di-sol®) het 'n uitgesproke verhoging in die absorpsie van R123 in die adsorptiewe rigting (nl. apikaal-na-basolateraal) meegebring terwyl 'n verlaging in R123 transport die sekretoriese-rigting (nl. basolateraal-na-apikaal) waargeneem was in vergelyking met die kontrole (nl. R123 alleen). Hierdie resultate bevestig dat Ac-di-sol® in staat is om effluks-transport deur middel van P-gp-modulering op 'n konsentrasie-afhanklike wyse te inhibeer. Hoë konsentrasies van mikrokristallyne sellulose (Avicel® PH-200) het 'n verlaging in R123 transport in beide rigtings bewerkstellig in vergelyking met die kontrole, maar het ook 'n skynbare inhibisie van P-gp by laer konsentrasies veroorsaak. Die resultate was egter onvoldoende om geldige gevolgtrekkings vanaf te maak weens die feit dat multi-molekulêre komplekse moontlik gevorm het wat aanleiding gegee het tot wisselvallige R123 transport by hoër konsentrasies. Natrium-styselglikolaat (Explotab®) het 'n inhiberende effek op R123 transport in beide rigtings veroorsaak by alle toetskonsentrasies. 'n Moontlike verduidelik vir hierdie verskynsel is dat transport as gevolg van 'n vergroting in die diffusieafstand belemmer was. Kruisgebonde povidoon (Kollidon® CL-M) het ook 'n konsentrasie-afhanklike inhibisie van effluks getoon, maar tot 'n mindere mate in vergelyking met Ac-di-sol®. Natriumalginaat het geen direkte effekte op P-gp getoon nie, maar het wel 'n

konsentrasie-afhanklike toename in TEEW, in beide rigtings, veroorsaak. ’n Toename in TEEW waardes dui daarop dat intersellulêre-aansluitings meer saamgetrek is, wat ’n skynbare toename in effluks weens die inhibisie van parasellulêre transport veroorsaak.

Die resultate van hierdie studie het bevestig dat sommige disintegrante ’n invloed op die omvang van geneesmiddelabsorpsie mag hê weens effluks-inhibisie of modulering van ander transportmegansimes en dit kan gevolglik tot ’n verandering in biobeskikbaarheid van sommige geneesmiddels lei.

Sleutelwoorde: P-glikoproteïen, Rhodamien 123, *ex vivo*, Sweetana-Grass diffusie apparaat, farmakokinetiese interaksies, vulstof-geneesmiddel interaksies, disintegrante, natrium-kruiskarmellose, mikrokristallyne-sellulose, natrium-styselglikolaat, kruisgebonde povidoon, natriumalginaat.

CONGRESS PROCEEDINGS

Effect of selected disintegrants on drug membrane permeation. Presented at the 37th Conference of the Academy of Pharmaceutical Sciences held from 5-8 October 2016 at the Misty Hills Hotel and Conference Centre in Muldersdrift, South Africa by the Department of Pharmaceutical Sciences from the Tshwane University of Technology and the Department of Pharmacology and Therapeutics at the Sefako Makgatho Health Sciences University. (See Addendum A)

TABLE OF CONTENTS

LIST OF FIGURES

LIST OF TABLES

LIST OF ABBREVIATIONS

ABC	ATP-binding cassettes
ADS	Ac-di-sol®
ANOVA	Analysis of variance
A-B	Apical-to-basolateral
API	Active pharmaceutical ingredient
ATP	Adenosine triphosphate
AVC	Avicel® PH-200
B-A	Basolateral-to-apical
Caco-2	Human colorectal carcinoma cells
CLM	Kollidon® CL-M
CO_2	Carbon dioxide
DMSO	Dimethyl sulfoxide
e.g.	*Exempli gratia* (for example)
ER	Efflux ratio
EV	Effluks verhouding
GIT	Gastrointestinal tract
HPC	Hydroxypropyl cellulose
i.e.	*Id est* (in other words)
KRB	Krebs-Ringer bicarbonate
LOD	Limit of detection
LOQ	Limit of quantification

MDCK	Madin-Darby canine kidney cells
MRP	Multidrug-resistance-associated protein 2
O_2	Oxygen
P_{app}	Apparent permeability coefficient/Skynbare permeabiliteitskoëffisiënt
P-gp	P-glycoprotein/P-glikoproteïen
R123	Rhodamine 123/Rhodamien 123
r^2	Correlation coefficient
RSD	Relative standard deviation
S	Regression line slope
SAL	Sodium alginate
SD	Standard deviation
SLC	Solute carriers
T_x	Time of specific (*x*) interval
TEER	Trans-epithelial electrical resistance
TEEW	Transepiteliale elektriese weerstand
w/v	Weight per volume (g/100ml)
w/w	Weight per weight (g/100g)
XPT	Explotab®

CHAPTER 1: INTRODUCTION

1.1 Background and justification

1.1.1 Excipient-drug pharmacokinetic interactions

Excipients such as binders or fillers, disintegrants, lubricants, colourants and flavourants are used in virtually all immediate release solid oral dosage forms (García-Arieta, 2014:89). Excipients were initially intended to be pharmacologically inert, but as early as 1967 it was reported that excipients may have an effect on drug levels in the body. It was, for example, found that dimethyl sulfoxide (DMSO) can cause an increase in blood and brain levels of magnesium pemoline (Brink & Stein, 1967:1480). It was later discovered that various excipients can have significant effects on drug permeation across biological membranes through mechanisms such as opening of tight junctions and modulation of drug efflux mediated by P-glycoproteins (P-gp's). Furthermore, it was found that different excipients exhibit different effects depending on the intestinal region and excipient concentration. For example: when using hydroxypropyl cellulose (HPC) at a concentration of 0.02% (w/v), the membrane permeation of 5(6)-carboxyfluorescein in the jejunum and ileum decreased, but increased in the same regions when using a 0.20% (w/v) solution (Takizawa, Kishimoto, *et al.*, 2013:363,366-367).

1.1.2 Disintegrants

Disintegrants, a subgroup of excipients, are included in solid oral dosage forms to ensure that the tablet/capsule is broken down into its most primary particles, thus exposing a larger surface area for full dissolution and subsequent optimal absorption and bioavailability of the active substance (Alderborn, 2007:450; Mohanachandran *et al.*, 2011:105). The mechanistic action of disintegration of solid oral dosage forms can be divided into three main phases. Water imbibition (wicking) into capillary spaces is considered as the first stage of disintegration. Although wicking is not believed to be able to cause full disintegration on its own, it is believed to serve as a prerequisite for swelling, strain recovery, heat of interaction or a combination of one or more of these mechanisms. Lastly, interruption of intermolecular bonds takes place as a result of these mechanisms and leads to the breakup of the tablet matrix (Alderborn, 2007:450; Desai *et al.*, 2016:2552-2553).

A wide variety of compounds exhibit disintegration properties, but for the purpose of this study, representatives will be selected from different subgroups of disintegrants. Croscarmellose sodium and microcrystalline cellulose fall within the subgroup of celluloses (Galichet, 2005:132; Guest, 2005:211), sodium starch glycolate is a modified starch (Edge &

Miller, 2005:701), crospovidone is classified within the subgroup of polyvinylpyrrolidones (Kibbe, 2005:214) and sodium alginate is a salt form of natural polysaccharide polymers found in brown seaweeds (Cable, 2005:656; Mohanachandran *et al.*, 2011:106-107; Tønnesen & Karlsen, 2002:622).

1.1.2.1 Croscarmellose sodium (Ac-di-sol®)

Croscarmellose sodium, commercially available as Ac-Di-Sol®, is specifically used as a disintegrant at concentrations ranging from 0.5 - 5.0% (w/w) in tablets and 10 – 25% (w/w) in capsules (Guest, 2005:211). Classified as a superdisintegrant, the properties of croscarmellose sodium can be attributed to the cross-linking of carboxymethylcellulose. These highly absorbent cross-linkages mediate the effective swelling of croscarmellose sodium by channeling water into the tablet through an action known as wicking (Desai *et al.*, 2016:2546,2548; Priyanka & Vandana, 2013:79). Croscarmellose sodium has previously been reported to increase the trans-epithelial transport of 5(6)-carboxyfluorescein across rat jejunum (Takizawa, Kishimoto, *et al.*, 2013:366).

1.1.2.2 Microcrystalline cellulose (Avicel® PH-200)

Microcrystalline cellulose, commercially available in different grades of Avicel®, is a multifunctional excipient that can be deployed as either an adsorbent and binder or a disintegrant, depending on the concentration used in the dosage form. At higher concentrations in tablets, adsorbent and binding effects can be noticed whereas disintegrant properties are prominent at lower concentrations. Concentrations used specifically for disintegrating effects of microcrystalline cellulose range between 5 and 15% (w/w) (Galichet, 2005:132; Priyanka & Vandana, 2013:81). Between these concentrations, it has recently been suggested that the disintegration mechanism of microcrystalline cellulose may be dependent on the capillary absorption of water, which causes disruption of intermolecular bonds which in turn ensures disintegration of the tablet (Desai *et al.*, 2016:2548; Priyanka & Vandana, 2013:81). In an earlier study conducted by Takizawa, Kishimoto, *et al*. (2013:366), it was reported that the inclusion of microcrystalline cellulose had no significant effect on the total amount of 5(6)-carboxyfluorescein permeation across the ileum and jejunum of rats using the everted sac method. However, this study measured neither changes in trans-epithelial electric resistance (TEER) nor modulation of the efflux of 5(6)-carboxyfluorescein in the basolateral-to-apical direction.

1.1.2.3 Sodium starch glycolate (Explotab®)

Sodium starch glycolate, commercially available as Explotab®, is exclusively used as a disintegrant, even though it has previously been reported to be useful as a suspending vehicle. The preferred concentration, which is commonly used in most solid oral drug formulations is 4% (w/w), however, concentrations ranging from 2 – 8% (w/w) have previously been used with success (Edge & Miller, 2005:701). The proposed mechanism of disintegration is by facilitating water uptake into the dosage form resulting in swelling of up to 300 times its own volume (Desai *et al.*, 2016:2549; Edge & Miller, 2005:702). Sodium starch glycolate has also been classified as a superdisintegrant by Desai *et al.* (2016:2549) due to the fact that full disintegration of most dosage forms can be achieved in less than two minutes.

1.1.2.4 Crospovidone (Kollidon® CL-M)

Crospovidone, commercially available as Kollidon® CL-M, was initially used solely as a tablet disintegrating agent at concentrations ranging between 2 - 5% (w/w). However, it was later also found to be a useful aid in improving the solubility of poorly water soluble drugs (Kibbe, 2005:214). Tablet disintegration by crospovidone seems to be largely dependent on the strain recovery of the compound when submerged in an aqueous environment, resulting in it being tested as a superdisintegrant (Desai *et al.*, 2016:2548; Kibbe, 2005:214; Thibert & Hancock, 1996:1255-1256). The disintegration method can be substantiated by studies mentioned by Kibbe (2005:214), where larger particles of crospovidone caused faster disintegration of analgesic tablets.

1.1.2.5 Sodium alginate

Sodium alginate is a multi-functional excipient that can be used as either a tablet disintegrant at concentrations ranging between 2.5 - 10% (w/w) or as a binder between 1 - 3% (w/w). However, sodium alginate has been widely used as a matrix in delayed- and sustained release tablets, of which their function can be attributed to the slow dissolution rate and the poorly water-soluble properties of sodium alginate. Furthermore, sodium alginate has also been deployed therapeutically as an antacid or haemostatic agent in dressings (Cable, 2005:656). The mechanism of disintegration is caused by wicking followed by rapid swelling (Mohanachandran *et al.,* 2011:108).

1.1.3 Intestinal absorption models

The oral route is the most commonly preferred means of drug administration and acceptable bioavailability of the active ingredient is of the utmost importance to ensure a therapeutically successful treatment outcome (Alderborn, 2007:442; Desai *et al.*, 2016:2545; Liu *et al.*, 2009:265). It is therefore important to have models at our disposal, which simulate *in vivo* conditions accurately in order to assess a marker compound's ability to permeate biological membranes. The most frequently used models are listed below (Alqahtani *et al.*, 2013:2-5):

- *In vitro* models include among others, adenocarcinoma cells of the colon (Caco-2), Madin-Darby canine kidney (MDCK) cells and other immortalised cell lines.

- *Ex vivo* models are used to conduct experiments on excised tissue from animals used in Ussing-type diffusion apparatus such as the Sweetana-Grass diffusion apparatus or the everted-sac method.

- *In situ* models where a predetermined region of the intestine of an anesthetised living organism are used to determine a compound's absorption, metabolism or physico-chemical interactions.

- *In vivo* models where live animals are used to determine a drug's bioavailability and metabolism.

- *In silico* models where computer software is used to predict certain pharmacokinetic properties of the test compound.

Some of these models are not ideally suited to the ever changing scientific environment, especially with increasing legislative, public and moral pressure to replace, reduce and refine experimental animals. This concept is referred to as "The Three R's" principle (Zurlo *et al.*, 1996). "Replace" refers to the use of alternative experimental models instead of live animals; "reduce" refers to using fewer animals by employing more sophisticated experimental procedures to generate accurate data from smaller test groups while "refining" focuses on the minimization of stress causing procedures performed on the experimental animals. In view of "The Three R's" principle, the most suitable/feasible option would be to use *in vitro* or *ex vivo* models for pharmacokinetic studies as far as possible (Zurlo *et al.*, 1996).

1.2 Problem statement

Excipients, and more specifically to this study, disintegrants, were originally developed to be pharmacologically inert. However, studies have shown that membrane permeability can be

altered in either a positive or negative way by the addition of excipients, such as disintegrants, to a dosage form (García-Arieta, 2014:89-90; Takizawa, Kishimoto, *et al*., 2013:363). If it can be proven that the presence of disintegrants can increase permeability or absorption, certain suggestions can be made to improve the bioavailability of poorly permeable drugs. Alternatively, certain disintegrants may need to be avoided in medicinal products containing drugs with narrow therapeutic indices to prevent adverse or toxic effects. These reasons, among others, will increase cost-effectiveness and may also be able to improve safety of oral dosage form regimes.

1.3 Goals and objectives

1.3.1 General aim

The aim of this study is to determine if selected disintegrants can affect drug transport across excised intestinal epithelial tissues and to disseminate the type of interaction (e.g. opening of tight junctions or modulation of efflux).

1.3.2 Specific objectives

- To select disintegrants, which are commonly used in solid oral dosage forms and that represent different disintegrant types.
- To choose a suitable model compound with fluorescence capabilities for the transport studies, which is a known P-glycoprotein (P-gp) substrate.
- To conduct bi-directional transport studies with the model compound in the presence and absence of selected disintegrants across excised pig intestinal tissue.
- To obtain trans-epithelial electrical resistance (TEER) measurements in the presence and absence of selected disintegrants across excised pig intestinal tissue.
- To calculate apparent permeability coefficient (P_{app}) values, efflux ratio (ER) values and %TEER changes in order to determine the effect of selected disintegrants on tight junctions as well as model compound efflux.
- To validate a plate reader method for analysis of the fluorescent model compound.

1.4 Ethics

Pig intestinal tissue will be obtained from pigs slaughtered for meat production purposes and not for research purposes. The only aspects which require ethical consideration include

control regarding the site of tissue collection (e.g. authorised abattoir that applies disease control on animals slaughtered) and the correct disposal of the intestinal tissue after completion of the transport studies. An ethics application was submitted to the Ethics Committee (AnimCare) of the North-West University for evaluation and was approved (Addendum B, reference number NWU-00025-15-A5).

1.5 Dissertation layout

Chapter 1: Description of the rationale and motivation for this study along with a general aim and specific objectives.

Chapter 2: Contains a literature review which covers the basic gastro-intestinal tract (GIT) physiology, followed by the different transport mechanisms across the GIT. Different excipients are also mentioned, with specific focus on disintegrants, and different models are discussed which may be employed to test the excipients' effects on drug transport.

Chapter 3: A full description of experimental methods and materials used for this study along with the determination of validation procedure for the sample analyses method.

Chapter 4: All results and conclusion of this study, along with explanations of P_{app} values, ER values and %TEER changes gained from experimental and statistically analised data.

Chapter 5: Final conclusions and future recommendations.

CHAPTER 2: EXCIPIENT-DRUG PHARMACOKINETIC INTERACTIONS

2.1 Introduction

Excipients such as fillers, binders, lubricants, disintegrants, flavourants and colourants are used in almost all immediate release solid oral dosage forms. More specific to this study, virtually all tablet formulations contain a disintegrating agent to help facilitate breakup of the tablet matrix, exposing a larger surface area for dissolution and consequently absorption of the drug (Alderborn, 2007:450; Liu *et al.*, 2009:265; Mohanachandran *et al.*, 2011:105). Traditionally, excipients were thought to be pharmacologically inert, but recently, an increasing number of studies have shown that they may play a part in either increasing or decreasing drug membrane permeation through mechanisms such as opening of tight junctions and modulation of drug efflux mediated by P-glycoprotein (P-gp) transporters (García-Arieta, 2014:89-90; Takizawa, Kishimoto, *et al.*, 2013:363).

Ex vivo and *in vitro* models are considered appropriate approaches to determine to which extent disintegrants may have an effect on drug transport. Transport studies using excised pig intestinal tissue are especially advantageous because of its close resemblance to human intestinal tissue and ease of access. Furthermore, experiments are done on functional cells in viable tissues, as it would have happened in a live specimen (Alqahtani *et al.*, 2013:3; Antunes *et al.*, 2013:13).

This chapter focuses on the gastrointestinal tract of the human and how drugs/drug-like compounds are absorbed together with the factors influencing absorption. Furthermore, it will explain the different excipients that can be found in tablet formulations. Lastly, an explanation of different models and experiments, which can be used to test the effect of excipients on drug absorption, is given.

2.2 The gastrointestinal tract

The gastrointestinal tract (GIT) is a continuous muscular tube of approximately 6 m in length (Figure 2.1). The GIT can be divided into four different regions including the mouth and esophagus, the stomach, the small intestine and the colon, each with varying diameters. Even though each region in the GIT has slightly different roles in terms of transport, digestion and absorption, its main physiological function is to digest orally ingested food and the subsequent absorption of nutrients. At the same time, the GIT is also tasked to be a barrier to toxic materials and xenobiotics (Ashford, 2007:271; Lundquist & Artursson, 2016).

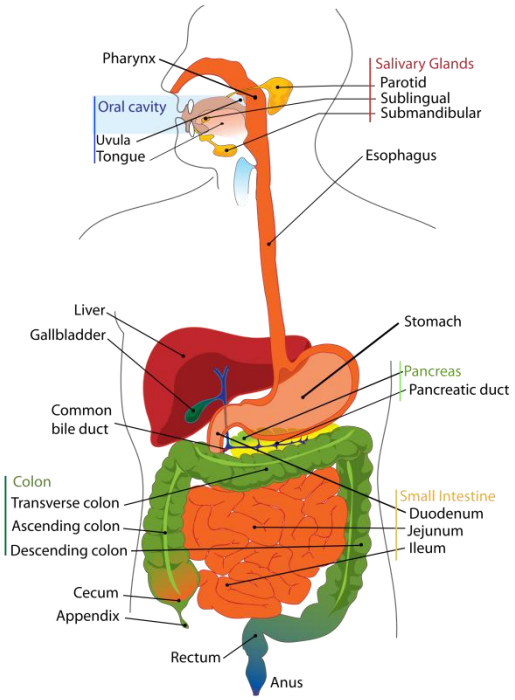

Figure 2.1: Illustration of the complete human gastrointestinal tract showing all four main anatomical areas, namely the mouth and esophagus, the stomach, the small intestine and the colon (Newhealthadvisor, 2014)

2.2.1 Anatomy of the gastrointestinal tract

As depicted in Figure 2.2, the GIT wall has four concentric histological layers throughout its entire length. The innermost layer, the mucosa, is further divided into the mucus secreting epithelium layer, the connective tissue lamina propria and the muscularis mucosa, which is a muscle that is able to alter the local conformation of the mucosa layer. The submucosa is a connective tissue layer mainly responsible for blood supply and lymphatic drainage. Circular and longitudinal muscles make up the next layer, the muscularis externa, which is responsible for peristalsis. Longitudinal muscles shorten the GIT, while the circular muscle closes the tract for a small period thus ensuring that food does not travel backwards and at the same time propelling the food forwards. Lastly, the outermost layer, the serosa is a densely packed layer of epithelial cells that acts as an external protective barrier for the GIT and is also regarded to be impenetrable for drugs and xenobiotics (Ashford, 2007:271; Renukuntla *et al.*, 2013:76).

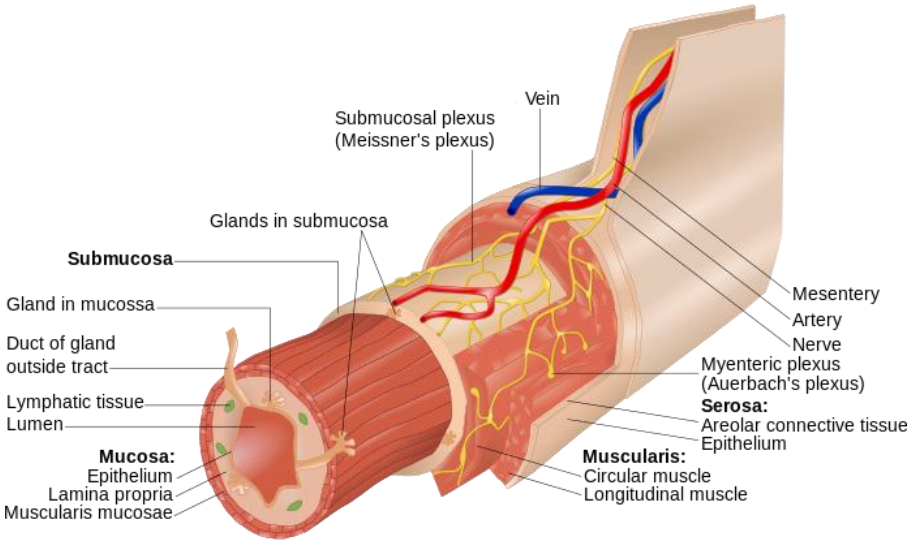

Figure 2.2: Schematic illustration of the gastrointestinal tract wall and the layers thereof (Wikimedia, 2014)

Villi (Figure 2.3) are fingerlike projections covering the surface of the intestinal epithelium and thereby increasing the effective absorption area by as much as 600 times. Each villus contains arterioles, venules and lymphatic vessels, which aid the villi in their main function of absorption. Furthermore, to increase the absorption area even further, a brush-like structure called microvilli, covers each villus (Ashford, 2007:273; Lundquist & Artursson, 2016; Renukuntla *et al.*, 2013:76).

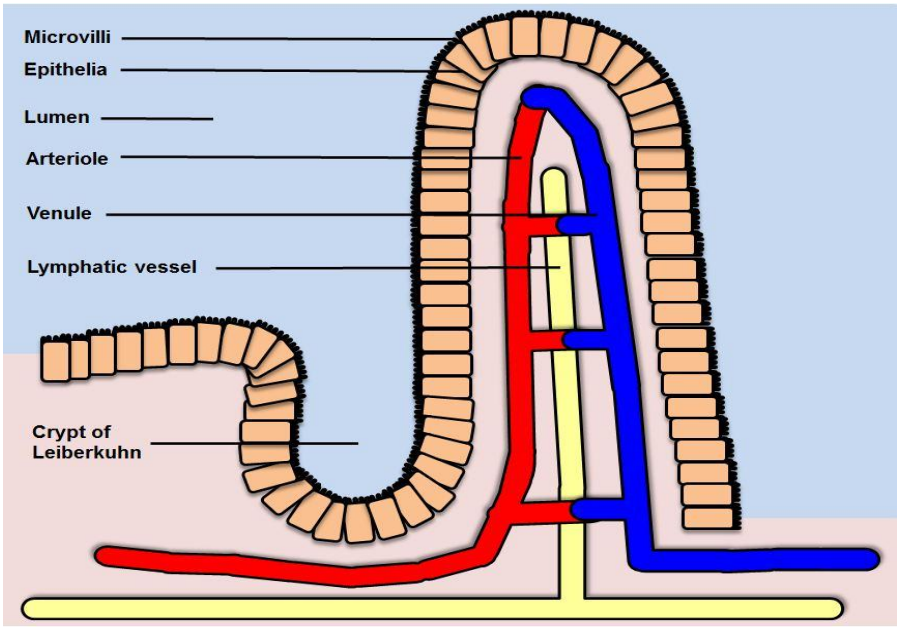

Figure 2.3: Schematic depiction of a single villus in the human gastrointestinal tract (Adapted from Ashford, 2007:274)

2.3 Drug absorption pathways

Any orally administered drug should be absorbed into the bloodstream to have a systemic effect. There are, however, many barriers that must be crossed in order for a drug molecule to reach the circulatory system, one of which is biological membranes. Absorption across membranes is a multi-pathway process where a drug may be transported by one or more mechanisms. Transport of drugs can occur passively, where the drug can either move in between the cells or through the cells. This is known as passive paracellular and transcellular transport, respectively (Figure 2.4 A and B). Energy-dependent mechanisms may also be encountered, which include trancytosis, carrier-mediated uptake and efflux transport (Figure 2.4 C, D and E) (Balimane *et al.*, 2006:E1-E2; Sarmento *et al.*, 2012:608-609).

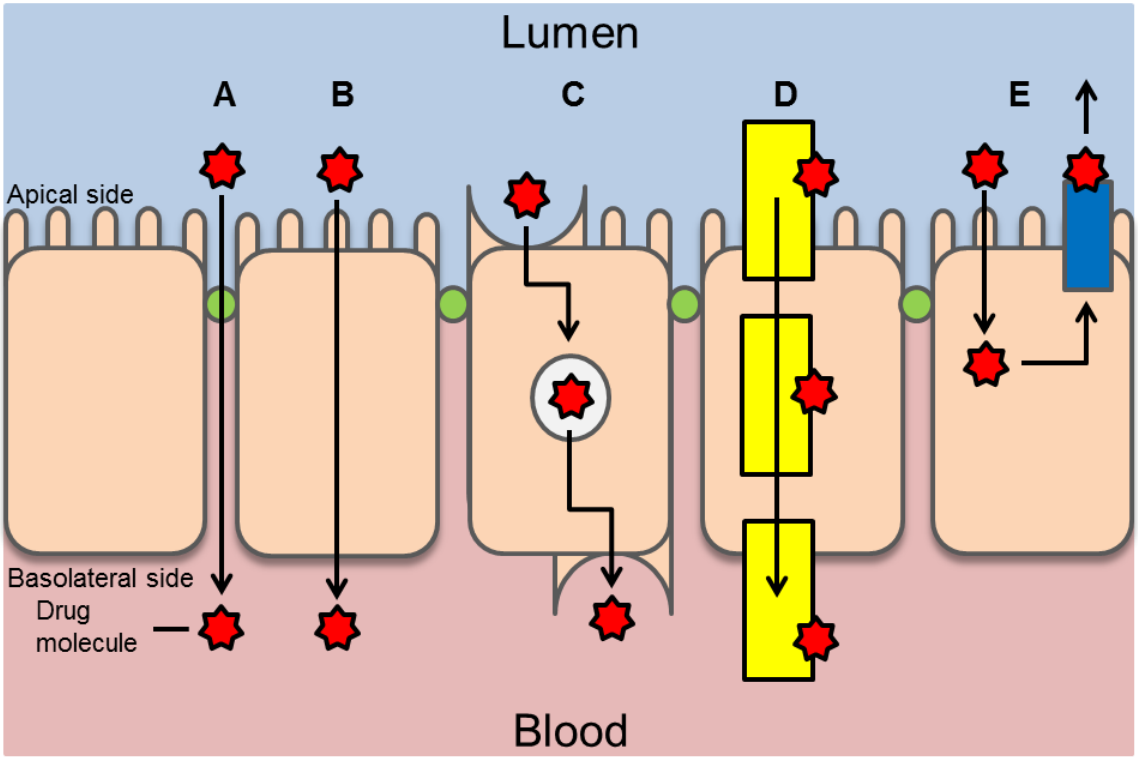

Figure 2.4: Schematic illustration of different absorption pathways across a biological membrane: A) Passive paracellular transport via intercellular tight junctions. B) Passive transellular transport along with the concentration gradient. C) Vesicular transport (trancytosis) depicting endocytosis on the apical side and exocytosis on the basolateral side. D) Carrier-mediated transport which may or may not be energy dependent. E) Efflux transport (Adapted from Balimane *et al.*, 2006:E2; Chan *et al.*, 2004:26; Sugano *et al.*, 2010:598)

2.3.1 Passive paracellular transport

Passive paracellular transport (Figure 2.4 A) occurs when drugs passively move or diffuse through the aqueous spaces in between cells, typically from high to low concentrations. Paracelluar transport depends on the chemical properties of the molecule being transported, but also on morphology of the cells between which the molecule is transported. For instance, the small intestinal intercellular spaces are much wider compared to the smaller/tighter cell junctions found in the blood-brain barrier. Drugs transported through intercellular spaces are usually small hydrophilic compounds and it has been documented that positively charged ions permeate more easily than neutral molecules, which in turn permeates easier than anions (Linnankoski *et al.,* 2010:2167; Sugano *et al.*, 2010:599).

2.3.2 Passive transcellular transport

Passive transcellular transport (Figure 2.4 B) is perhaps the most common transport mechanism, where the drug is transported through the cell. It is considered a diffusion process where the transport is driven by a concentration gradient (i.e. from high to low concentrations). Furthermore, because passive transport is not subject to site specific binding, it is not saturable and is less sensitive to the stereo-chemical structure of the compound being transported across the membrane. During transcellular transport, the compound being absorbed must first partition into the membrane and then move through the lipid bilayer of the cell membrane on the apical side of the cell. The drug/drug-like compound being transported across the membrane should possess certain physico-chemical properties such as favourable molecular charge, partition coefficient, pKa, solubility and molecular size to pass through the hydrophilic outer layers as well as the hydrophobic center of the membrane. Once across the cell membrane on the apical side of the cell, the drug moves through the cytoplasm and undergoes the same process across the cell membrane on the basolateral side of the cell (Chan *et al.*, 2004:26; Sugano *et al.*, 2010:597-598). Vesicular and carrier-mediated transport form part of the transcellular transport pathway.

2.3.3 Vesicular transport

Vesicular transport (Figure 2.4 C) can be sub-divided into different processes. Initially endocytosis takes place, which can be divided further into two processes, namely: i) pinocytosis where fluids or solutes are engulfed or ii) phagocytosis where solids are engulfed. During endocytosis the cell membrane on the apical side invaginates to surround the material and then engulfs it to internalize into the cell in a carrier vesicle or vacuole. The

vacuole moves through the cell and releases the contents from the cell on the basolateral side by the process of exocytosis (Lundquist & Artursson, 2016; Shargel *et al.*, 2005:381).

2.3.4 Carrier-mediated transport

Carrier-mediated transport is a transcellular transport mechanism (Figure 2.4 D) where a protein, called a transporter, is responsible for carrying the permeating molecules across the cell membrane. Two main membrane transporter families have been identified namely ATP (Adenosine triphosphate)-binding cassettes (ABC) and solute carriers (SLC). Transporters require energy in the form of ATP directly or indirectly to function. This enables the transporter proteins to move drugs/drug-like compounds against the concentration gradient. ABC transporters use ATP directly to activate the transport process, whereas the SLC family of transporters utilise ion gradients, which are ATP-dependent. However, membrane proteins may also act as a facilitated transporter, which isn't energy dependent, restricting transport to occur only with the concentration gradient. As the transporters are fixed proteins and stereo-specific, the possibility exists for the proteins to become saturated, or even blocked by a compound other than the drug (i.e an inhibitor). Saturation occurs when the number of drug molecules to be transported is greater than the number of transporters present on the membrane (Sugano *et al.,* 2010:598).

2.3.5 Efflux transport

Efflux transporters are mainly ABC proteins situated on the apical side of the cell membrane (Figure 2.4 E). They are found throughout the body and most noticeably in the small intestine, the liver and the blood-brain barrier. Efflux transport decreases absorption of any compound by actively transporting it back into the lumen after being absorbed into the epithelial cells. Sub-family members of the ABC proteins, like P-gp and multidrug-resistance-associated protein 2 (MRP2) are therefore very important in reducing/preventing uptake of potentially toxic substances, but also influence the final bioavailability of orally administered drugs or other therapeutic substances that are substrates of these efflux proteins (Chan *et al.*, 2004:25-27; Varma *et al.*, 2003:348).

2.4 Factors influencing drug absorption

Transport mechanisms play an important role in the rate and extent of drug absorption but Liu *et al.* (2009:281-282) and Shargel *et al.* (2005:414-145) described other factors that can also influence drug absorption, and therefore bioavailability, to a significant extent.

2.4.1 Physico-chemical factors

- Lipophilicity: For drug absorption to take place, drug molecules must penetrate the lipid bilayer of cell membranes. It is widely accepted that lipophilic drugs penetrate cells more easily than hydrophilic drugs. However, if a compound is too lipophilic it may remain in the hydrophobic center of the membrane and is then unable to enter the intracellular aqueous environment (Liu *et al.,* 2009:282).

- Molecular size: Cells throughout the body are joined together by tight junctions. These junctions may be small/tight, like in the colon or the blood-brain barrier, or they may be looser, like in the small intestinal epithelia. Therefore, the size of a molecule may have a significant effect on the capability of moving paracellularly or transcellularly over a membrane. It is accepted that mainly hydrophilic drugs with a molecular weight of less than 200 Da are able to move via the paracellular route, while molecules less than 500 Da are usually able to cross via the transcellular route. The resultant potential energy of the concentration difference over a membrane for a large molecule may not be high enough to partition the molecule in the lipid bilayer, which is necessary for transcellular absorption (Liu *et al.*, 2009:267).

- Charge: Generally, it is accepted that uncharged molecules tend to present with higher absorption rates. However, different molecular charges (positive, negative or uncharged) may prefer different mechanisms of transport as mentioned earlier (Liu *et al.,* 2009:282).

- Dissolution and solubility: Dissolution is the process of a solid substance becoming dissolved in a solvent, whereas solubility is a constant property which can be defined as the specific mass of a solute that dissolves in a specific volume of solvent at a specific temperature. Drugs need to be dissolved in order to be absorbed. These two factors play an indispensable role in drug absorption and consequently the bioavailability of the drug (Liu *et al.,* 2009:282; Shargel *et al.*, 2005:414).

2.4.2 Physiological factors

The following physiological factors may influence drug absorption from the GIT (Liu *et al.*, 2009:282-284; Shargel 2005:383-395):

- Transit time: Many physico-chemical and physiological factors can affect the gastro-intestinal transit time of an ingested oral dosage form. The optimal absorption of a drug, however, hinges on a fine balance where peristaltic movements should be

strong enough to thoroughly mix the drug with the GIT fluids, but should not be so forceful that the drug passes optimal absorption areas (i.e. the absorption window) too quickly.

- pH: Depending on the chemical stability and pKa value of the drug, the different pH values throughout the GIT may cause the drug to either precipitate or stay in solution and will also determine if the drug exists mainly in the ionized or unionized state. It is therefore important to consider when the dosage form is given. In the fasting state, gastric fluid may have pH values as low as 2, but can then increase to approximately 6-7 after a meal.

- Food: Food can either directly or indirectly affect the bioavailability of a drug. It does so by delaying the gastric emptying rate, stimulating bile secretion, increasing splanchnic blood flow and/or by physically or chemically interacting with the drug.

- Enzymatic activity: Enzymes like pepsin, protease and amylase are found throughout the GIT. The function of enzymes in the body is to degrade proteins and nutrients into smaller, absorbable entities. For example, peptide drugs and drugs that resemble nutrients are highly susceptible to breakup and inactivation by these enzymes, thus leading to a lower bioavailability (Lundquist & Artursson, 2016).

- Disease states: Drug absorption and, in turn, bioavailability are often unpredictably affected by disease states. Diseases may mediate changes in intestinal blood flow and enzymatic secretion, changes in GIT motility and emptying rates or altered membrane integrity by either causing inflammation or perforation. Based on the abovementioned physico-chemical and physiological factors, certain disease states may cause variable drug absorption due to physiological changes and should therefore be taken into account when administering medicines.

2.5 Pharmaceutical excipients

Pharmaceutical excipients can be defined as any components added to a dosage form other than the active pharmaceutical ingredient(s). Although they are generally regarded as pharmacologically and physiologically inert, excipients are included in medicinal formulations to provide functions with regards to dosage form design, manufacturing and drug release kinetics (Bele & Derle, 2012:756; Dave *et al.*, 2015:906; Shargel *et al*., 2005:418-419).

2.5.1 Types and functions of pharmaceutical excipients in tablets

2.5.1.1 Diluents

Diluents, also referred to as fillers, are mainly used to ease handling and dosage uniformity by increasing the size and weight of the final dosage form. This is particularly advantageous during manufacturing of oral dosage forms (such as tablets) as the active ingredient(s) dose is often too small in quantity to be compressed into a tablet on its own. Due to the high percentage of diluents incorporated into a single dosage form, they play an important role in the drug release kinetics of the completed product including the disintegration and dissolution rate (de la Luz Reus Medina & Kumar, 2006:31; García-Arieta, 2014:89). Furthermore, compounds from different chemical classes can be used as diluents. These include sugars, celluloses and inorganic salts, each of which is chosen for their individual properties that may positively contribute to the specific dosage form being produced. Examples include, but are not limited to lactose, glucose, sorbitol and mannitol (sugars), di-calcium phosphate and calcium carbonate (salts) and microcrystalline cellulose and cellulose acetate (celluloses) (Alderborn, 2007:449-450).

2.5.1.2 Lubricants

Lubricants are mainly used in the manufacturing of tablets, during which they act by decreasing the friction between the powder mass and the metal die during tablet ejection. The importance of reducing friction between tablet and die wall is to ensure that tablets get easily ejected and are uniformly pressed and shaped. When powders get compressed, particles lose their natural shape but tend to move back to their original shape after the pressure is removed. It is the radial pressure that the particles exert outwards that causes tablets to scratch and crack while being ejected. Furthermore, the flow rate, filling properties and the fluidity of the bulk powder can be improved by adding lubricants (Late *et al.*, 2009:4). Lubricants used during manufacturing can either be the fluid lubrication or the more popular dry powder boundary lubrication (Figure 2.5). Fluid lubrication act by creating a layer between the two solid objects' surfaces, which reduces friction. Alderborn (2007:452) notes that effervescent tablet manufacturing was done using liquid paraffin as an example of fluid lubrication. In the case of boundary lubrication, the powder mass is directly in contact with the tablet press. The dry powder lubricant gets mixed thoroughly with the powder mixture of the tablet formulation and tends to adhere to the larger particles, as the lubricant powder usually consists of small particles. This causes a thin layer of particles to form between the two moving surfaces, which in turn lower the kinetic friction coefficient (Alderborn, 2007:452-453; Aoshima *et al.*, 2005:28). Most commonly used lubricants (e.g. magnesium stearate)

are hydrophobic compounds. Therefore, an alteration in disintegration and dissolution rates are usually observed with the addition of these compounds to a dosage form. Water infiltration into the tablet is greatly reduced and can therefore not force the particles apart. Furthermore, contact between particles is also reduced when the lubricant covers the surface of bigger particles, leading to a reduction in tablet strength. Lubricants, for this reason are always used at the lowest possible concentration, which ranges from 0.25% to 5% w/w, but are also mixed for the shortest amount of time to prevent wide coverage of particle surfaces (Alderborn, 2007:453; Allen & Luner, 2005:430-431).

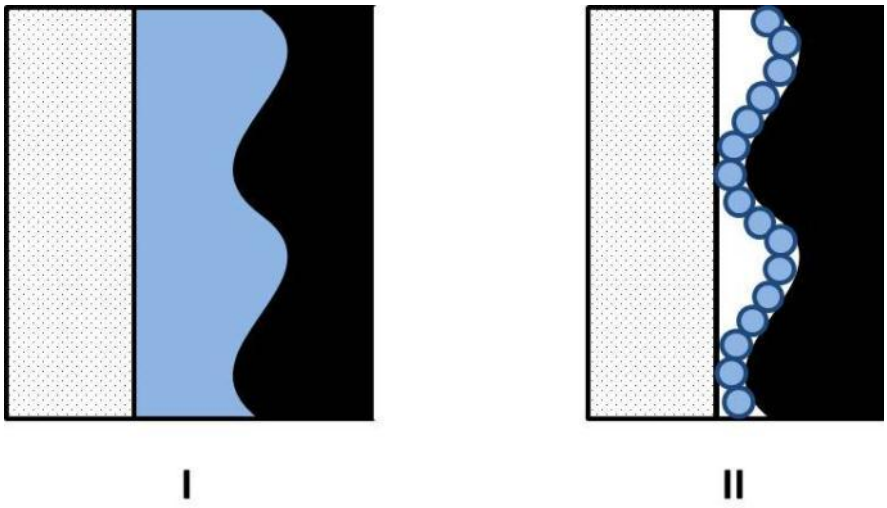

Figure 2.5: A schematic presentation of (I) fluid lubrication and (II) boundary lubrication between the die wall and drug particles (Adapted from Alderborn, 2007:452)

2.5.1.3 Binders

Binders, also sometimes referred to as adhesives, are excipients used mainly during manufacturing of tablets where it is incorporated to increase the compressibility of the bulk powder mixture and hardness of the final product. Compressibility is a term that is used to describe the ability of forces to arise between individual particles when forced to come into very close contact with each other. These forces increase the mechanical strength of a tablet. Binders can be incorporated into the powder mixture in three different ways: it can be added as a dry powder together with other excipients before wet agglomeration, it can be added as a solution that is used as an agglomeration liquid during wet agglomeration (solution binder) or mixed into the bulk powder before direct compaction (dry binder). Most commonly used today are solution binders, especially when manufacturing granules or beads. The granules formed after wet agglomeration, however, may be mixed together with a dry binder to further increase the compressibility of the powder (Alderborn, 2007:452).

2.5.1.4 Flavouring and colouring agents

Flavouring and colouring agents are mostly used to improve the organoleptic properties of oral dosage forms and therefore play a big role in patient compliance to drug therapy. Active ingredients and other excipients in a dosage form often exhibit unappetizing properties in its natural form. Therefore, flavouring agents are added, often in addition to sweeteners, to oral dosage forms especially in lozenges, fluids and effervescent tablets. It is furthermore very important to take into consideration a type of flavour that will best suit the target market of the product as well as the type of source (i.e. natural or synthetic). Colouring agents are added to mask other ingredients' colour, to distinguish between different strengths of the same dosage form, to increase aesthetic value of a dosage form or to compliment the flavouring agents used (Billany, 2007:369-370; York, 2007:13).

2.5.1.5 Disintegrants

For an active pharmaceutical ingredient (API) to be released from a solid oral dosage form and to be systemically absorbed from the GIT, the dosage form (e.g. tablet) needs to break up into smaller particles in order to undergo faster dissolution (Alderborn, 2007:450; Mohanachandran *et al.*, 2011:105; Shargel *et al*., 2005:414). A disintegrant is the pharmaceutical excipient mainly responsible for breaking the dosage form such as a tablet apart into smaller particles. Only after disintegration and dissolution of the dosage form can the API(s) become pharmaceutically available, therefore indirectly contributing to the effectiveness of the medication. The disintegration process itself can be divided into different phases where the dosage form firstly breaks into coarse particles and then sub-dividing into very fine primary units (Desai *et al.,* 2016:2546; Mohanachandran *et al.*, 2011:105). Even though some experts believe that disintegration is a combination of mechanisms (illustrated in Figure 2.6), the mechanisms can be individually described as wicking, swelling, strain recovery, heat of interaction and interruption of intermolecular bonds.

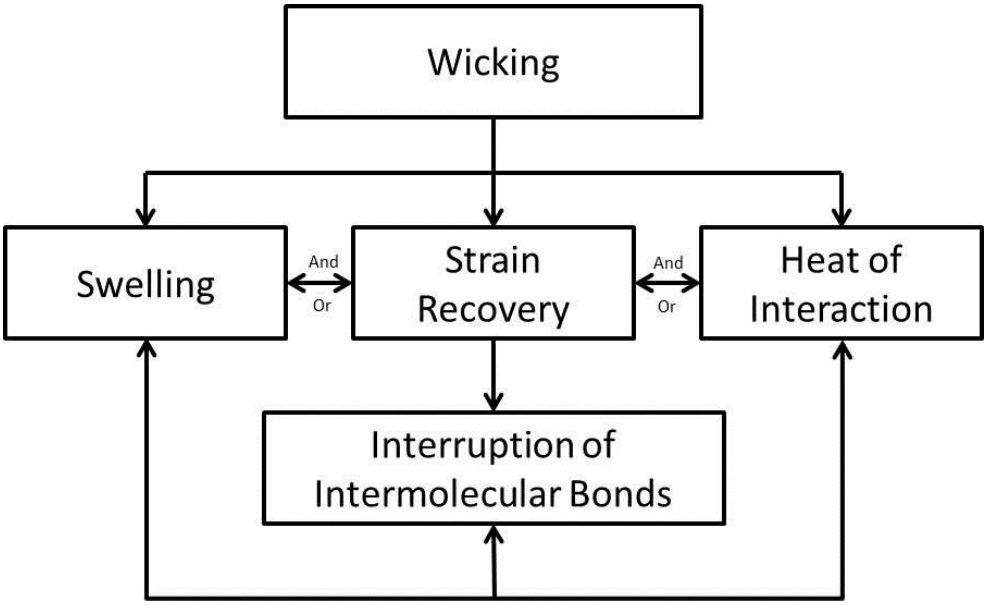

Figure 2.6: Schematic illustration of different disintegrating mechanisms and the interactions between mechanisms to cause tablet disintegration (Adapted form Desai *et al.*, 2016:2553)

- Wicking: This prerequisite mechanism of disintegration relies on capillary action to draw water into pores of the dosage form. Desai *et al*. (2016:2547) stated that most researchers agree that wicking alone cannot be responsible for full disintegration, while Quodbach *et al.* (2014:249) suggested that wicking may be a precursor required for swelling to occur or to cause strain recovery of the disintegrant particles. Furthermore, it is assumed that when increased compression forces are used to manufacture tablets, the disintegration rate is decreased for disintegrants that act mainly by wicking and swelling because of tighter intermolecular spaces (Desai *et al.*, 2012:2162).

- Swelling: Regarded as the most commonly accepted mechanism for disintegration by Desai *et al.* (2016:2546). Swelling occurs when the particles of disintegrants enlarge after coming into contact with water and start to exert forces outwards, forcing particles further away from each other, which causes the dosage form to break apart (Quodbach *et al*., 2014:249).

- Strain recovery: During tablet manufacturing, the bulk of the powder gets exposed to high amounts of pressure, which causes densely packed particles to form weak intermolecular bonds. Strain (or elastic) recovery is the process where, after coming into contact with water, the particle recovers its original form (Figure 2.7). The outwards pressure caused by recovery may cause tablets to disintegrate (Desai *et*

al., 2016:2548; Mohanachandran *et al.*, 2011:106). Furthermore, Patel *et al.* (2007:116) found that a higher compression force led to a higher tendency of strain recovery, especially as particle size increased.

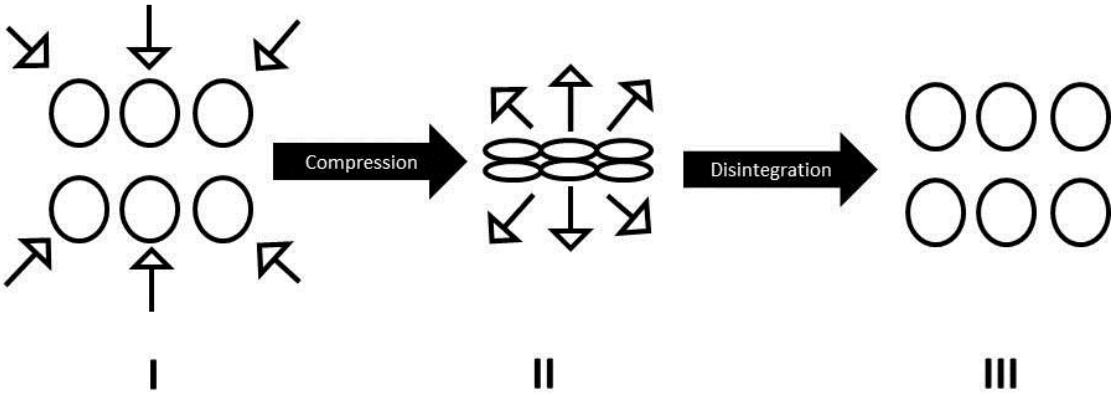

Figure 2.7: Illustration of disintegrant particles undergoing strain recovery where: (I) the free disintegrant particles get compressed during tablet manufacturing, (II) the disintegrant particles expand and (III) return to their original form after coming into contact with water (Adapted from Desai *et al.*, 2012:2162)

- Heat of interaction: A highly theoretical mechanism that posits the exothermic reactions that arise from certain disintegrants' reaction to water, which may produce enough heat energy to cause expansion of air trapped inside the dosage forms, leading to disintegration. Desai *et al.* (2016:2548) listed different contradictory statements on this proposed mechanism and stated that further studies are needed to determine its role in disintegration.

- Interruption of intermolecular bonds: It is known that many bonds between particles form under the pressure of compression during tableting and have been described as solid bridges, mechanical interlocking and intermolecular forces. Intermolecular forces are widely accepted as the most common bonding mechanism. Another mechanism for disintegration is believed to break these bonds which are locking the particles together to cause repulsion, thus breaking the dosage form apart. However, this action alone is not believed to be able to mediate full disintegration. Wicking and swelling may contribute to the intermolecular bonds breaking therefore causing disintegration of the tablet matrix (Desai *et al.*, 2016:2548; Ferrari *et al.*, 1996:78-79).

2.5.1.5.1 Croscarmellose sodium (Ac-di-sol®)

Croscarmellose sodium, commercially available as Ac-di-sol®, falls under a sub-group of disintegrants referred to as superdisintegrants due to its superior disintegrating capabilities at low concentrations. Whilst utilising wicking, swelling and strain recovery, Ac-di-sol® is capable of swelling four to eight times its own weight in less than ten seconds (Desai *et al.*, 2016:2550; Solaiman *et al.*, 2016:89). Used as a disintegrant only, concentrations of 10 - 25% (w/w) are incorporated in capsules and 0.5 – 5% (w/w) in tablets (Guest, 2005:211). Even though it is expected that disintegrants are chemical and biological inert substances, relatively recent studies by Takizawa *et al.* (2013:366) have shown a significant increase in paracellular transport of 5(6)-carboxyfluorescein in the presence of croscarmellose sodium across excised rat jejunum tissue.

2.5.1.5.2 Microcrystalline cellulose (Avicel® PH-200)

Avicel® has many uses as an excipient ranging from anti-adherent and disintegrating properties at low concentrations (5 - 15% w/w) to being a binding or adsorbent agent at very high concentrations (20 - 90% w/w). Avicel® is arguably the most used excipient in direct compression methods of manufacturing, even though efficacy during wet granulation has also been proven (de la Luz Reus Medina & Kumar, 2006:31; Galicet, 2005:132). During compression, microcrystalline cellulose undergoes plastic deformation, while still maintaining sufficient internal porosity to allow capillary uptake (wicking) of water into the tablet, thus ensuring fast disintegration (Al-khattawi *et al.*, 2014; Desai *et al.*, 2016:2550). Furthermore, Takizawa *et al.* (2013:366) found that microcrystalline cellulose had no significant intestinal permeability altering effects in the rat model specifically but remarked that permeation altering effects might in fact be plausible and that further studies are warranted.

2.5.1.5.3 Sodium starch glycolate (Explotab®)

Sodium starch glycolate, available as Explotab®, is a superdisintegrant synthesized from natural starches. It is used solely as a disintegrant in tablets and capsules, where only small concentrations ranging from 2 - 8% (w/w) are required because of its exceptional swelling capabilities (Edge & Miller, 2005:701; Mohanachandran *et al.*, 2011:106; Thibert & Hancock, 1996:1256). Experimental data by Young *et al.* (2005:252-253) proved this by showing a 45 - 50% increase in mass of sodium starch glycolate when exposed to conditions of 90% relative humidity, while Edge & Miller (2005:702) noted that Explotab® can sweel up to 300 times its own volume in water.

2.5.1.5.4 Crospovidone (Kollidon® CL-M)

Crospovidone, commercially available as Kollidon®, is a synthetic cross-linked polyvinylpyrrolidone that is employed as both a disintegrant as well as a dissolution enhancing agent at concentrations of 2 - 5 % (w/w) (Desai *et al.*, 2016:2550; Kibbe, 2005:214). The mechanism of disintegration, however, has been open to many debates as Kibbe (2005:214) suggested that crospovidone mediates tablet disintegration by swelling following capillary wicking. In a newer publication, Desai *et al.* (2012:2162) found that crospovidone disintegrated by strain recovery (see section 2.5.1.5, Figure 2.7) rather than the initially believed wicking only. This explains why disintegration occurs faster when relatively larger particles of crospovidone are used than in comparison with relatively smaller particles.

2.5.1.5.5 Sodium Alginate

Alginic acid is a natural polysaccharide polymer extracted from brown seaweed, which is then neutralized with sodium bicarbonate to form sodium alginate. Sodium alginate is a multifunctional compound which can be used as an excipient or therapeutically. Sodium alginate has been deployed therapeutically for the management of gastro-esophageal reflux and as a haemostatic agent in wound dressings amongst others. As an excipient, sodium alginate has been used as a thickening and suspending agent in topical formulations, as an agent to delay dissolution in oral dosage forms and as a binder or disintegrant at relatively low concentrations (2.5 - 10% w/w) in solid oral dosage forms (Cable, 2005:656; Tønnesen & Karlsen, 2002:622-623).

2.6 Prediction of drug absorption

From as early as the 1950's, pressure was mounting on scientists from different fields to find more humane scientific techniques when conducting pharmacokinetic and other experiments that involved animals. In 1956, Charles Hume proposed a new approach, which he referred to as "The Three R's" concept. "The Three R's" represent key concepts such as a reduction in the number of animals required per study, refinement of the experimental methods and replacement alternatives for laboratory animals such as *in vitro* or *ex vivo* experimental approaches (Zurlo *et al.*, 1996).

Reduction in the number of animals used in research may refer to two possible interpretations: firstly, to use a smaller number of animals to gain the same levels of information or secondly, to gain more information from a specified number of animals. Thus, in both situations, the total cost in terms of animal stressors is greatly decreased.

Furthermore, better experimental designs and statistical analyses can be used to aid in the reduction of animal usage (Zurlo *et al.*, 1996).

Alternatives to refine animal experiments focus mainly on keeping any form of discomfort to a minimum for the animal. Discomfort may include physiological-, psychological- and/or environmental stressors caused by, amongst others, surgery, disease, food and water deprivation and the like. Zurlo *et al.* (1996) suggested that more resources should be allocated to standardisation of an objective way of assessing animal pain and stress.

Lastly, replacement alternatives refer to experimental methods that can be used to achieve the scientific goal without the use of laboratory animals (more detail will be given in section 2.6.1). Alternatives can be classified as either relative replacements or absolute replacements. Relative replacements are explained by Zurlo *et al.* (1996) as the humane killing of animals for purposes other than experimental work in order to gain cells, tissues and organs for use in *ex vivo* studies, whereas absolute replacement are methods where no animals are involved at all (e.g. use of synthetic and artificial membranes).

2.6.1 Classification of models that can be used for drug absorption studies

2.6.1.1 *In vivo* models

In vivo experiments make use of live animals, which are mainly used to determine absorption, distribution, metabolism and excretion (in other words, the bioavailability) of drugs from different routes of administration as well as toxicity. Drugs may be orally administered or infused into a specific gastric region via a tube that is inserted through the mouth or anus of the animal. Thereafter, samples (e.g. blood, excrement or organ tissue) are withdrawn or collected at specific time intervals after insertion and analysed to establish the drug concentration present in each sample. Higher order vertebrates such as rats, rabbits, dogs and pigs are preferred for *in vivo* experiments since they show more evolved transport and metabolism mechanisms (Alqahtani *et al.*, 2013:5; Gamboa & Leong, 2013:805).

The *in vivo* experimental approach has certain attributes that make it a desirable experimental option such as the presence of a fully functional metabolic system, blood circulation, lymphatic absorption, nerve supply and intact intestinal membranes. However, the *in vivo* model does have some drawbacks, which include the physiological differences between humans and animals, the large amount of resources and time required and the difficulty associated with isolating individual absorption mechanisms. These factors are the reason why *in vivo* experiments are often considered to be impractical and not suitable for high-throughput drug screening purposes (Alqahtani *et al.*, 2013:5-6).

Gamboa & Leong (2003:805) stated that *in vivo* experiments will always eventually be required to obtain conclusive data in terms of the pharmacokinetics of a drug, no matter how sophisticated any of the other models may be.

2.6.1.2 *In situ* models

In situ studies refer to a process where solutions with selected concentrations of test compounds are perfused through a pre-determined part of intestinal tissue for a specific amount of time in an anaesthetized animal or human (Figure 2.8). Concentrations of the test compounds are calculated from the outlet flow, after known concentrations were deposited at the inlet. The differences in said concentrations indicate drug absorption and metabolism and can be used to measure the region specific membrane permeability of the drug. *In situ* models are especially advantageous because of intact blood flow, nervous systems and full biological enzyme and protein expression, thus closely mimicking *in vivo* conditions. High costs, trained personnel and anesthesia's effect in absorption include some of the disadvantages linked to this technique (Alqahtani *et al.*, 2013:5; Gamboa & Leong, 2013:805).

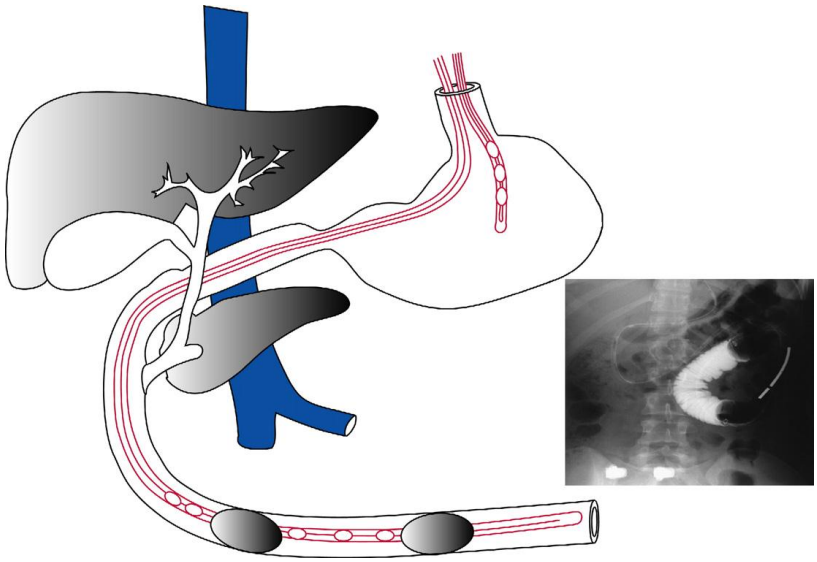

Figure 2.8: Illustration showing the Loc-I-Gut *in situ* technique where two balloons are placed approximately 10 cm from each other in a pre-determined intestinal region. Tubes are then used to infuse and deliver a test compound at a known concentration to the specific region (Lennernäs, 2007:1108)

2.6.1.3 *In silico* models

The term *in silico* refers to predictions made with regards to pharmacokinetic properties (i.e. absorption, distribution, metabolism and excretion) of compounds by using computer

software, when provided with certain factors such as pH, molecular weight etc. Some of the many different available software programs include GastroPlus®, SimCYP® and PKSim, which may be used to predict intestinal transit, absorption and other relevant parameters. During pre-formulation of pharmaceuticals, *in silico* models play an important role to reduce time and cost in determining novel compounds' kinetic characteristics (Alqahtani *et al.*, 2013:8-9).

2.6.1.4 *In vitro* models

In vitro is a term used to describe experimental models where primary or immortalized cells are used to mimic physiological conditions outside of the body in order to characterize the absorption and permeability tendencies of drugs during early stages of drug development (Alqahtani *et al.*, 2013:2; Sarmento *et al.*, 2012:607).

2.6.1.4.1 Cell culture-based *in vitro* models

Sarmento *et al.* (2012:610) listed some of the most preferred cell lines for intestinal permeability studies as Caco-2 (Figure 2.9), MDCK, HT29-MTX and IEC-18 cells, to name a few. Immortalized epithelial cells have continuously been used as *in vitro* models because of their ability to grow as polarized monolayers (where there is a definite apical and basolateral side), to express different enzymes and transporters and because tight junctions, like in enterocytes, are present (Alqahtani *et al.*, 2013:2). Furthermore, cell lines contribute considerably in reducing and replacing animal experimentation.

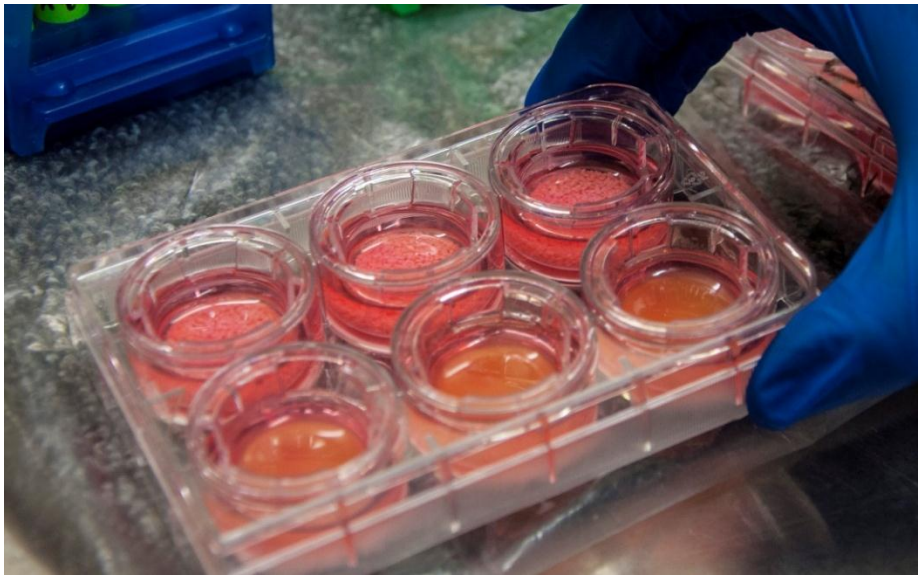

Figure 2.9: Image showing a 6-well Transwell® plate with Caco-2 cell monolayers used for *in vitro* experiments

Unfortunately, cell lines do have some shortcomings such as the lengthy time that is required for the cells to mature, to form tight junctions and to express transporter proteins as well as enzymes. Variance between different laboratories and passage numbers, relative difficult technique of culturing cells and a tendency to mediate less paracellular transport due to much tighter intercellular junctions than in normal enterocytes may also prove to be problematic (Alqahtani *et al.*, 2013:2).

2.6.1.5 *Ex vivo* models

Ex vivo refers to excised animal/human tissues being used in experiments outside the body. This model has the advantage that experiments are conducted on viable and functional cells in order to determine drug transport as it would occur in the live specimen (Alqahtani *et al.*, 2013:3; Antunes *et al.*, 2013:13).

Some disadvantages that are associated with *ex vivo* techniques include dissection of the tissue and removal of serosal layers from the small intestine, which is regarded as the biggest drawback of this model. These techniques are difficult to master and may cause damage to the underlying tissue, which in its own right, can cause drastic fluctuations in the extent of drug transport. Furthermore, inter-experimental variations between tissue samples, prolonged setup times and low-throughput rates contribute to the difficulties associated with the use of *ex vivo* models (Antunes *et al.*, 2013:13).

Certain advantages and other desirable attributes are associated with the use of *ex vivo* models. For instance, the intestinal integrity is preserved which closely mimic *in vivo* conditions, which enables researchers to investigate intestinal transport in different regions and species. Metabolism of a drug can be investigated simultaneously with bi-directional transport, which may include both inhibitory and absorptive transporters/enzymes (Antunes *et al.*, 2013:13). Furthermore, in line with the ethical concerns of experimental work as mentioned previously by Zurlo *et al.* (1996), *ex vivo* assays succeed in reducing, replacing and refining laboratory animal experimentation, since intestinal tissue are often collected from animals designated for slaughter for meat production purposes.

2.6.1.5.1 Sweetana-Grass diffusion apparatus

The Sweetana-Grass diffusion apparatus (Figure 2.10) was originally developed from the Ussing chamber, where the latter was used only to study transepithelial ion transport, while the former was optimized to study drug transport. During permeation studies with this system, a small piece of intestine is mounted between the diffusion chamber half-cells. Both sides are usually initially incubated with Krebs-Ringer bicarbonate buffer (KRB), while

carbogen gas (95% O_2:5% CO_2) is constantly pumped through the solution. The gas serves the purpose to supply oxygen to the tissue, but also to circulate the fluids in the chamber. An important advantage of this system is that the experimental solution can be incubated on either side of the membrane, i.e. the mucosal or the serosal side. Therefore, transport can be studied in either an absorptive or a secretory direction (Antunes *et al.*, 2013:13; Legen *et al.*, 2005:185).

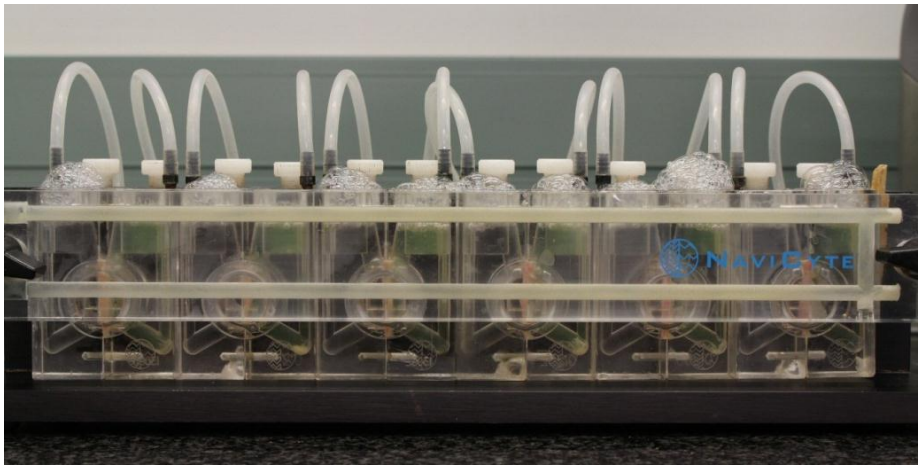

Figure 2.10: Image showing a Sweetana-Grass diffusion apparatus used for *ex vivo* experiments, shown here connected to a carbogen supply and heating block

2.7 Summary

Drug products are mainly administered via the oral route of drug administration due to its ease of administration, safety and patient compliance. Active pharmaceutical ingredients (API's) are almost never given alone, but together with other compounds namely excipients. Excipients were believed to be pharmacologically inert, but from the literature it is clear that this is not the case and that the different types of excipients may present drug absorption modulating effects.

Many models are available to test the possible effects that excipients (in this case, disintegrants specifically) might have, which include models ranging from computer simulations (*in silico*), through tests on excised tissue and immortilised cells (*ex vivo* and *in vitro* respectively) to experiments on living subjects (*in situ* and *in vivo*).

With increased pressure on the worldwide scientific community to replace, reduce and refine animal testing, it is our moral and ethical responsibility to find surrogate experimental models. *In vitro* and *ex vivo* models are thus excellent experimental approaches in reaching these goals. Using excised pig intestinal tissue in a Sweetana-Grass diffusion apparatus is

an excellent way to do preliminary permeation experiments as this intestinal tissue is easy to procure from an abattoir, its close resemblance to human intestinal tissue and because of ethical considerations (animals are not bred and sacrificed for research purposes, but for meat production purposes).

CHAPTER 3: MATERIALS AND METHODS

3.1 Introduction

In this study, a Sweetana-Grass diffusion apparatus was used to determine if selected disintegrants had an effect on the bi-directional transport of a known P-gp substrate, rhodamine 123 (R123) (Crawford & Putnam, 2014:1462; Zhao *et al.*, 2016:1527). Excised pig intestinal tissues were used for the transport studies as it is fairly easily obtainable, but also due to its close anatomical and physiological resemblance to the human intestinal tract (Pietzonka *et al.*, 2002:40). Bi-directional transport across intestinal tissue entails studies in both apical-to-basolateral (absorptive) and basolateral-to-apical (secretory) directions, where the apical side represents the intestinal lumen and the basolateral side, the blood circulation.

Furthermore, during the development of the experimental design and the execution of the analytical procedures, validation of said procedures is of extreme importance. Validation can be defined as the process where it is established that the performance characteristics of the analytical procedure meet certain criteria. These performance characteristics include: accuracy, precision, specificity, detection limits, quantification limits, linearity, range and robustness (USP-NF, 2016a).

3.2 Materials

R123, Krebs-Ringer bicarbonate (KRB) buffer and sodium alginate (batch number MKBN7680V) were purchased from Sigma-Aldrich (Johannesburg, South Africa). Croscarmellose sodium (Ac-di-sol®, batch number T017C) and microcrystalline cellulose (Avicel® PH-200, batch number M939C) were purchased from FMC Corporation (Cork, Ireland). Sodium starch glycolate (Explotab®, batch number SSGP0601) was purchased from Mirren (PTY) LTD and crospovidone (Kollidon® CL-M, batch number 91416136W0) was purchased from BASF (Ludwigshafen, Germany). Costar® 96-well plates (lot number 07914036) were purchased from The Scientific Group (Randburg, South Africa). Pig intestine was collected at a local abattoir in Potchefstroom, South Africa.

3.3 Fluorescence spectrometry method validation

A Spectramax Paradigm® (Serial nr 33270-1142) multi-mode detection platform plate reader was used to do a fluorescence spectroscopic analysis of all samples from the transport studies. Using a Costar® 96-well plate to analyse the R123 concentration in the samples, the plate reader was set at an excitation wavelength of 480 nm and an emission wavelength of 520 nm (Kaprelyants & Kell, 1992:412; Wang *et al.*, 2009:3).

3.3.1 Linearity

Linearity describes the ability of an analytical method to obtain test results that are directly proportionate to test samples over a specific concentration range. The concentration range used for determination of linearity should be selected to be in the same magnitude range as the expected sample concentrations, which may be encountered during the experimental procedures (USP-NF, 2016a). A correlation coefficient (r^2) of more than 0.999 should be achieved as proof of acceptable linearity and should be determined by a series of three to six tests over at least five concentrations (Shabir, 2003:63-64; Singh, 2013:29).

In order to determine linearity two stock solutions were prepared of 5 µM and 2.5 µM respectively. These stock solutions were diluted four and three times respectively by a factor of ten. The samples over the full concentration range (i.e. 5 µM, 2.5 µM, 0.5 µM, 0.25 µM, 0.05 µM, 0.025 µM, 0.005 µM, 0.0025 µM and 0.0005 µM) were analysed four times each and the regression of the calibration curve was calculated.

3.3.2 Limit of detection (LOD) and limit of quantification (LOQ)

The limit of detection (LOD) can be defined as the lowest concentration of analyte that can be detected by the analytical method of any given sample and can be calculated using Equation 1 (Shabir, 2003:62-63).

$$\text{Limit of Detection (LOD)} = 3.3 \times \left(\frac{SD}{S}\right) \qquad \text{(Eq. 1)}$$

The limit of quantification (LOQ) is the lowest concentration of analyte that can be quantified with optimal precision and accuracy. LOQ can be calculated using Equation 2 (Shabir, 2003:63).

$$\text{Limit of Quantification (LOQ)} = 10 \times \left(\frac{SD}{S}\right) \qquad \text{(Eq. 2)}$$

Where the factor constant (3.3 and 10 for Equations 1 and 2, respectively) represent the signal-to-noise ratio, SD represents the standard deviation of the plate blanks and S the slope of the standard regression line for both equations.

3.3.3 Accuracy

The accuracy of an analytical method can be defined as how close the concentration of the generated analytical values of a specific analyte is in comparison to a known concentration of the same analyte. Accuracy is determined by at least nine readings over at least three concentrations, i.e. a high, medium and low concentration sample should each be analysed

at least three times. The concentration values are then calculated as a percentage of the theoretical concentration in order to determine the accuracy of the analytical method (USP-NF, 2016a). Test results for an analytical method are considered as accurate when the mean recovery is 100 ± 2% (Shabir, 2003:61).

Six samples from each solution containing R123 at concentrations of 5 µM, 2.5 µM and 0.125 µM were analysed and the recovery from all three solutions complied with the 100 ± 2% recovery.

3.3.4 Precision

The precision of an analytical method is defined as the degree to which individual test samples concur with each other when analysed at different times. Precision is therefore used to indicate the degree of repeatability/reliability of an analytical method (USP-NF, 2016a). Precision was determined via intra-day and inter-day analysis.

3.3.4.1 Intra-day precision

Repeatability testing forms part of precision testing where results of an analytical method are compared over a relatively short time interval (i.e. on the same day). This is referred to as intra-day precision testing. During intra-day precision testing, three concentrations of the analyte are analysed thrice at three separate times during a single day (or during a 24 hour period). A percentage relative standard deviation (RSD) of ≤ 2% should be achieved to confirm the precision of the analytical method (Shabir, 2003:62).

Solutions with three different concentrations of R123 (5 µM, 2.5 µM and 0.125 µM) were analysed thrice at three separate times during a single day and standard deviation and %RSD values were calculated. The fluorescence analytical method used in this study was found to comply with the requirement of ≤ 2% RSD for intra-day precision.

3.3.4.2 Inter-day precision

The same three concentrations of R123 used for intra-day precision (5 µM, 2.5 µM, 0.125 µM) were used to determine inter-day precision at the same time over three consecutive days. The %RSD value for inter-day precision can also be accepted to be ≤ 2% (Shabir, 2003:62) and therefore the fluorescence analytical method complied with this requirement.

3.3.5 Specificity

The specificity of an analytical method refers to the ability of the experimental method and equipment to accurately detect the analyte in the presence of other compounds which may be present in the samples and impede detection of the specific analyte (USP-NF, 2016a).

In this case, Costar® 96-well plates were prepared to contain control solutions (5 µM R123 alone) alongside test solutions, which contained 5 µM R123 mixed with the particular disintegrant being tested for a specific experiment. After analysis, the mean fluorescent values of the test solutions were compared to that of the R123-alone control solution and the actual concentration R123 present was calculated. Using the actual concentration R123 found in the test solutions and comparing it to that of the controls, one could deduce whether the disintegrants interfered with the fluorescent yield of R123. The same criterion for accuracy, namely 100 ± 2% recovery of R123 in the presence of each disintegrant, is used to demonstrate acceptable specificity (Shabir, 2003:61; USP-NF, 2016b).

3.4 *Ex vivo* transport studies

3.4.1 Preparation of experimental solutions

Five commonly used tablet disintegrants were selected and tested for potential pharmacokinetic interactions with a model compound at four different concentrations. The chosen disintegrant concentrations were based on the minimum and maximum amounts of each disintegrant that are typically employed to formulate an oral dosage form (e.g. tablet) as described in the literature.

The selected concentrations of the disintegrants in the transport studies also took into account the fact that most oral dosage forms are taken together with fluid volumes ranging between 100 ml and 200 ml (Takizawa, Kishimoto, *et al.*, 2013:365). KRB was used as the solvent for all solutions in the transport experiments.

Disintegrant solutions/suspensions were freshly prepared to a final volume of 50 ml with KRB before every transport experiment. Table 3.1 shows the disintegrant concentrations used in the bi-directional transport studies to cover the complete range of potential concentrations of each disintegrant that a drug could be exposed to in the GIT when taken in a 200 mg tablet orally with two different volumes of fluid (i.e. 100 and 200 ml, respectively).

Table 3.1: Concentrations (% w/v) of each selected disintegrant for the bi-directional transport experiments (Cable, 2005:626; Edge & Miller, 2005:701; Galichet, 2005:132; Guest, 2005:211; Kibbe, 2005:214)

Disintegrant	Minimum and maximum concentration (% w/w) in tablet		Concentration of disintegrant (% w/v)	
			In 100 ml fluid	In 200 ml fluid
Ac-di-sol®	**Minimum concentration**	**0.5**	0.0010	0.0005
	Maximum concentration	**5.0**	0.0100	0.0050
Avicel® PH-200	**Minimum concentration**	**5.0**	0.0100	0.0050
	Maximum concentration	**15.0**	0.0300	0.0150
Explotab®	**Minimum concentration**	**2.0**	0.0040	0.0020
	Maximum concentration	**8.0**	0.0160	0.0080
Kollidon® CL-M	**Minimum concentration**	**2.0**	0.0040	0.0020
	Maximum concentration	**5.0**	0.0100	0.0050
Sodium alginate	**Minimum concentration**	**2.5**	0.0050	0.0025
	Maximum concentration	**10.0**	0.0200	0.0100

R123 was identified as a potential model compound because it is known to be a highly selective P-gp substrate (Crawford & Putnam, 2014:1462; Zhao *et al.*, 2016:1527). R123 was used as a marker transport compound in this study at a concentration of 5 µM to investigate if the selected disintegrants have any effect on the extent of P-gp-mediated bi-directional transport across excised pig intestinal tissue (Wang *et al.*, 2009:3).

When transport experiments were conducted in the apical-to-basolateral direction, sufficient R123 (to produce a final concentration of 5 µM) was mixed together with the amount of disintegrant required for the specific concentration being tested and was made up to a volume of 50 ml with KRB. A volume of 7 ml of the R123-disintegrant mixture was added to the apical side (i.e. each donor chamber) of the intestine in the Sweetana-Grass diffusion chamber.

Transport experiments in the basolateral-to-apical direction required two separate solutions. A 50 ml solution of R123 was prepared in KRB (with final concentration of 5 µM) and aliquots of 7 ml of this solution were added to the basoleteral side (i.e. each donor chamber) of the intestine. The apical side (i.e. each acceptor chamber) was incubated each with an aliquot of 7 ml of each disintegrant solution/suspension after the required amount of disintegrant was weighed off, mixed and made up to 50 ml with KRB.

Experiments were designed in this way to ensure that the solution/suspension containing the disintegrant was always added to the apical side in order to mimic normal physiological conditions, where a disintegrant will be available in the GIT lumen after swallowing an oral dosage form and not in the blood. Most disintegrants have large molecular weights and are too hydrophilic to get absorbed into the systemic circulation. Table 3.2 indicates the mass of each disintegrant used to make up to 50 ml solution/suspension for each individual experiment.

Table 3.2: Mass of each disintegrant used for preparing test solutions/suspensions for each transport experiment

Disintegrant	Concentration (% w/w) in tablet	Mass of disintegrant in 50 ml test solution/suspension (mg)	
		When taken with 100 ml fluid	When taken with 200 ml fluid
Ac-di-sol®	**0.5**	0.50	0.25
	5.0	5.00	2.50
Avicel® PH-200	**5.0**	5.00	2.50
	15.0	15.00	7.50
Explotab®	**2.0**	2.00	1.00
	8.0	8.00	4.00
Kollidon® CL-M	**2.0**	2.00	1.00
	5.0	5.00	2.50
Sodium alginate	**2.5**	2.50	1.25
	10.0	10.00	5.00

3.4.2 Preparation of pig intestinal tissue for transport studies

Pig jejunum tissue was collected at a local abattoir in Potchefstroom, South Africa. Immediately after the pigs were slaughtered, a piece of proximal jejunum (± 20 cm) was excised, rinsed and submerged in freshly prepared ice-cold KRB buffer and placed in a cooler box for transfer to the laboratory. In the laboratory, the jejunum segment was pulled over a glass test tube. The serosal layer was then stripped off by means of blunt dissection and the piece of jejunum was cut along the mesenteric border with a scalpel as shown in Figure 3.1 (A, B and C) (Legen *et al.*, 2005:185; Pietzonka *et al.*, 2002:41).

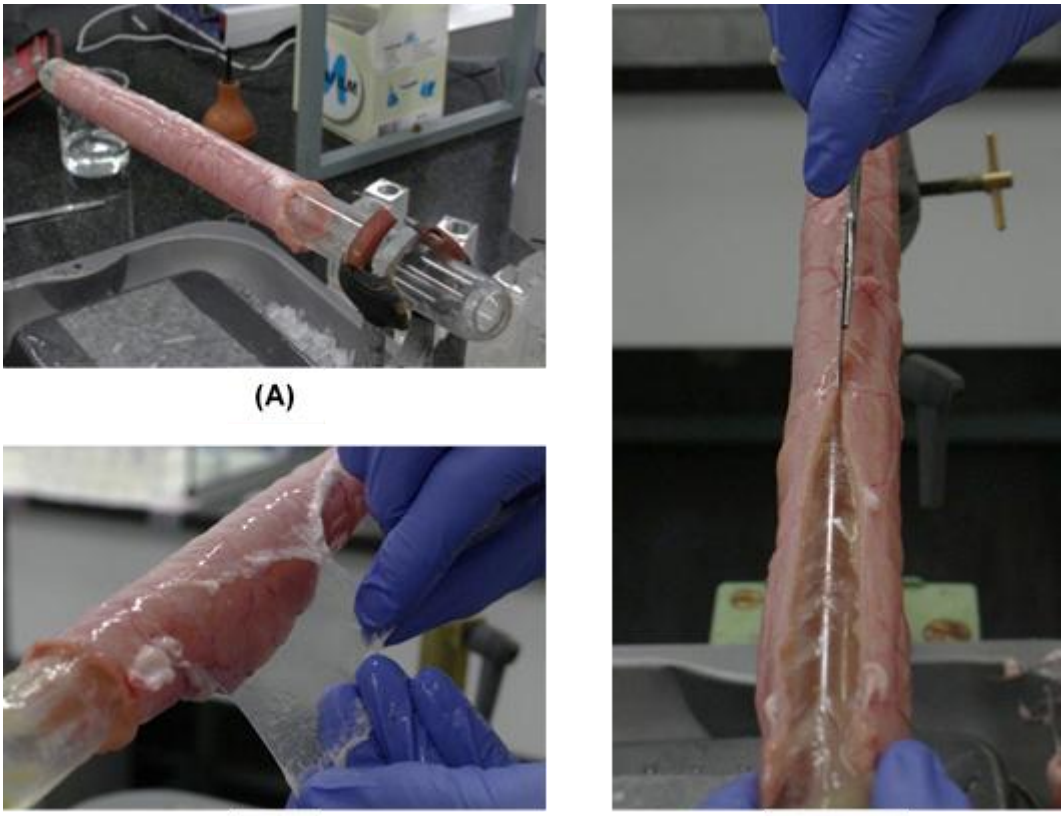

Figure 3.1: Images illustrating (A) a segment of proximal jejunum mounted on a glass tube showing the mesenteric border, (B) the serosal layer being removed and (C) the jejunum being cut along the mesenteric border before being washed off the glass tube onto filter paper

The resultant jejunum sheet was washed off from the glass tube onto a sheet of filter paper. The jejunum sheet was then cut into smaller segments, which were mounted onto Sweetana-Grass diffusion chamber half-cells, thus exposing an average surface area of 1.72 cm^2 available for the trans-membrane transport of molecules (Figures 3.2 and 3.3).

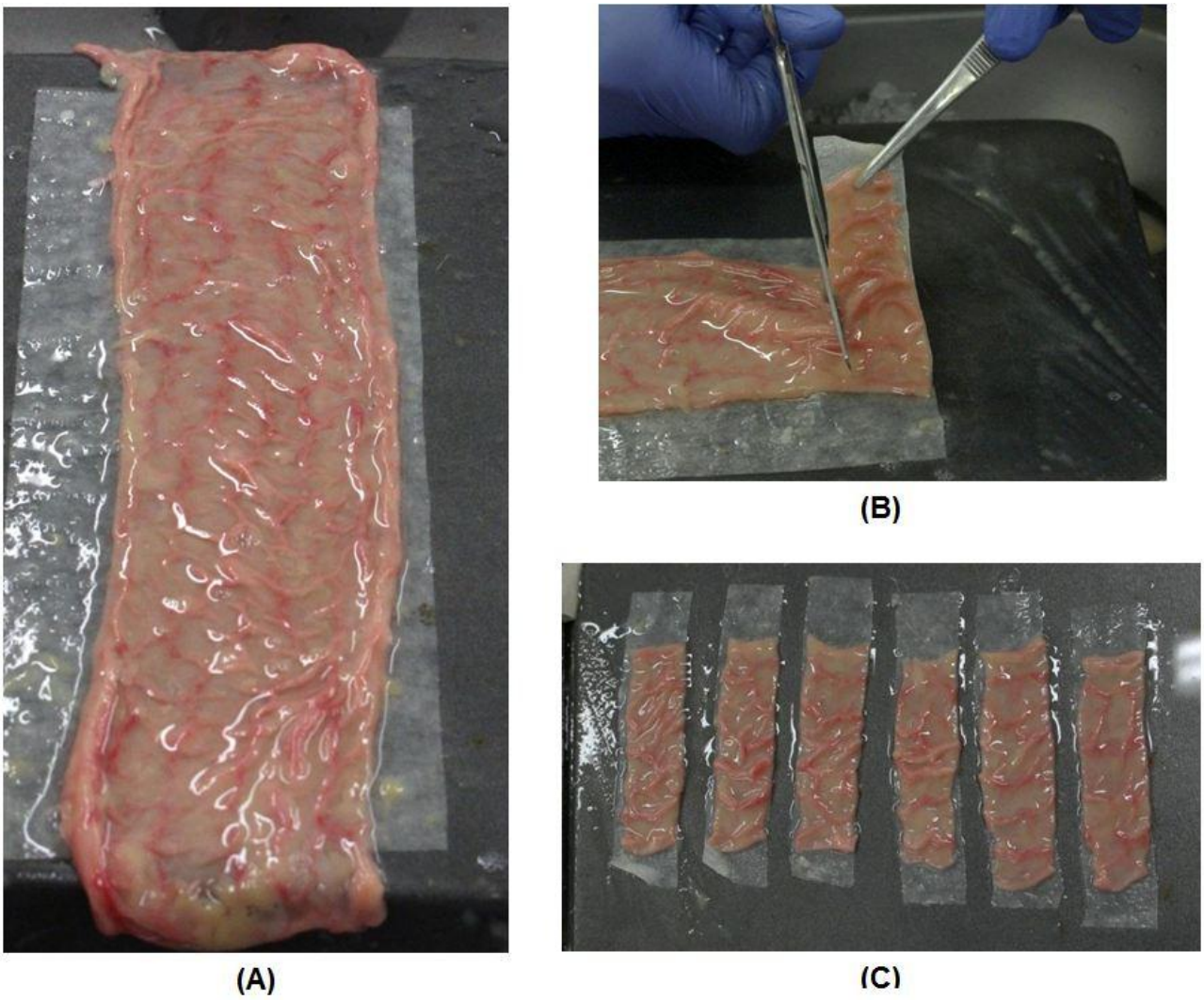

Figure 3.2: Images illustrating (A) the proximal jejunum sheet spread open after being cut open and washed off from the glass tube onto filter paper and (B and C) process of cutting the tissue sheet into smaller segments

(A)

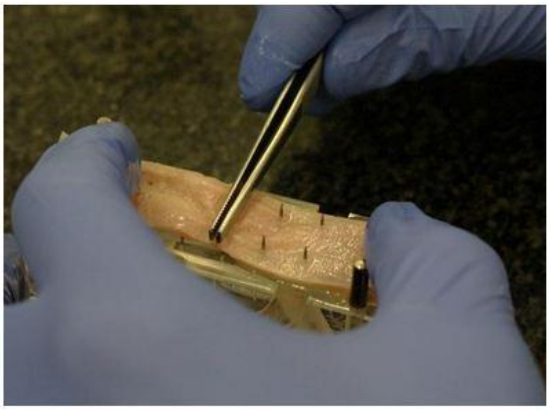

(B)

(C)

(D)

Figure 3.3: Images illustrating (A, B and C) the process of mounting the jejunum segments onto half cells and removal of filter paper and (D) assembling two-half cells into a single diffusion chamber

Peyer's patches, which is regarded as epithelial adaptations that can affect drug absorption, was avoided whilst cutting intestinal tissue into smaller segments (Figure 3.4).

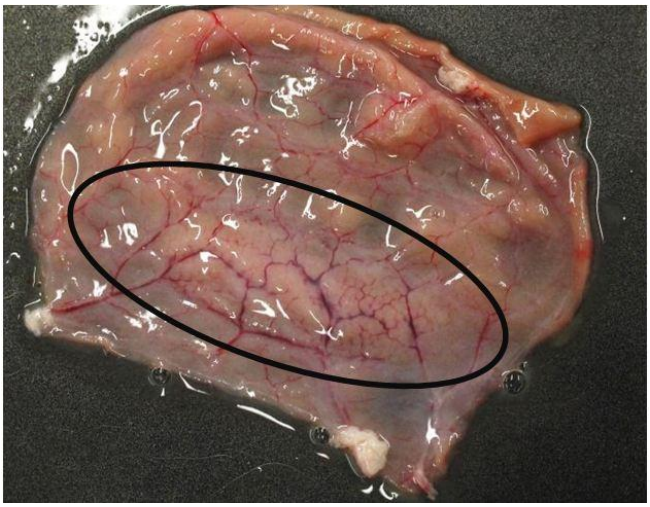

Figure 3.4: A Peyer's patch encircled on a section of intestinal tissue

Each of the six assembled diffusion chambers was then linked to a heating block (37°C) and a carbogen (95% O_2:5% CO_2) supply (Figure 3.5) (Legen *et al.*, 2005:185).

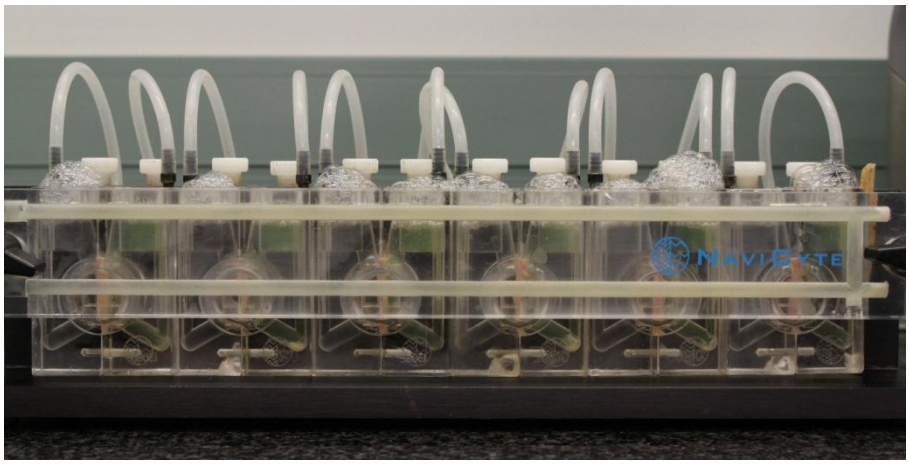

Figure 3.5: Image illustrating an assembled Sweetana-Grass diffusion apparatus with the heating block and connected to a carbogen (95% O_2:5% CO_2) supply

Trans-epithelial electrical resistance (TEER) was measured using a Warner Instruments® EC-825A epithelial voltage clamp (Serial nr 211) every 20 min (Figure 3.6) to ensure membrane integrity was maintained and/or to register any effects on tight junctions by the disintegrants.

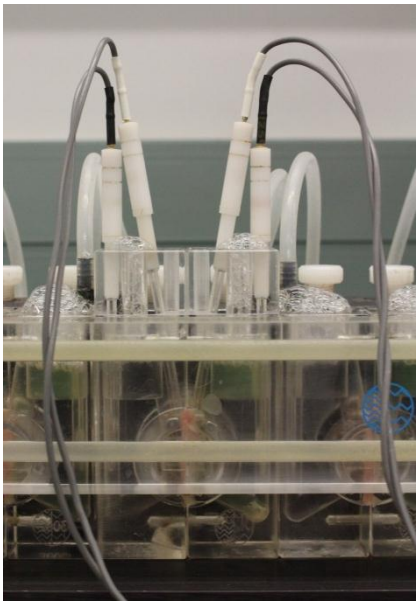

Figure 3.6: Image illustrating electrodes connected to a Sweetana-Grass diffusion chamber to measure trans-epithelial electrical resistance (TEER)

3.4.3 Transport studies using the Sweetana-Grass diffusion apparatus technique

All transport studies on R123 were conducted in triplicate in two directions (i.e. apical-to-basolateral [A-B] direction and basolateral-to-apical [B-A] direction) across the excised pig intestinal tissue. Both sides of the diffusion chamber were filled with 7 ml KRB for 15 min to allow the tissue to acclimatise in the new environment. The 7 ml KRB was then removed from the donor chamber and the tissue was incubated with a R123 solution (5 µM) in the presence (experimental solutions) and absence (control group) of the disintegrant solutions of the same volume. Samples of 180 µl were taken from the acceptor chamber at 20 min intervals over a total time of 2 h. Each withdrawn sample was replaced with an equal volume of freshly prepared and pre-heated KRB (transport in the A-B direction) or the disintegrant solution (transport in the B-A direction).

3.4.4 Analysis of test samples

The R123 concentration in each of the transport samples was determined by a validated fluorescence spectroscopic method using a Spectramax Paradigm® (Serial nr 33270-1142) multi-mode detection platform plate reader.

3.5 Data processing and statistical analysis

3.5.1 Percentage transport (% Transport)

The percentage transport of each sample was calculated at each time interval (Equation 3) after correction for dilution and was expressed as cumulative drug transport values (percentage of initial dose). The resultant values were then plotted on a percentage transport versus time curve for each individual study.

$$\% \text{ Transport} = \frac{\text{Mean value at specific time}}{\text{Mean value of donor solution}} \times 100 \qquad \text{(Eq. 3)}$$

3.5.2 Apparent permeability coefficient (P_{app})

The apparent permeability coefficient (P_{app}) is used to collectively describe the sum of passive and carrier-mediated transport across a membrane normalized for absorption surface and concentration applied without considering the effects of the aqueous boundary layer and paracellular transport (Sugano *et al.*, 2010:610).

The P_{app} values for R123 in the absence and presence of the selected disintegrants were calculated using Equation 4:

$$P_{app} = \frac{dQ}{dt}\left(\frac{1}{A.60.C_0}\right) \qquad \text{(Eq. 4)}$$

Where P_{app} is the apparent permeability coefficient ($cm \cdot s^{-1}$), $\frac{dQ}{dt}$ is the permeability rate (amount permeated per minute), A is the diffusion area of the membrane (cm^2) and C_0 is the initial concentration of R123 (Legen *et al.*, 2005:186).

3.5.3 Efflux ratio (ER)

The efflux ratio (ER) was calculated using equation 5 to obtain a ratio which indicates the extent to which R123 undergoes efflux.

$$ER = \frac{P_{app}\ (B\text{-}A)}{P_{app}\ (A\text{-}B)} \qquad \text{(Eq. 5)}$$

Where P_{app} (B-A) is the permeability coefficient for the permeation in the basolateral to the apical direction and P_{app} (A-B) the same variable in the apical to basolateral direction.

3.5.4 Statistical analysis of results

Statistical analysis was performed on experimental data obtained from bi-directional transport data. Analysis of variance (ANOVA) was performed to determine any statistically significant differences in P_{app} values between the control groups (R123 alone) and experimental (disintegrant containing) groups in both directions. The Dunnett's t-test and the Kruskal-Wallis test were post-hoc tests used to analyse non-parametric data. Data was deemed statistically significant if $p \leq 0.05$.

CHAPTER 4: RESULTS AND DISCUSSION

4.1 Introduction

Transport studies were conducted to determine the effect of five selected disintegrants on the bi-directional transport of Rhodamine 123 (R123) across excised pig intestinal jejunum. All studies were conducted in triplicate using a Sweetana-Grass diffusion apparatus and expressed as cumulative transport over a period of 2 h. Apparent permeability coefficient (P_{app}) values of R123 were calculated from percentage transport curves in the presence and absence of selected disintegrants and expressed as an average together with the standard deviation of the three experiments. Furthermore, all P_{app} values were statistically analysed and compared to the control group in both transport directions, i.e. R123 alone in the apical-to-basolateral (A-B) and basolateral-to-apical (B-A) direction, respectively. Efflux ratio (ER) values and effect on trans-epithelial electrical resistance (TEER) were also calculated to bring all the possible transport mechanisms that could be affected into context with each other.

Successful experimental outcomes are dependent on the capability of the analytical method to accurately and consistently analyse samples generated from the experimental method. Validation of any analytical method should therefore be conducted first in order to portray compliance with all the necessary validation parameters.

4.2 Fluorescence spectrometry method validation

Analysis of the R123 content in all transport samples was done by means of fluorescence spectrometry, which was performed with a Spectramax Paradigm® plate reader with the excitation and emission wavelengths set at 480 nm and 520 nm, respectively (Kaprelyants & Kell, 1992:412; Wang *et al.*, 2009:3). Validity of the analysis method was ensured by determining linearity, limit of detection, limit of quantification, accuracy, precision and specificity.

4.2.1 Linearity

As described in Chapter 3, linearity was determined on a standard curve after analysis of a series of R123 concentrations (Table 4.1). The regression curve obtained where fluorescent values were plotted as a function of R123 concentration is shown in Figure 4.1.

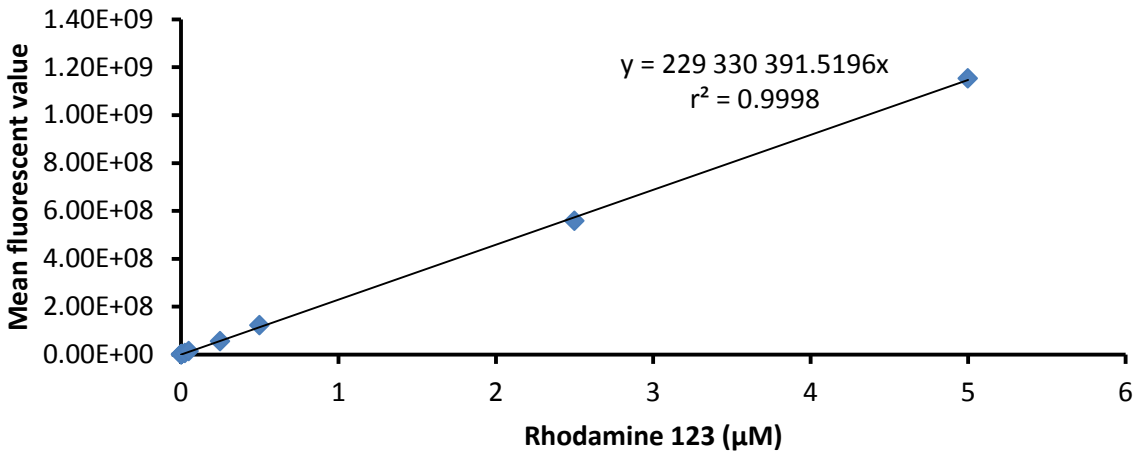

Figure 4.1: Linear regression curve of Rhodamine 123 shown with the straight line equation and correlation coefficient (r^2)

Table 4.1: Mean fluorescent values of Rhodamine 123 over a specified concentration range

R123 concentration (µM)	Mean fluorescent value
0.0005	433097
0.0025	963073
0.005	1940977.2500
0.025	6298660
0.05	13526329.5000
0.25	55634348.5000
0.5	122319631.5000
2.5	558466059.5000
5	1153376940
Slope	229330391.5196
r^2	0.9998

From Figure 4.1 and Table 4.1, it is clear that the analytical method did meet the proposed criterium for a correlation coefficient (r^2) value of > 0.999 as stated in the literature (Shabir, 2003:64; Singh, 2013:29).

4.2.2 Limit of detection and limit of quantification

The limit of detection (LOD) and limit of quantification (LOQ) were mathematically determined using the standard deviation of the blanks (i.e. the noise as shown in Table 4.2) and the slope of the regression curve (Figure 4.1 and Table 4.1).

Table 4.2: Background noise (fluorescent values of the blanks) and standard deviation of the blanks

Background noise	Average	Standard deviation
160275	170228.500	11084.829
159418		
197082		
172981		
165845		
171170		
168885		
166172		

The LOD was calculated (as discussed in section 3.3.2) to be 1.60 x 10^{-4} µM and the LOQ to be 4.83 x 10^{-4} µM for R123 using this analytical method. Concentrations of R123 used in experiments were higher than the LOD and LOQ and thus indicates the analytical method were able to detect and quantify R123 accurately in the concentrations obtained in the transport experiments.

4.2.3 Accuracy

Table 4.3 shows that the accuracy (% recovery) of the analytical method was satisfactory for all three concentrations of R123 and complied with the specification of 100 ± 2% recovery as recommended in the literature (Shabir, 2003:61).

Table 4.3: Data obtained from sample analysis to determine accuracy across a selected concentration range

Theoretical concentration (µM)	**5**	**2.5**	**0.125**
Fluorescent values	1132599564	561839883.500	29988431.500
	1144131596	573806539.500	29070773.500
	1109870604	560227275.500	28737417.500
	1120979724	573634251.500	29594415.500
	1141132556	569021195.500	28714197.500
	1204865292	571057355.500	28850937.500
Average fluorescent values	1142263222	568264416.800	29159362.170
Actual concentration (µM)	4.981	2.478	0.127
Accuracy (% recovery)	99.617	99.117	101.720

4.2.4 Precision

4.2.4.1 Intra-day precision

Table 4.4 shows a summary of standard deviation and percentage relative standard deviation (%RSD) values obtained from the three R123 concentrations (i.e. 5 µM, 2.5 µM and 0.125 µM) analysed to determine intra-day precision.

Table 4.4: Data obtained for intra-day precision of Rhodamine 123

Concentration (µM)	Repeat	Mean fluorescent value	Standard deviation	%RSD
5	1	1142263222	21860317.62	1.69
	2	1377161449		
	3	1336923222		
2.5	1	568264416.80	8911704.35	1.52
	2	608115928		
	3	583749043.40		
0.125	1	29159362.17	370256.35	1.22
	2	31286167.38		
	3	30540887.61		

It is clear from Table 4.4 that the analytical method complied with the precision standards as stated by the literature and that all RSD values were < 2% (Shabir, 2003:62).

4.2.4.2 Inter-day precision

Inter-day precision of the analytical method complied with the recommended accepted %RSD of < 2% (Shabir, 2003:62), as can be seen in Table 4.5. The average fluorescent values of each concentration (i.e. 5 µM, 2.5 µM and 0.125 µM) were calculated from values obtained on each day and used to calculate the standard deviation and the resultant %RSD.

Table 4.5: Data obtained for inter-day precision of Rhodamine 123

Concentration (µM)	Day	Mean fluorescent value	Standard deviation	%RSD
5	1	1292608602	20338899.66	1.55
	2	1327986228		
	3	1358933318		
2.5	1	586709796.10	10027076.09	1.68
	2	605204358.60		
	3	611918144.60		
0.125	1	30339967.92	379216.82	1.24
	2	31088272.32		
	3	30301176.34		

4.2.5 Specificity

Specificity of the analytical method used for R123 analyses in the presence of selected disintegrants was determined and the required accuracy of 100 ± 2% (Shabir, 2003:61; USP-NF, 2016b) recovery of R123 was achieved in the presence of all disintegrants. Table 4.6 depicts the concentrations and percentage accuracy of R123 achieved during the specificity validation when analysed alone and in the presence of disintegrants.

Table 4.6: Summary of specificity validation

Mixture	Theoretical concentration (µM)	Mean fluorescent value	Actual concentration (µM)	Accuracy (%)
Rhodamine 123 alone	5	881625406.10	4.98	99.65
Ac-di-sol®	4.98	872392450.60	4.93	98.95
Avicel® PH-200	4.98	869837730.60	4.92	98.66
Explotab®	4.98	872473618.60	4.93	98.96
Kollidon® CL-M	4.98	882121359.60	4.99	100.06
Sodium alginate	4.98	862633378.60	4.88	97.85

4.2.6 Summary of validation results

From all the data obtained for each individual validation test as shown above, it was found that the analysis method for R123 using the Spectramax Paradigm® plate reader complied with all validation criteria.

4.3 Transport studies

Bi-directional transport studies were conducted on selected disintegrants at four different concentrations each (Table 3.1). R123, a known P-gp substrate (Crawford & Putnam, 2014:1462; Zhao *et al.*, 2016:1527), was used as a model compound at a concentration of 5 µM to evaluate bi-directional transport across excised pig intestinal tissue. The collected transport samples were corrected for dilution and the apparent permeability coefficient (P_{app}) values for R123 were calculated for each transport study. Statistical analysis of the data was performed using Dunnett's t-test and a Kruskal Wallis post-hoc test on P_{app} values.

4.3.1 Croscarmellose sodium (Ac-di-sol®)

Croscarmellose sodium, commercially available as Ac-di-sol®, is a superdisintegrant and its transport altering effects were studied at concentrations of 0.0005% (w/v), 0.001% (w/v), 0.005% (w/v) and 0.01% (w/v). All transport studies were conducted in triplicate. Figure 4.2 shows the average percentage transport of R123 in the apical-to-basolateral (A-B) direction, while Figure 4.3 depicts the transport in the basolateral-to-apical (B-A) direction over a period of 2 h for each concentration.

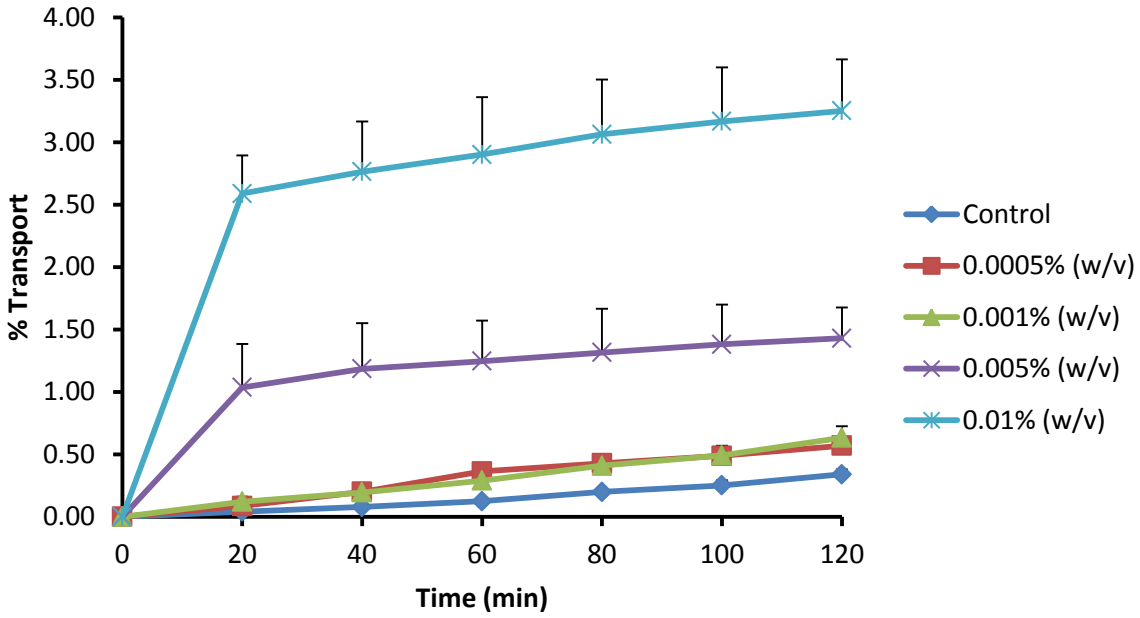

Figure 4.2: Apical-to-basolateral percentage transport of Rhodamine 123 in the presence of croscarmellose sodium (Ac-di-sol®) across excised pig jejunum plotted as a function of time

Ac-di-sol® mediated a concentration dependent increase in transport of R123 in the A-B direction. The two lower concentrations (0.0005% (w/v) and 0.001% (w/v)) of Ac-di-sol® did not show a pronounced difference in R123 transport when compared with each other. However, these two concentrations virtually doubled the percentage transport of R123 when compared to the control (R123 alone). Ac-di-sol® at a concentration of 0.005% (w/v) increased transport of R123 approximately 4-fold, whereas 0.01% (w/v) increased R123 transport by approximately 9.5-fold relative to the control. Furthermore, with reference to a study conducted by Takizawa, Kitazato, *et al.* (2013:33) and taking the measured decrease in trans-epithelial electrical resistance (TEER) into account (discussed in section 4.5, Table 4.8), we may attribute the large concentration dependent increase in R123 transport by Ac-di-sol® partly to the opening of tight junctions, which improved the paracellular transport of R123.

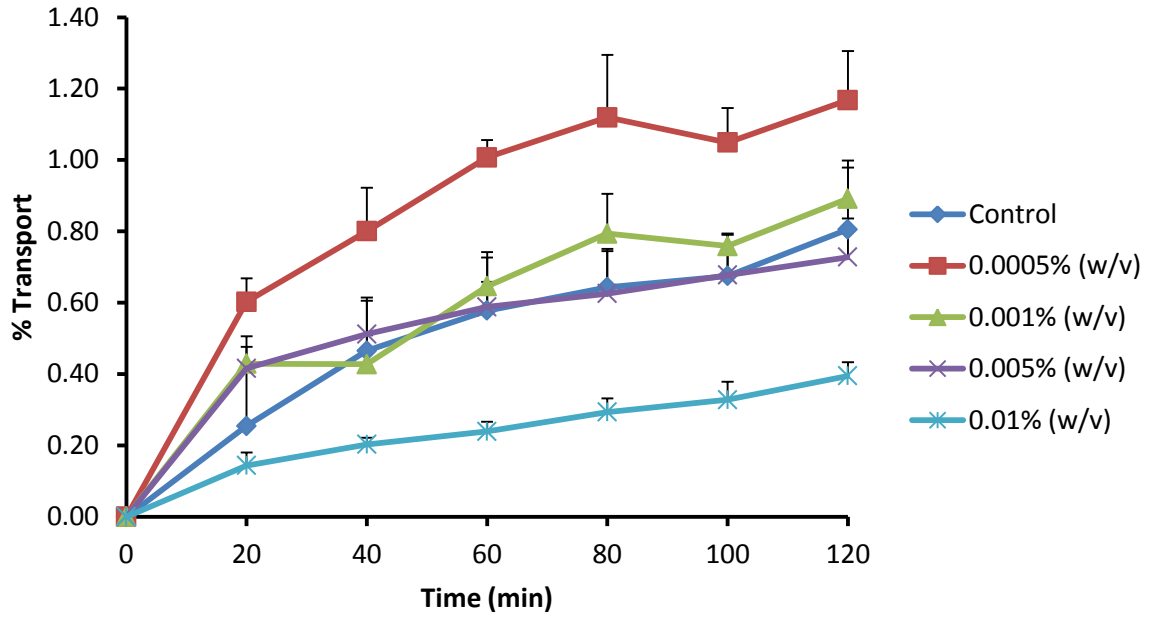

Figure 4.3: Basolateral-to-apical percentage transport of Rhodamine 123 in the presence of croscarmellose sodium (Ac-di-sol®) across excised pig jejunum plotted as a function of time

Figure 4.3 shows that the percentage transport of the R123 alone (control group) in the B-A (secretory) direction was more than double that of the transport in the A-B (absorptive) direction. This finding confirms that R123 is a P-gp substrate and that it is highly susceptible to efflux. Furthermore, even though transport of R123 in the presence of Ac-di-sol® at concentrations of 0.0005% (w/v) and 0.001% (w/v) were slightly higher than that of the control, there was an apparent concentration dependent decrease in R123 transport as the concentration of Ac-di-sol® had increased. The increase in R123 transport at the lower two Ac-di-sol® concentrations relative to the control may be explained by a reduction in TEER (Table 4.8), which is an indication of tight junction modulation (i.e. opening of tight junctions) that may have caused an increase in paracellular transport of R123. Therefore, this study proved that different transport routes for R123 were modulated by Ac-di-sol®, but did not determine to which extent R123 moved via each transport route.

A summary of the P_{app} values are given in Figure 4.4 and the data shows that Ac-di-sol® inhibits efflux and thereby also secretory transport in a concentration dependent manner and subsequently enhances uptake transport. The efflux ratio values and possible transport mechanisms involved in the transport modulation are discussed in section 4.4. Statistically significant modulation of R123 transport by Ac-di-sol® was observed at concentrations of

0.005% (w/v) and 0.01% (w/v) in the absorptive direction and 0.0005% (w/v) and 0.01% (w/v) in the secretory direction.

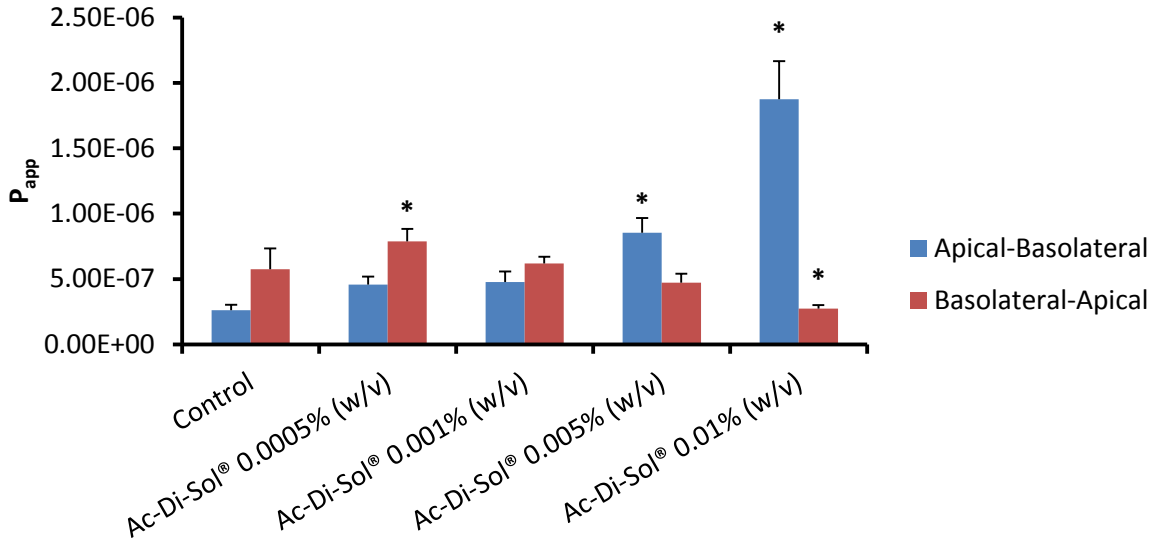

Figure 4.4: Average P_{app} values for bi-directional transport of Rhodamine 123 in the presence of croscarmellose sodium (Ac-di-sol®) across excised pig jejunum (*statistically significant differences compared to the control, $p \leq 0.05$)

4.3.2 Microcrystalline cellulose (Avicel® PH-200)

Avicel® PH-200 is a multifunctional excipient which consists of large particles (approximately 180 µm) and is virtually insoluble in water (Galichet, 2005:132,134). Concentrations of 0.005% (w/v), 0.01% (w/v), 0.015% (w/v) and 0.03% (w/v) were studied in triplicate and bi-directionally to determine any effects Avicel® PH-200 may have had on R123 transport. Figure 4.5 shows the average R123 transport in the A-B direction, while B-A transport results of R123 are shown in Figure 4.6.

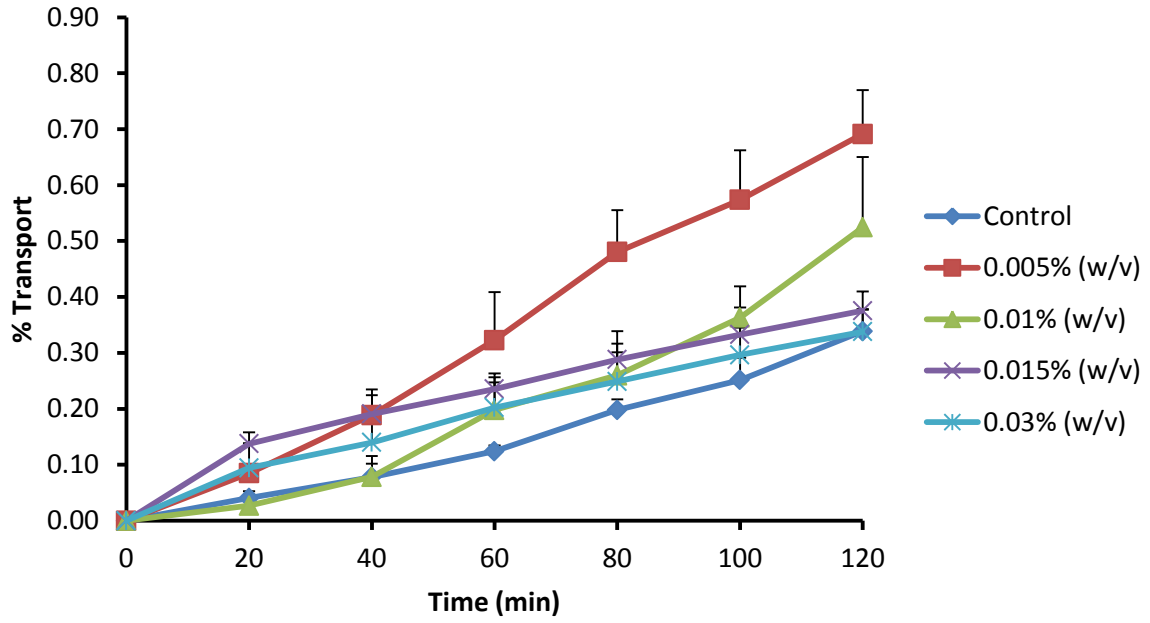

Figure 4.5: Apical-to-basolateral percentage transport of Rhodamine 123 in the presence of microcrystalline cellulose (Avicel® PH-200) across excised pig jejunum plotted as a function of time

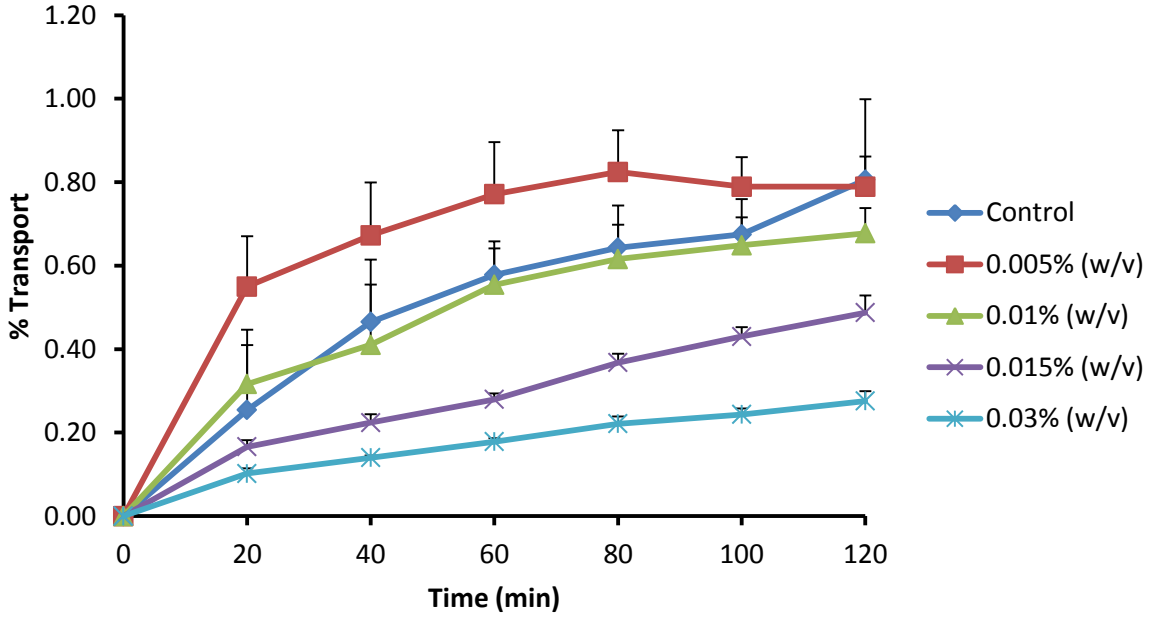

Figure 4.6: Basolateral-to-apical percentage transport of Rhodamine 123 in the presence of microcrystalline cellulose (Avicel® PH-200) across excised pig jejunum plotted as a function of time

Figures 4.5 and 4.6 show that Avicel® PH-200 mediated an increase in R123 absorptive (A-B) transport and a decrease in transport of R123 in the secretory direction (B-A) when compared to the control. This may be attributed to the inhibition of efflux when compared to the control group. However, the absorptive transport enhancement effect decreased with an increase in concentration of Avicel® PH-200, while the extent of efflux inhibition increased with Avicel® PH-200 concentration in the secretory direction. The concentration dependent decrease in absorptive transport enhancement can potentially be explained by physical or chemical interactions between R123 and Avicel® PH-200.

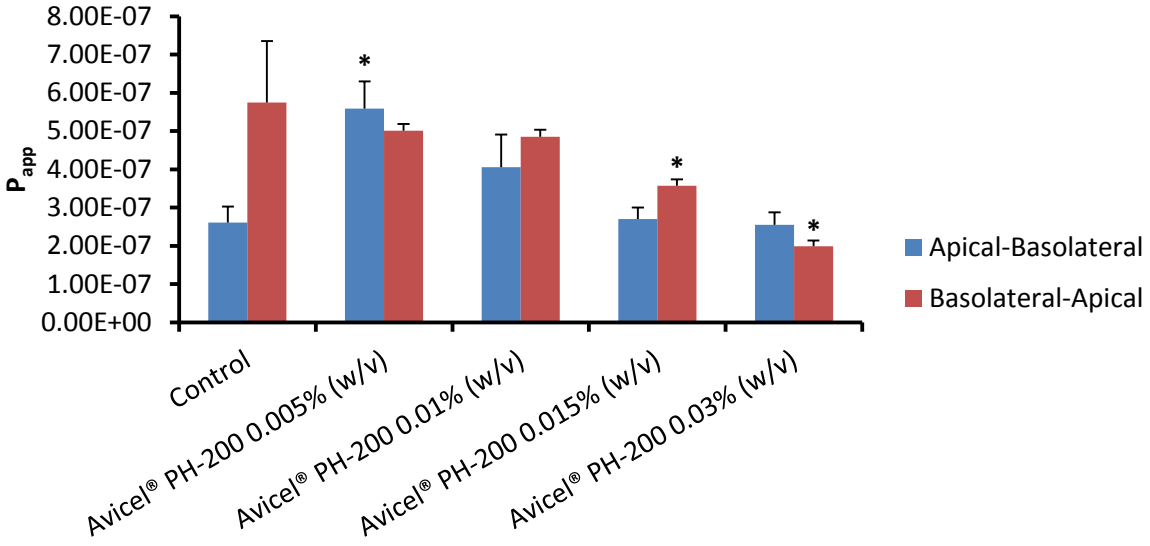

Figure 4.7: Average P_{app} values for bi-directional transport of Rhodamine 123 in the presence of microcrystalline cellulose (Avicel® PH-200) across excised pig jejunum (*statistically significant differences compared to the control, $p \leq 0.05$)

The large size and relative insoluble nature of Avicel® PH-200 particles may have led to aggregation of the particles while being suspended in the aqueous Krebs-Ringer bicarbonate buffer solution. These aggregates could possibly have caused mechanical entrapment of R123 molecules or may have formed intermolecular bonds with R123 molecules. Molecular entrapment of R123, in the presence of surfactants, has recently been reported where R123 was incorporated into micelles whenever concentrations surpassed the critical micelle concentration (Zhao *et al.*, 2016:1532). Furthermore, if any intermolecular bonds had formed between Avicel® PH-200 particles and R123 molecules, the resultant molecule complex would be too large to cross the biological membrane and less R123 would be detectable on the acceptor side. However, this explanation is only applicable to the absorptive transport of R123 due to the fact that the disintegrant and the model compound were both incubated on

the apical side of the excised intestinal tissue sheet. Figure 4.7 shows that Avicel® PH-200 had mediated a statistically significant increase in R123 transport in the A-B direction when applied in a concentration of 0.005% (w/v). The possibility exists that Avicel® PH-200 reached a critical concentration where there were enough particles in the suspension to initiate interactions with R123, as discussed earlier, which may have led to the decreased absorption enhancement effect.

During the B-A transport studies, disintegrants were incubated on the apical side and R123 on the basolateral side of the excised intestinal tissue sheet. Figure 4.7 shows a concentration dependent decrease in P_{app} in the secretory direction when compared to the control group. Inhibition of R123 efflux explains this phenomenon. Secretory transport of R123 in the presence of Avicel® PH-200 at concentrations of 0.015% (w/v) and 0.03% (w/v) was inhibited to such an extent that P_{app} values were statistically significantly different from the control.

4.3.3 Sodium starch glycolate (Explotab®)

Explotab® is a superdisintegrant that mediates disintegration of solid oral dosage forms via a swelling mechanism. It is known to swell up to 300 times its own volume and can form a highly hydrated gel layer in cold water at concentrations of approximately 2% w/v (Edge & Miller, 2005:702). Explotab® in concentrations of 0.002% (w/v), 0.004% (w/v), 0.008% (w/v) and 0.016% (w/v) were used in bi-directional transport studies of R123 as model compound. The percentage A-B transport of R123 as a function of time in the presence of Explotab® is shown in Figure 4.8, while the B-A transport is shown in Figure 4.9.

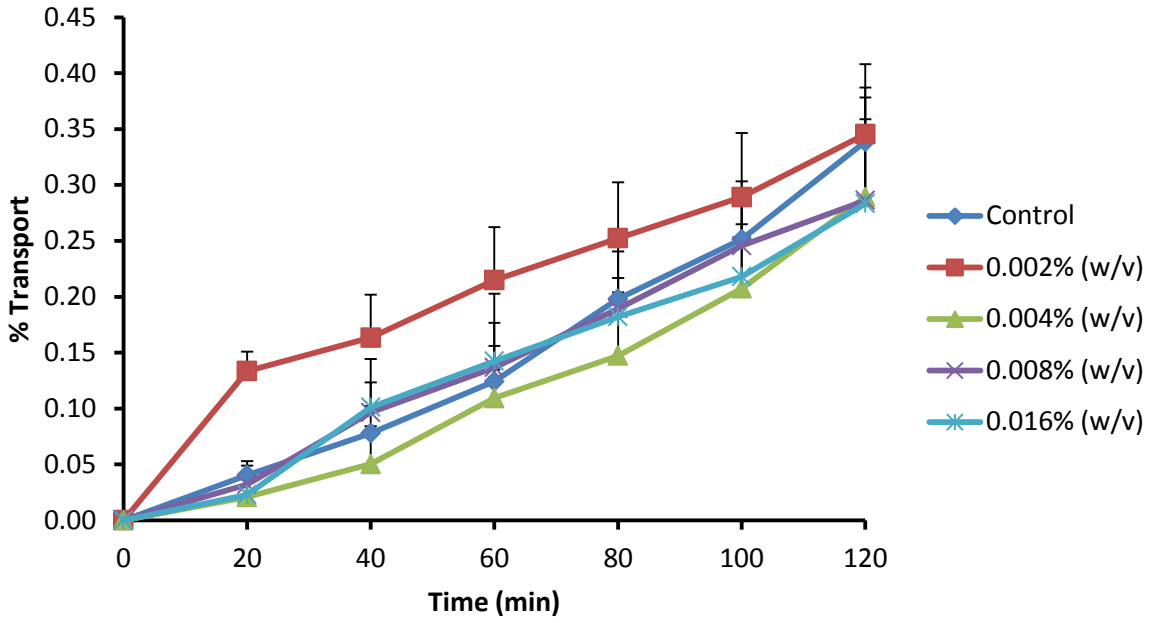

Figure 4.8: Apical-to-basolateral percentage transport of Rhodamine 123 in the presence of sodium starch glycolate (Explotab®) across excised pig jejunum plotted as a function of time

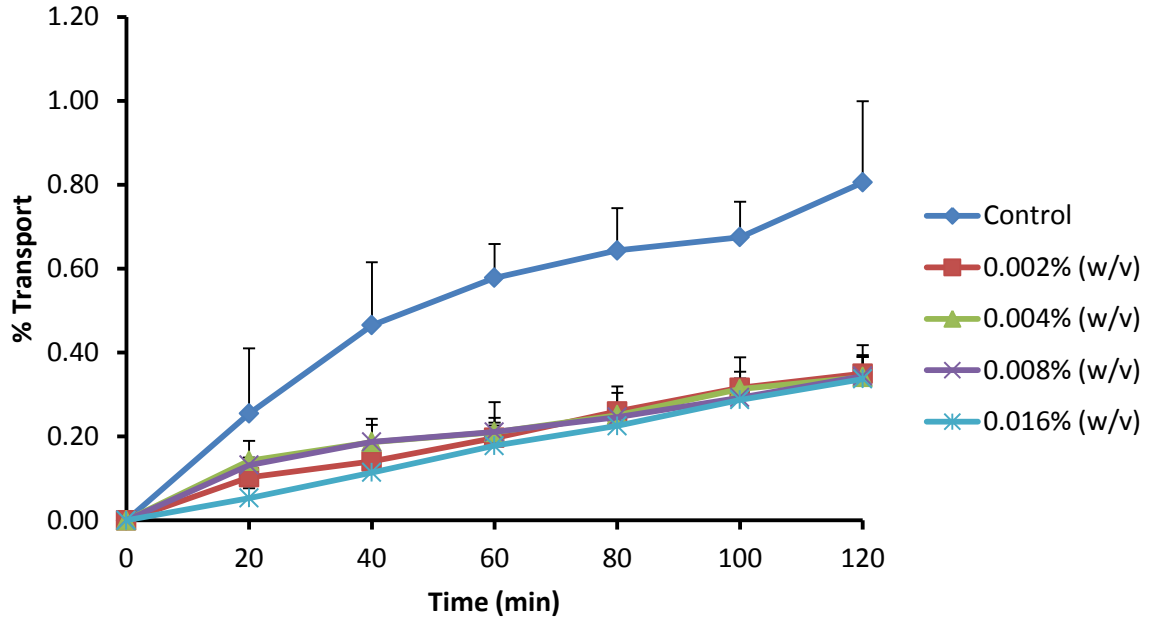

Figure 4.9: Basolateral-to-apical percentage transport of Rhodamine 123 in the presence of sodium starch glycolate (Explotab®) across excised pig jejunum plotted as a function of time

In both the absorptive and secretory directions, transport of R123 in the presence of Explotab® was restricted to approximately 0.3% of the initial concentration of 5 µM (Figures 4.8 and 4.9). The physico-chemical properties of Explotab® can be used to explain the effect on the bi-directional transport of R123 across the intestinal tissue. As mentioned earlier, Explotab® is known to form a highly hydrated stagnant gel layer. If such stagnant layer had formed on the membrane, the diffusion distance would increase according to Fick's 1st law of diffusion and the diffusion rate of R123 would decrease over the same period of time. Furthermore, formation of a highly viscous layer (due to Explotab's® excellent swelling capabilities) would have impeded R123 molecules to cross the excised tissue sheet. Figure 4.10 shows that the P_{app} values for R123 in the presence of Explotab® remained constant at approximately 2.40 x 10^{-7} cm/s in both directions, which is indicative of restricted membrane permeation of R123. Although Explotab® was applied to the apical side while R123 was applied to the basolateral side during the B-A transport study, the formation of a stagnant layer on the apical side of the excised tissue sheet may still have impeded R123 molecules to reach the acceptor chamber, as it would have in the A-B study when both R123 and Explotab® were both incubated on the apical side.

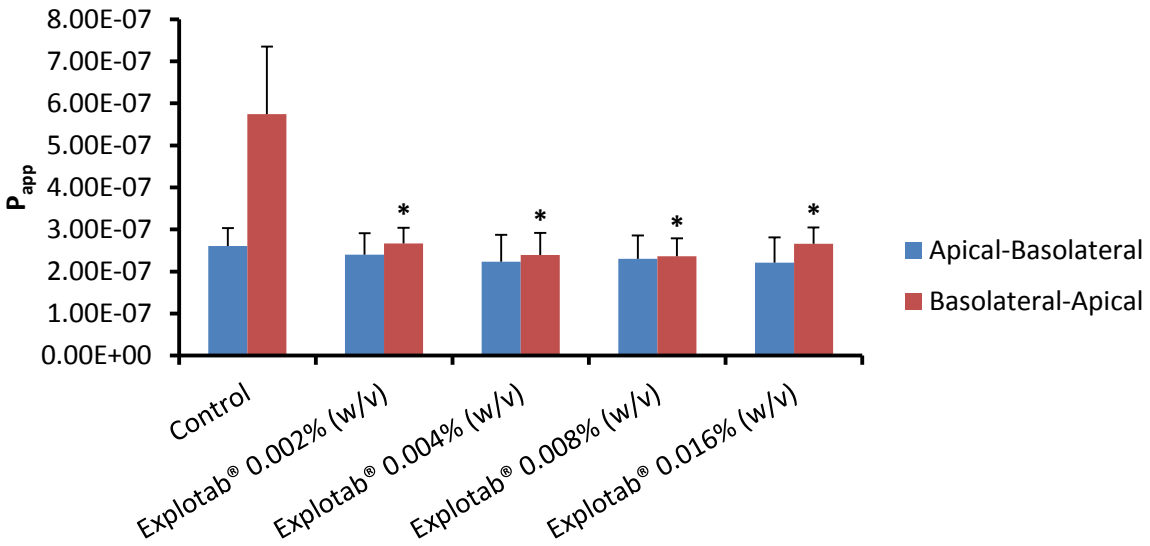

Figure 4.10: Average P_{app} values for bi-directional transport of Rhodamine 123 in the presence of sodium starch glycolate (Explotab®) across excised pig jejunum (*statistically significant differences compared to the control, $p \leq 0.05$)

An overall average increase in TEER readings (Table 4.8) indicates a decrease in ion transport across the biological membrane. If Explotab® formed a layer on the biological membrane that increased the diffusion distance or viscosity of the stagnant layer, ions would have had increased difficulty passing through the membrane. Increased TEER values

therefore serve as an additional explanation for possible effects Explotab® had on the transport results of R123.

4.3.4 Crospovidone (Kollidon® CL-M)

Kollidon® CL-M yielded a concentration dependent increase in R123 transport in the absorptive direction (Figure 4.11), while simultaneously causing a concentration dependent decrease in R123 transport in the secretory direction (Figure 4.12). For A-B studies, Kollidon® CL-M increased R123 transport as much as 2.5-fold, whereas secretory transport studies saw Kollidon® CL-M decreasing R123 transport to a total of almost 5-fold compared to the control.

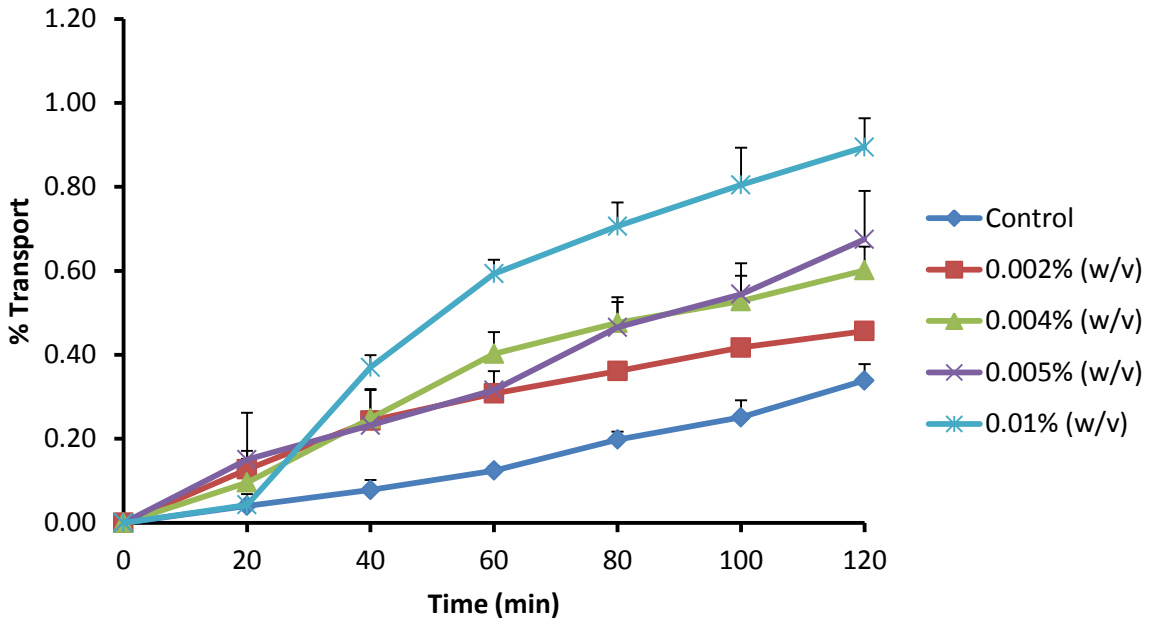

Figure 4.11: Apical-to-basolateral percentage transport of Rhodamine 123 in the presence of crospovidone (Kollidon® CL-M) across excised pig jejunum plotted as a function of time

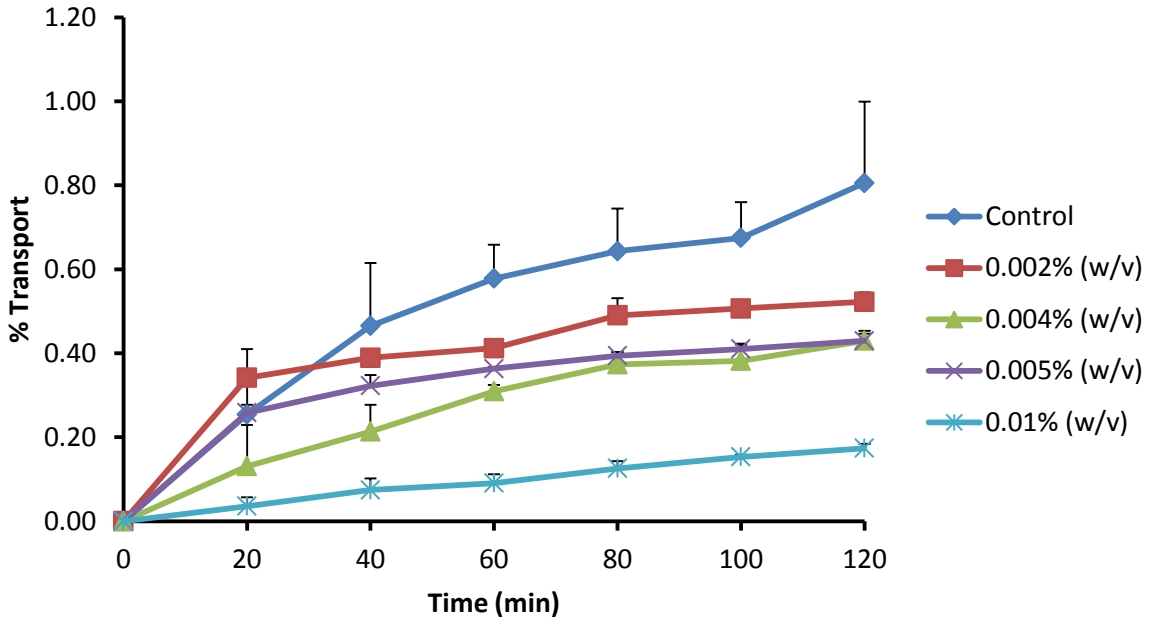

Figure 4.12: Basolateral-to-apical percentage transport of Rhodamine 123 in the presence of crospovidone (Kollidon® CL-M) across excised pig jejunum plotted as a function of time

P_{app} values obtained for R123 in the presence of Kollidon® CL-M (Figure 4.13) indicated that Kollidon® CL-M is a concentration dependent efflux pump inhibitor and statistically significant interactions occurred at all concentrations in the secretory transport of R123. The only statistically significant interaction in the absorptive transport of R123 occurred at a concentration of 0.01% (w/v) Kollidon® CL-M. As an increase and decrease in TEER values indicate closing and opening of tight junctions respectively, the contribution of tight junction modulation to the resultant paracellular transport of R123 may have been negligibly small when considering the change in TEER values at all concentrations tested (Table 4.8). For all of the tested Kollidon® CL-M concentrations, the P_{app} values were found to be lower in the secretory direction than in the absorptive direction, which suggests that the transport enhancement effect on R123 had only taken place by means of inhibition of efflux transporters. The calculated efflux ratios are discussed in more detail in section 4.4.

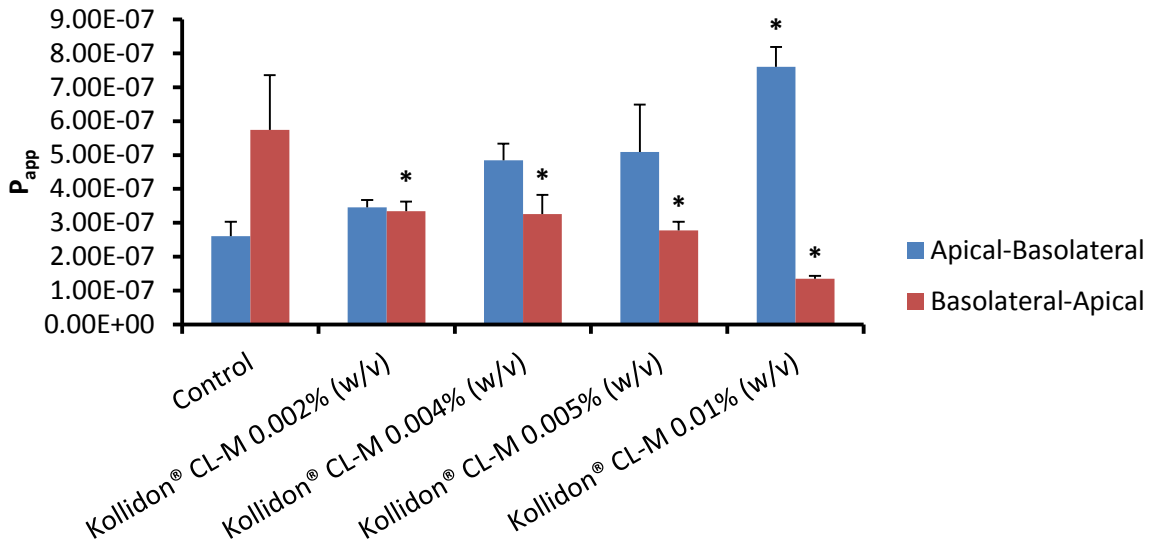

Figure 4.13: Average P_{app} values for bi-directional transport of Rhodamine 123 in the presence of crospovidone (Kollidon® CL-M) across excised pig jejunum (*statistically significant differences compared to the control, $p \leq 0.05$)

4.3.5 Sodium alginate

Sodium alginate is a multi-functional excipient, which is utilised as a tablet disintegrant at quantities ranging from 2.5% - 10% (w/w) in tablet formulations (Cable, 2005:656). Four concentrations of this disintegrant (i.e 0.0025% (w/v), 0.005% (w/v), 0.01% (w/v) and 0.02% (w/v)) were employed in bi-directional transport studies of R123. The percentage transport of R123 in the A-B direction in the presence of sodium alginate plotted as a function of time is shown in Figure 4.14, while the transport in the B-A direction is shown in Figure 4.15.

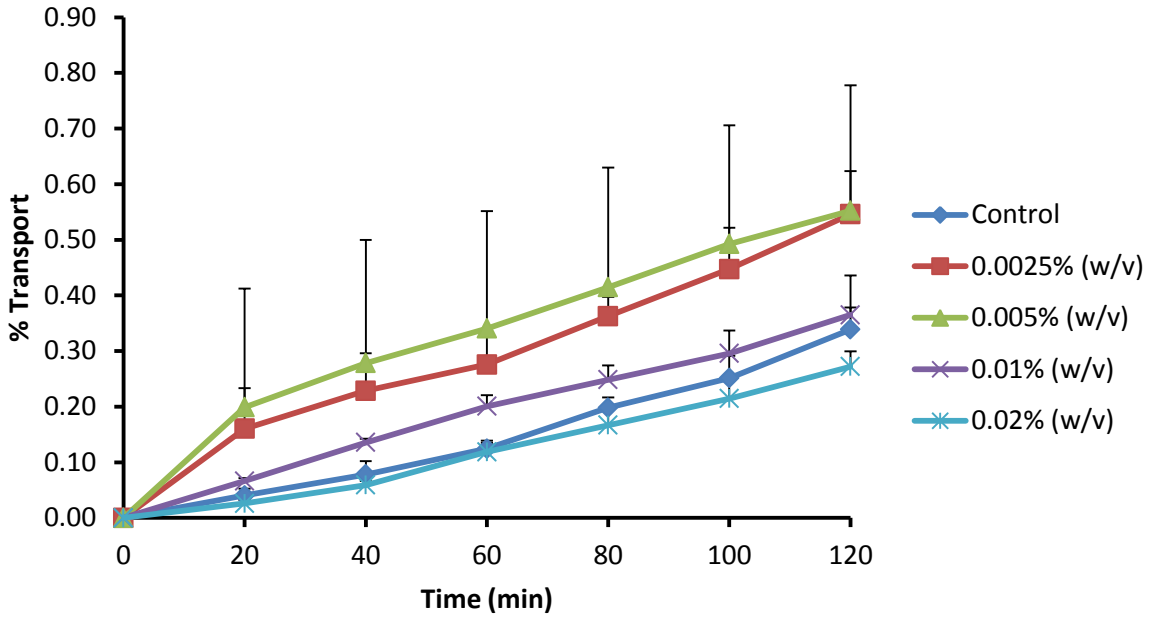

Figure 4.14: Apical-to-basolateral percentage transport of Rhodamine 123 in the presence of sodium alginate across excised pig jejunum plotted as a function of time

From Figure 4.14, it is evident that sodium alginate at concentrations of 0.0025% (w/v), 0.005% (w/v) and 0.01% (w/v) had mediated an increase in the percentage transport of R123 in the absorptive direction with regards to the control. However, inhibition of R123 transport took place at the highest sodium alginate concentration (0.02% (w/v)), to less than that of the control group. The lower three concentrations of sodium alginate that presented with transport higher than that of the control may indicate that other possible transport mechanisms for R123 may be affected in the presence of sodium alginate.

Figure 4.15 shows that sodium alginate caused a decrease in the percentage transport of R123 in the secretory direction with regards to the control, which correlates well with the transport trends of R123 in the absorptive direction.

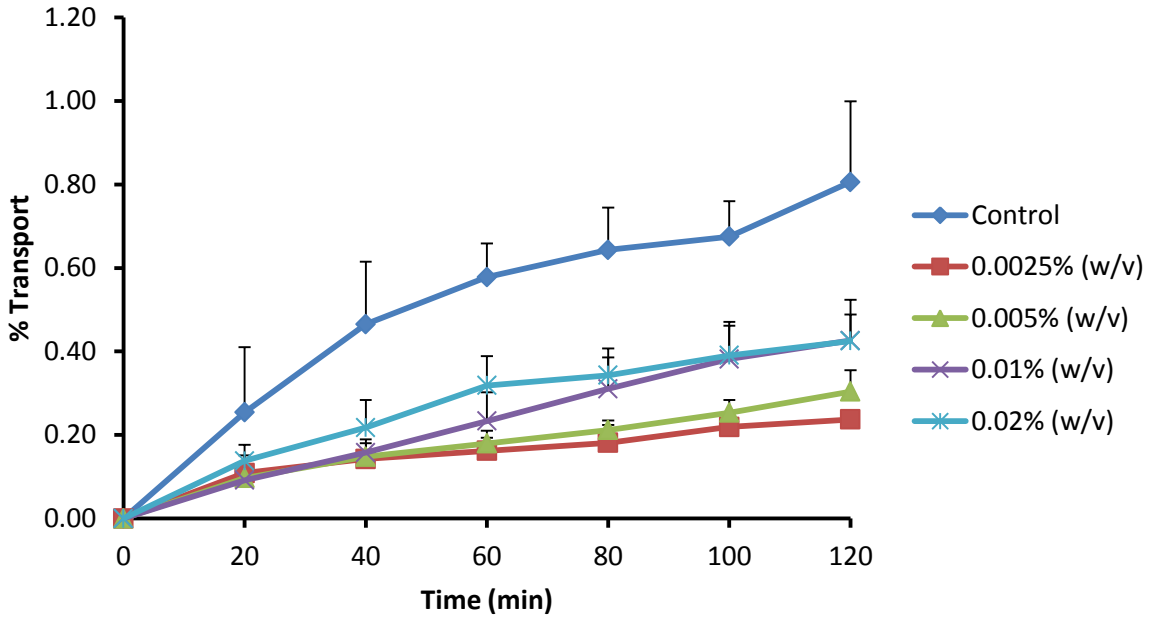

Figure 4.15: Basolateral-to-apical percentage transport of Rhodamine 123 in the presence of sodium alginate across excised pig jejunum plotted as a function of time

Figure 4.16 indicates absorptive transport of R123 increased slighty and the secretory transport decreased. However, the summarised data in Table 4.8 shows a concentration dependent increase in the TEER values which indicate that the tight junctions had progressively closed more tightly at higher sodium alginate concentrations which in turn reduced the paracellular transport of R123. Paracellular transport of R123 has already been reported (Takizawa, Kitazato, *et al.*, 2013:33). Taking the progressive increase in TEER differences and resultant tighter tight junctions into account, one can deduce that R123 could show a higher affinity for efflux transport if it is not capable of moving via the paracellular pathway. The apparent induction of efflux transport at higher sodium alginate concentrations (shown in Figure 4.16 and later discussed in section 4.4) was however still lower than that of the control group, which indicates that full inhibition of paracellular transport did not take place initially, but only to a certain extent. Furthermore, the two lower concentrations of sodium alginate (0.0025% (w/v) and 0.005% (w/v)) had seemingly inhibited efflux while an apparent induction of efflux was evident at higher concentrations (0.01% (w/v) and 0.02% (w/v)). Therefore, the probability exist that sodium alginate reaches a certain critical concentration (approximately 0.0075% (w/v)) where it starts to inhibit the tight junctions leading to a decrease in R123 transport via the paracellular route, resulting in more R123 being transported via efflux proteins.

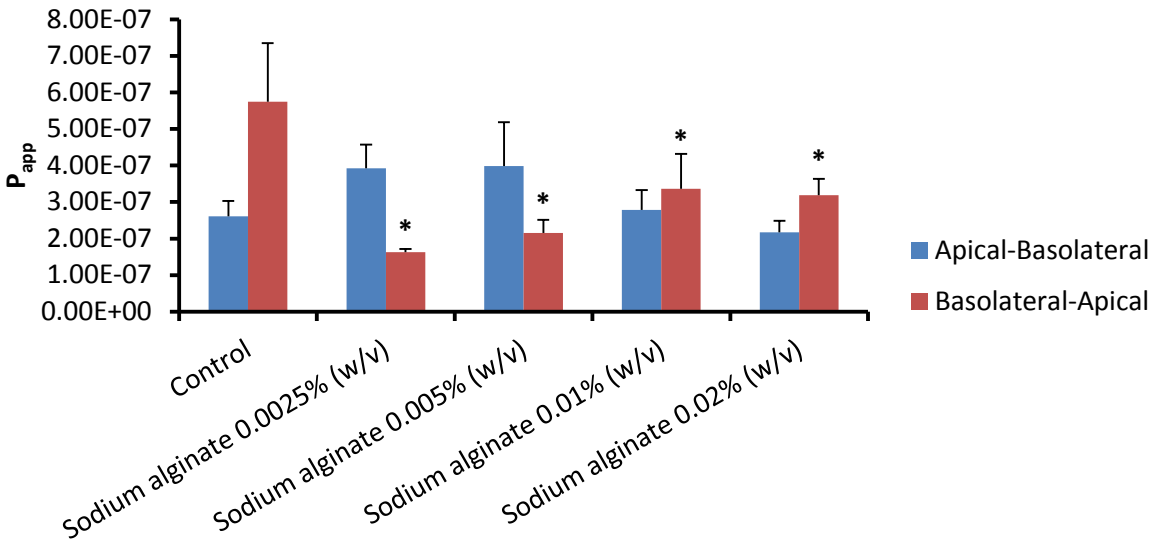

Figure 4.16: Average P_{app} values for bi-directional transport of Rhodamine 123 in the presence of sodium alginate across excised pig jejunum (*statistically significant differences compared to the control, $p \leq 0.05$)

Further evaluation of the effects of sodium alginate on different transport mechanisms are required to investigate at which concentration this turning point takes place and to what extent each individual transport mechanism is affected.

4.4 Evaluation of efflux ratios

Efflux ratio (ER) values take the extent of transport in both directions into consideration to give an indication of the main transport mechanism. An ER >> 1 indicates that a compound is susceptible to active efflux transport and when ER = 1 it indicates that the compound is mainly transported by means of passive diffusion, while an ER << 1 indicates active absorptive uptake (Bock *et al.*, 2003). The ER values obtained for R123 in the presence of the selected disintegrants are shown in Table 4.7

Table 4.7: Summary of the average P_{app} values and efflux ratio (ER) values for selected disintegrants at the selected concentrations

	Control (R123 alone)			
Mean P_{app} (B-A)	5.74E-07			
Mean P_{app} (A-B)	2.61E-07			
Efflux ratio (ER)	2.20			
	Ac-di-sol®			
	0.0005 (% w/v)	**0.001 (% w/v)**	**0.005 (% w/v)**	**0.01 (% w/v)**
Mean P_{app} (B-A)	7.88E-07	6.19E-07	4.71E-07	2.75E-07
Mean P_{app} (A-B)	4.58E-07	4.77E-07	8.54E-07	1.87E-06
Efflux ratio (ER)	1.72	1.30	0.55	0.15
	Avicel® PH-200			
	0.005 (% w/v)	**0.01 (% w/v)**	**0.015 (% w/v)**	**0.03 (% w/v)**
Mean P_{app} (B-A)	5.01E-07	4.85E-07	3.57E-07	1.99E-07
Mean P_{app} (A-B)	5.59E-07	4.06E-07	2.70E-07	2.55E-07
Efflux ratio (ER)	0.90	1.20	1.32	0.78
	Explotab®			
	0.002 (% w/v)	**0.004 (% w/v)**	**0.008 (% w/v)**	**0.016 (% w/v)**
Mean P_{app} (B-A)	2.67E-07	2.39E-07	2.36E-07	2.66E-07
Mean P_{app} (A-B)	2.40E-07	2.24E-07	2.30E-07	2.21E-07
Efflux ratio (ER)	1.11	1.07	1.02	1.20
	Kollidon® CL-M			
	0.002 (% w/v)	**0.004 (% w/v)**	**0.005 (% w/v)**	**0.01 (% w/v)**
Mean P_{app} (B-A)	3.34E-07	3.26E-07	2.78E-07	1.35E-07
Mean P_{app} (A-B)	3.46E-07	4.84E-07	5.09E-07	7.60E-07
Efflux ratio (ER)	0.97	0.67	0.55	0.18
	Sodium alginate			
	0.0025 (% w/v)	**0.005 (% w/v)**	**0.01 (% w/v)**	**0.02 (% w/v)**
Mean P_{app} (B-A)	1.63E-07	2.15E-07	3.36E-07	3.19E-07
Mean P_{app} (A-B)	3.92E-07	3.98E-07	2.79E-07	2.17E-07
Efflux ratio (ER)	0.41	0.54	1.21	1.47

In the graphic representation of the efflux ratios for each individual disintegrant used in this study (Figure 4.17), the following three different trends can be identified:

Avicel® PH-200 and Explotab® showed no significant effects on efflux modulation at any of the test concentrations. Physical and/or chemical interactions between R123 and Avicel® PH-200 may serve as possible reasons that relatively low permeation of R123 occurred across the biological membrane. The lack of effect on P_{app} of Explotab® may be attributed to the possible barrier effect it has on the membrane as discussed earlier in section 4.3.3.

Ac-di-sol® and Kollidon® CL-M showed a concentration dependent inhibition of R123 efflux. It is important to consider the possibility that Ac-di-sol® might have had transport modulatory effects on transport mechanisms other than efflux (Section 4.5). This particular study, however, did not endeavor to distinguish between different transport mechanisms and mechanism based studies are warranted in future projects. It has been reported previously that P-gp may be inhibited by either blocking of the drug binding site, interfering with the ATP hydrolysis site or by altering cell membrane lipid integrity (Varma *et al.*, 2003:349). Ac-di-sol® and Kollidon® CL-M both have very large molecular weights. A probable explanation for the interaction with efflux pumps can therefore be either competitive or non-competitive receptor blocking. Furthermore, allosterical changes of the efflux pump can also be induced by the disintegrants on the drug and/or ATP binding sites.

Inhibition of paracellular transport by sodium alginate at high concentrations may have played a significant role in the transport of R123. An apparent induction of efflux (as indicated by ER values > 1) has occurred at the two highest concentrations of sodium alginate when the secretory transport is compared to the absorptive transport of R123 in this experimental group. However, the B-A transport of R123 in the presence of sodium alginate was below that of the control group at all the concentrations of sodium alginate investigated.

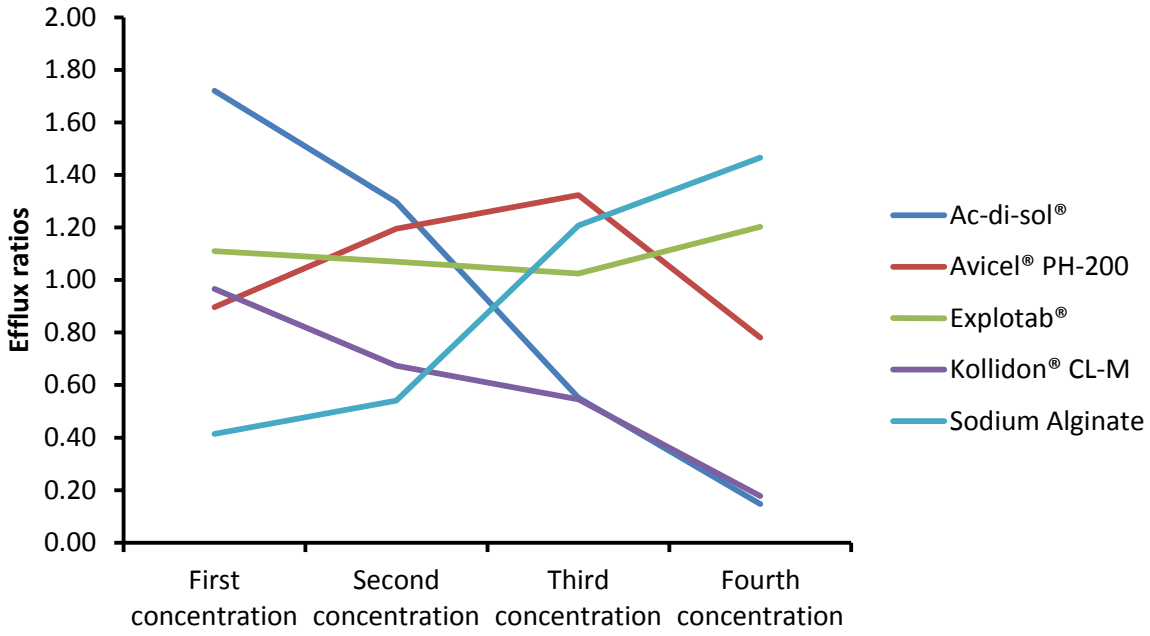

Figure 4.17: Graphic representation of the efflux ratio values of each of the selected disintegrants at each of the four selected concentrations

4.5 Comparison and evaluation of trans-epithelial electrical resistance (TEER)

Trans-epithelial electrical resistance (TEER) is the electrical resistance across a membrane measured to monitor membrane integrity and/or possible effects that any test compound may have on paracellular transport or intercellular tight junctions. Higher resistance readings indicate a denser or thicker membrane and vice versa (Alqahtani *et al.*, 2013:2-3; Sarmento *et al.*, 2012:611-613).

During this study, TEER readings were taken at 20 min intervals, and the average percentage changes in TEER were calculated between the T_0 and T_{120} readings (Table 4.8).

Table 4.8: Average percentage trans-epithelial electrical resistance (TEER) for excised tissue exposed to each selected disintegrant over a 120 min period (all values are expressed as average percentage of the initial T_0 value at T_{120})

	Ac-di-sol®			
	0.0005 (% w/v)	**0.001 (% w/v)**	**0.005 (% w/v)**	**0.01 (% w/v)**
Apical-basolateral	52.11	59.63	79.31	35.56
Basolateral-apical	57.69	44.71	78.40	45.80
	Avicel® PH-200			
	0.005 (% w/v)	**0.01 (% w/v)**	**0.015 (% w/v)**	**0.03 (% w/v)**
Apical-basolateral	71.38	93.44	64.37	77.78
Basolateral-apical	153.13	155.62	200.22	141.70
	Explotab®			
	0.002 (% w/v)	**0.004 (% w/v)**	**0.008 (% w/v)**	**0.016 (% w/v)**
Apical-basolateral	92.56	127.47	117.29	54.02
Basolateral-apical	180.16	193.76	132.70	153.11
	Kollidon® CL-M			
	0.002 (% w/v)	**0.004 (% w/v)**	**0.005 (% w/v)**	**0.01 (% w/v)**
Apical-basolateral	72.77	116.25	121.22	89.87
Basolateral-apical	103.73	110.78	141.59	106.67
	Sodium alginate			
	0.0025 (% w/v)	**0.005 (% w/v)**	**0.01 (% w/v)**	**0.02 (% w/v)**
Apical-basolateral	81.62	93.54	84.92	105.03
Basolateral-apical	58.71	85.70	124.85	131.04

From Table 4.8, it is clear that only Ac-di-sol® and sodium alginate had pronounced effects on the TEER and therefore tight junction modulation. An increase in TEER indicates tight junctions closing, while a decrease in TEER indicates opening of tight junctions. Ac-di-sol® mediated a decrease in the TEER in both directions (i.e. A-B and B-A) at all test concentrations and may explain the large increase in A-B percentage transport of R123 as mentioned earlier in section 4.3.1. It could not be determined from the data to what extent R123 will be transported via the paracellular route in the presence of Ac-di-sol®.

Sodium alginate showed a concentration dependent increase in TEER values in each direction of transport (i.e. A-B and B-A). The increase in TEER, due to the presence of

sodium alginate, together with the apparent induction of efflux (Section 4.3.5) explains the reduction in A-B transport of R123 at the highest concentration of sodium alginate.

Increased TEER readings found in the presence of Explotab® may indicate a decreased flow of ions through the biological membrane. This effect may have presented because of the possible increase in diffusion distance and/or the possible increase in diffusion layer viscosity that Explotab® might cause against the biological membrane.

4.6 Conclusion

The analytical method complied with validation specifications of linearity, selectivity, precision and accuracy. The studies conducted with R123 in the presence of Ac-di-sol® and Kollidon® CL-M showed that the disintegrants had statistically significant transport altering effects on efflux related transport mechanisms probably due to inhibition of P-gp. Furthermore, it was shown that R123 was also transported via the paracellular route in addition to being a P-gp substrate as illustrated by a reduction in transport when the TEER was increased by sodium alginate. The presence of Ac-di-sol® had shown a tendency to increase paracellular transport of R123 as a result of a reduction in TEER values. Avicel® PH-200 had an apparent inhibitory effect on P-gp, but results were inconclusive due to multi-molecular complex formation that may have occurred at higher Avicel® PH-200 concentrations. Explotab® yielded inconclusive results as its swelling properties might have interfered with trans-membrane transport by increasing the diffusion distance, thus decreasing the percentage transport and P_{app} of R123.

CHAPTER 5: FINAL CONCLUSIONS AND FUTURE RECOMMENDATIONS

5.1 Final conclusions

The evaluation of the effects of selected disintegrants on drug membrane permeation was successfully completed across excised pig intestinal tissue in the Sweetana-Grass diffusion apparatus. The study aimed to determine the effect of selected disintegrants (Ac-di-sol®, Avicel® PH-200, Explotab®, Kollidon® CL-M and sodium alginate) on the transport of a model compound (Rhodamine 123 or R123) across excised pig jejunum tissue as well as elucidate the mechanism of interaction involved (e.g. modulation of efflux transporters and/or tight junctions).

The results of the study clearly indicated that Ac-di-sol® and Kollidon® CL-M had pronounced effects on the efflux transport of R123 by concentration dependent inhibition of P-glycoprotein (P-gp). Avicel® PH-200 also exhibited a concentration dependent efflux inhibitory effect, but this effect was only visible in the basolateral-to-apical direction. Results regarding R123 transport in the apical-to-basolateral direction in the presence of Avicel® PH-200 were inconclusive and could not be fully explained due to possible intermolecular interactions between R123 and Avicel® PH-200 particles. Sodium alginate presented with a relative increase in efflux transport for each individual concentration tested, although total percentage transport of R123 was lower than that of the control group.

Both Ac-di-sol® and sodium alginate showed tight junction modulation, which directly influences paracellular transport, albeit in an opposite manner. Ac-di-sol® mediated an increase in paracellular transport by opening intercellular tight junctions as proven by a reduction in trans-epithelial electrical resistance (TEER). Sodium alginate, on the other hand, decreased paracellular transport in a concentration dependent manner, thus explaining the relative increase in P-gp transport.

Explotab® yielded inconclusive results in terms of R123 transport in the chosen *ex vivo* transport model. An increased diffusion distance and/or increase in viscosity of the diffusion layer may have been mediated by the excellent swelling capabilities of Explotab®. Both of these mechanisms may be probable explanations for the constant relatively low percentage R123 transport found in both directions across the excised intestinal tissue as well as for the increase in TEER values.

The analytical method was validated and complied with all specifications as stated in the literature in terms of linearity, limit of quantification, limit of detection, accuracy, precision and specificity and therefore the results were deemed accurate and trustworthy.

This study confirmed that not all excipients are necessarily inert substances and that they can interfere with drug pharmacokinetics. These excipients may cause unwanted effects on drug pharmacokinetics but may also be employed to function as multi-functional excipients, for example to enhance the absorption of poorly permeable compounds. However, this study served as a screening to identify potential pharmacokinetic interactions and follow-up *in vivo* clinical trials are needed to be conclusive in terms of clinical significance of these interactions.

5.2 Future recommendations

Certain attributes of selected disintegrants on R123 permeation were investigated in this study, but there are still various aspects that require further exploration. Future studies should be structured to investigate the following aspects:

- To study and characterise the mechanisms of interaction between Ac-di-sol®, Kollidon® CL-M, sodium alginate and P-gp.
- To investigate the potential use of multifunctional excipients in the formulation of pharmaceutical products that contain efflux transport substrates in order to improve their absorption and bioavailability.
- To characterise the mechanism of interaction between intercellular tight junctions and Ac-di-sol® and sodium alginate, respectively.
- To conclusively determine the physical and/or chemical interactions which take place between Avicel® PH-200 and R123 and to determine to which extent these interactions takes place.
- To conclusively determine if Explotab® has any effect on the diffusion surface thickness and how this could inhibit R123 transport.
- To quantify and characterise the different mechanisms by which R123 is absorbed to help explain the apparent efflux induction by sodium alginate for each individual concentration.
- To conduct disintegrant-transporter-interaction studies in *in vivo* models to determine if there is any correlation between data generated from *ex vivo* and *in vitro* models with the clinical findings as well as to determine if the pharmacokinetic interactions are clinically significant.

REFERENCES

Al-khattawi, A., Alyami, H., Townsend, B., Ma, X. & Mohammed, A.R. 2014. Evidence-based nanoscopic and molecular framework for excipient functionality in compressed orally disintegrating tablets. *PLoS ONE*, 9(7). http://journals.plos.org/plosone/article?id=10.1371/journal.pone.0101369 Date of access: 26 Oct. 2016.

Alderborn, G. 2007. Tablets and compaction. (*In* Aulton, M.E., *ed*. Aulton's pharmaceutics the design and manufacture of medicines. 3rd ed. Edinburgh: Churchill Livingston. p. 441-482).

Allen, L.V. & Luner, P.E. 2005. Magnesium Stearate. (*In* Rowe, R.C., Sheskey, P.J. & Owen, S.C., *eds.* Handbook of Pharmaceutical Excipients. 5th ed. London: Pharmaceutical Press. p. 430-433).

Alqahtani, S., Mohamed, L.A. & Kaddoumi, A. 2013. Experimental models for predicting drug absorption and metabolism. *Expert Opinion on Drug Metabolism & Toxicology*, 9(10):1-14.

Antunes, F., Andrade, F., Ferreira, D., Nielsen, H.M. & Sarmento, B. 2013. Models to predict intestinal absorption of therapeutic peptides and proteins. *Current Drug Metabolism*, 14(1):4-20.

Aoshima, H., Miyagisnima, A., Nozawa, Y., Sadzuka, Y. & Sonobe, T. 2005. Glycerin fatty acid esters as a new lubricant of tablets. *International Journal of Pharmaceutics*, 293:25-34.

Ashford, M. 2007. Gastointestinal tract – physiology and drug absorption. (*In* Aulton, M.E., *ed*. Aulton's Pharmaceutics the Design and Manufacture of Medicines. 3rd ed. Edinburgh: Churchill Livingston. p. 270-285).

Balimane, P.V., Han, Y-H. & Chong, S. 2006. Current industrial practices of assessing permeability and P-glycoprotein interaction. *The AAPS Journal,* 8(1):E1-E13.

Bele, M.H. & Derle, D.V. 2012. Effect of polacrilin potassium as disintegrant on bioavailability of diclofenac potassium in tablets: a technical note. *AAPS PharmSciTech,* 13(3):756-759.

Billany, M.R. 2007. Solutions. *(In* Aulton, M.E., *ed*. Aulton's pharmaceutics the design and manufacture of medicines. 3rd ed. Edinburgh: Churchill Livingston. p. 361-373).

Bock, U., Kottke, T., Gindorf, C. & Haltner, E. 2003. Validation of caco-2 cell monolayer system for determining the permeability of drug substances according to the Biopharmaceutics Classification System (BCS). (Unpublished)

Brink, J.J. & Stein, D.G. 1967. Pemoline levels in brain: Enhancement by dimethyl sulfoxide. *Science*, 158(3807):1479-1480.

Cable, C.G. 2005. Sodium alginate. (*In* Rowe, R.C., Sheskey, P.J. & Owen, S.C., *eds*. 2006. Handbook of pharmaceutical excipients, 5th ed. London: Pharmaceutical Press. p. 656-658).

Chan, L.M.S., Lowes, S. & Hirst, B.H. 2004. The ABCs of drug transport in intestine and liver: efflux proteins limiting drug absorption and bioavailability. *European Journal of Pharmaceutical Sciences,* 21:25-51.

Crawford, L. & Putnam, D. 2014. Synthesis and characterization of macromolecular rhodamine tethers and their interactions with P-glycoprotein. *Bioconjugate Chemistry*, 25:1462-1469.

Dave, V.S., Saoji, S.D., Raut, N.A. & Haware, R.V. 2015. Excipient variability and its impact on dosage form functionality. *Journal of Pharmaceutical Sciences*, 104:906-915.

de la Luz Reus Medina, M. & Kumar, V. 2006. Evaluation of cellulose II powders as a potential multifunctional excipient in tablet formulations. *International Journal of Pharmaceutics*, 322:31-35.

Desai, P.M., Liew, C.V. & Heng, P.W.S. 2012. Understanding disintegrant action by visualization. *Journal of Pharmacaeutical Sciences,* 101(6):2155-2164.

Desai, P.M., Liew, C.V. & Heng, P.W.S. 2016. Review of disintegrants and the disintegration phenomena. *Journal of Pharmaceutical Sciences,* 105(9):2545-2555.

Edge, S. & Miller, R.W. 2005. Sodium starch glycolate. (*In* Rowe, R.C., Sheskey, P.J. & Owen, S.C., *eds*. 2006. Handbook of pharmaceutical excipients, 5th ed. London: Pharmaceutical Press. p. 701-704).

Ferrari, F., Bertoni, M., Bonferoni, M.C., Rossi, S., Caramella, C. & Nyström, C. 1996. Investigation on bonding and disintegration properties of pharmaceutical materials. *International Journal of Pharmaceutics,* 136:71-79.

Galichet, L.Y. 2005. Cellulose, microcrystalline. (*In* Rowe, R.C., Sheskey, P.J. & Owen, S.C., *eds*. 2006. Handbook of pharmaceutical excipients, 5th ed. London: Pharmaceutical Press. p. 132-135).

Gamboa, J.M. & Leong, K.W. 2013. *In vitro* and *in vivo* models for the study of oral delivery of nanoparticles. *Advanced Drug Delivery Reviews,* 65:800-810.

García-Arieta, A. 2014. Interactions between active pharmaceutical ingredients and excipients affecting bioavailability: Impact on bioequivalence. *European Journal of Pharmaceutical Sciences*, 65:89-97.

Guest, R.T. 2005. Croscarmellose sodium. (*In* Rowe, R.C., Sheskey, P.J. & Owen, S.C., *eds*. 2006. Handbook of pharmaceutical excipients, 5th ed. London: Pharmaceutical Press. p. 211-213).

Kaprelyants, A.S. & Kell, D.B. 1992. Rapid assessment of bacterial viability and vitality by rhodamine 123 and flow cytometry. *Journal of Applied Bacteriology*, 72:410-422.

Kibbe, A.H. 2005. Crospovidone. (*In* Rowe, R.C., Sheskey, P.J. & Owen, S.C., *eds*. 2006. Handbook of pharmaceutical excipients, 5th ed. London: Pharmaceutical Press. p. 214-216).

Late, S.G., Yu, Y-Y. & Banga, A.K. 2009. Effects of disintegration-promoting agent, lubricants and moisture treatment on optimized fast disintegrating tablets. *International Journal of Pharmaceutics*, 364:4-11.

Legen, I., Salobir, M. & Kerč, J. 2005. Comparison of different intestinal epithelia as models for absorption enhancement studies. *International Journal of Pharmaceutics,* 291:183-188.

Lennernäs, H. 2007. Animal data: The contributions of the Ussing Chamber and perfusion systems to predicting human oral drug delivery *in vivo*. *Advanced Drug Delivery Reviewes,* 59:1103-1120.

Linnankoski, J., Mäkelä, J., Palmgren, J., Mauriala, T., Vedin, C., Ungell, A-L., Lazorova, L., Artursson, P., Urtti, A. & Yliperttula, M. 2010. Paracellular porosity and pore size of the human intestinal epithelium in tissue and cell culture models. *Journal of Pharmaceutical Sciences,* 99(4):2166-2175.

Liu, Z., Wang, S., Hu, M. 2009. Oral absorption basics: Pathways, physico-chemical and biological factors affecting absorption. (*In* Qiu, Y., Chen, Y., Zhang, G.G.Z., Liu, L. & Porter, W.R., *eds*. Developing Solid Oral Dosage Forms. 1st ed. London: Elsevier. p. 264-288).

Lundquist, P., Artursson, P. 2016? Oral absorption of peptides and nanoparticles across the human intestine: Opportunities, limitations and studies in human tissues. *Advanced Drug Delivery Review* (In press).

Mohanachandran, P.S., Sindhumol, P.G. & Kiran, T.S. 2011. Superdisintegrants: An overview. *International Journal of Pharmaceutical Sciences Review and Research*, 6(1):105-109.

Newhealthadvisor.com. 2014. What is the order of the digestive system? http://www.newhealthadvisor.com/order-of-digestive-system.html Date of access: 6 Sep. 2016.

Patel, S., Kaushal, A.D. & Bansal, A.K. 2007. Effect of particle size and compression force on compaction behaviour and derived mathematical parameters of compressibility. *Pharmaceutical Research*, 24(1):111-124.

Pietzonka, P., Walter, E., Duda-Johner, S., Langguth, P. & Merkle, H.P. 2002. Compromised integrity of excised porcine intestinal epithelium obtained from the abattoir affects the outcome of in vitro particle uptake studies. *European Journal of Pharmaceutical Sciences*, 15:39-47.

Priyanka, S. & Vandana, S. 2013. A review article on: Superdisintegrants. *International Journal of Drug Research and Technology*, 3(4):76-87.

Quodbach, J., Moussavi, A., Tammer, R., Frahm, J. & Kleinebudde, P. 2014. Tablet disintegration studied by high-resolution real-time magnetic resonance imaging. *Journal of Pharmaceutical Sciences,* 103:249-255.

Renukuntla, J., Vadlapudi, A.D., Patel, A., Boddu, S.H.S. & Mitra, A.K. 2013. Approaches for enhancing oral bioavailability of peptides and proteins. *International Journal of Pharmaceutics,* 447:75-93.

Sarmento, B., Andrade, F., Baptista da Silva, S., Rodrigues, F., das Neves, J. & Ferreira, D. 2012. Cell-based *in vitro* models for predicting drug permeability. *Expert Opinion on Drug Metabolism & Toxicology,* 8(5):607-621.

Shabir, G.A. 2003. Validation of high-performance liquid chromatography methods for pharmaceutical analysis understanding the differences and similarities between validation requirements of the US Food and Drug Administration, the US Pharmacopeia and the International Conference on Harmonization. *Journal of Chromatography A*, 987:57-66.

Shargel, L., Wu-Pong, S. & Yu, A.B.C. 2005. Applied biopharmaceutics & pharmacokinetics. 5th ed. New York: McGraw-Hill.

Singh, R. 2013. HPLC method development and validation – an overview. *Indian Journal of Pharmaceutical Education and Research*, 4(1):26-33.

Solaiman, A., Suliman, A.S., Shinde, S., Naz, S. & Elkordy, A.A. 2016. Application of general multilevel factorial design with formulation of fast disintegrating tablets containing croscarmellose sodium and Disintequick MCC-25. *International Journal of Pharmaceutics,* 501:87-95.

Sugano, K., Kansy, M., Artursson, P., Avdeef, A., Bendels, S., Di, L., Ecker, G.F., Faller, B., Fischer, H., Gerebtzoff, G., Lennernaes, H. & Senner, F. 2010. Coexistence of passive and carrier-mediated processes in drug transport. *Nature Reviews Drug Discovery,* 9:597-614.

Takizawa, Y., Kishimoto, H., Nakagawa, M., Sakamoto, N., Tobe, Y., Furuya, T., Tomita, M. & Hayashi, M. 2013. Effects of pharmaceutical excipients on membrane permeability in rat small intestine. *International Journal of Pharmaceutics*, 453:363-370.

Takizawa, Y., Kitazato, T., Ishizaka, H., Kamiya, N., Ito, Y., Kishimoto, H., Tomita, M. & Hayashi, M. 2013. Changes in absorption and excretion of rhodamine 123 by sodium nitroprusside. *International Journal of Pharmaceutics*, 450:31-35.

Thibert, R. & Hancock, B.C. 1996. Direct visualization of superdisintegrant hydration using environmental scanning electron microscopy. *Journal of Pharmaceutical Sciences*, 85(11):1255–1258.

Tønnesen, H.H. & Karlsen, J. 2002. Alginate in drug delivery systems. *Drug Development and Industrial Pharmacy,* 28(6):621-630.

United States Pharmacopeial Convention. 2016a. Validation of compendial procedures. http://www.uspnf.com/uspnf/pub/index?usp=39&nf=34&s=0&officialOn=May%201,%202016 Date of access: 20 Jul. 2016.

United States Pharmacopeial Convention. 2016b. Fluorescence spectroscopy. http://www.uspnf.com/uspnf/pub/index?usp=39&nf=34&s=1&officialOn=August%201,%2020 16 Date of access: 18 Aug. 2016.

Varma, M.V.S., Ashokraj, Y., Dey, C.S. & Panchagnula, R. 2003. P-glycoprotein inhibitors and their screening: a perspective from bioavailability enhancement. *Pharmacological Research*, 48:347-359.

Wang, X., Meng, M., Gao, L., Liu, T., Xu, Q. & Zeng, S. 2009. Permeation of astilbin and taxifolin in Caco-2 cell and their effects on the P-gp. *International Journal of Pharmaceutics*, 378:1-8.

Wikimedia.org. 2014. File: Layers of the GI Tract english.svg. https://commons.wikimedia.org/wiki/File:Layers_of_the_GI_Tract_english.svg Date of access: 6 Sep. 2016.

York, P. 2007. Design of Dosage Forms. (*In* Aulton, M.E., *ed*. Aulton's pharmaceutics the design and manufacture of medicines. 3rd ed. Edinburgh: Churchill Livingston. p. 4-14).

Young, P.M., Edge, S., Staniforth, J.N., Steele, F. & Price, R. 2005. Dynamic vapor sorption properties of sodium starch glycolate disintegrants. *Pharmaceutical Developments and Technology,* 10:249-259.

Zhao, W., Uehera, S., Tanaka, K., Tadokoro, S., Kusamori, K., Katsumi, H., Sakane, T. & Yamamoto, A. 2016. Effects of polyoxyethylene alkyl ethers on the intestinal transport and absorption of rhodamine 123: a P-glycoprotein substrate by *in vitro* and *in vivo* studies. *Journal of Pharmaceutical Sciences*, 105:1526-1534.

Zurlo, J., Rudacille, D. & Goldberg, A.M. 1996. The three R's: The way forward. *Environmental Health Perspectives,* 104(8). http://caat.jhsph.edu/publications/Articles/3r.html Date of access: 23 Jun. 2016.

ADDENDUM A

CONGRESS PROCEEDINGS

Society: APSSA

Theme: Pharmaceutics

Presentation preference: Oral

Taking part in the young scientist competition: Yes

Title: Effect of selected disintegrants on drug membrane permeation

Werner Gerber[1], Josias H Hamman[1], Johan D Steyn[1]

[1]Centre of Excellence for Pharmaceutical Sciences, North-West University, Private Bag X6001, Potchefstroom, 2520, South Africa

E-mail-address: wgerber99@gmail.com

Purpose: Virtually all solid dosage forms contain a disintegrating agent to help facilitate breakup, dissolution and absorption. Traditionally, excipients were thought to be pharmacologically inert, but recently, an increasing number of studies have shown that they may play a part in either increasing or decreasing drug membrane permeation. This study focused on investigating the effects of selected disintegrants on intestinal epithelial drug permeation. Five different disintegrants were selected and tested together with a model compound that is a P-glycoprotein (P-gp) substrate, namely rhodamine 123 (Rho123).

Methods: Bi-directional transport studies were conducted across excised pig jejunum using a Sweetana-Grass diffusion chamber apparatus. Samples of 180 µl were taken at 20 min intervals over a period of 2 h and analyzed for Rho 123 by means of a validated fluorescence spectroscopic method using a Spectramax® plate reader. All transport studies were conducted in triplicate at four different concentrations of each selected disintegrant. The apparent permeability coefficient values as well as efflux ratio values were calculated from the transport data.

Results: Croscarmellose sodium (Ac-Di-Sol®) has shown remarkable increases in transport in the apical-to-basolateral (A-B) direction, while decreasing the transport in the basolateral-to-apical (B-A) direction in a concentration dependent way in comparison with the control group (Rho123 alone). This proved that croscarmellose sodium is capable of inhibiting P-gp-mediated efflux. Microcrystalline cellulose (Avicel PH 200®) caused less Rho123 transport at higher concentrations in both directions which suggests that other transport mechanisms, other than efflux, are affected. Sodium starch glycolate (Explotab®) exhibited

an inhibitory effect at all concentrations and in both directions, possibly indicating inhibition of all transport mechanisms barred passive transport. Two more disintegrants, sodium alginate and crospovidone will also be investigated.

Conclusions: The findings of this study indicate that some excipients, such as certain disintegrants, may act as multi-functional excipients and influence drug absorption by means of efflux inhibition or other mechanisms, which may result in changes in the bioavailability of the drug.

The Academy of Pharmaceutical Sciences of the Pharmaceutical Society of South Africa

hereby commends

Werner Gerber

As the winner of the
Young Scientist award for
Pharmaceutical Sciences
2016

Chairman

Secretary

ADDENDUM B

ETHICAL APPROVAL

NORTH-WEST UNIVERSITY
YUNIBESITI YA BOKONE-BOPHIRIMA
NOORDWES-UNIVERSITEIT

Private Bag X6001, Potchefstroom
South Africa 2520

Tel: (018) 299-4900
Faks: (018) 299-4910
Web: http://www.nwu.ac.za

Ethics Committee
Tel +27 18 299 4849
Email Ethics@nwu.ac.za

ETHICS APPROVAL OF PROJECT

The North-West University Research Ethics Regulatory Committee (NWU-RERC) hereby approves your project as indicated below. This implies that the NWU-RERC grants its permission that provided the special conditions specified below are met and pending any other authorisation that may be necessary, the project may be initiated, using the ethics number below.

Project title: Excised pig buccal and intestinal tissues as in vitro models for pharmacokinetic studies

Project Leader: Prof Sias Hamman

Ethics number: NWU-00025-15-A5
(Institution – Project Number – Year – Status)

Status: S = Submission; R = Re-Submission; P = Provisional Authorisation; A = Authorisation

Approval date: 2015-04-16 **Expiry date: 2020-04-15**

Special conditions of the approval (if any): None

General conditions:

While this ethics approval is subject to all declarations, undertakings and agreements incorporated and signed in the application form, please note the following:

- *The project leader (principle investigator) must report in the prescribed format to the NWU-RERC:*
  - *annually (or as otherwise requested) on the progress of the project,*
  - *without any delay in case of any adverse event (or any matter that interrupts sound ethical principles) during the course of the project.*
- *The approval applies strictly to the protocol as stipulated in the application form. Would any changes to the protocol be deemed necessary during the course of the project, the project leader must apply for approval of these changes at the NWU-RERC. Would there be deviated from the project protocol without the necessary approval of such changes, the ethics approval is immediately and automatically forfeited.*
- *The date of approval indicates the first date that the project may be started. Would the project have to continue after the expiry date, a new application must be made to the NWU-RERC and new approval received before or on the expiry date.*
- *In the interest of ethical responsibility the NWU-RERC retains the right to:*
  - *request access to any information or data at any time during the course or after completion of the project;*
  - *withdraw or postpone approval if:*
    - *any unethical principles or practices of the project are revealed or suspected,*
    - *it becomes apparent that any relevant information was withheld from the NWU-RERC or that information has been false or misrepresented,*
    - *the required annual report and reporting of adverse events was not done timely and accurately,*
    - *new institutional rules, national legislation or international conventions deem it necessary.*

The Ethics Committee would like to remain at your service as scientist and researcher, and wishes you well with your project. Please do not hesitate to contact the Ethics Committee for any further enquiries or requests for assistance.

Yours sincerely

Linda du Plessis

Digitally signed by Linda du Plessis
DN: cn=Linda du Plessis, o=NWU, Vaal Triangle Campus, ou=Vice-Rector: Academic, email=linda.duplessis@nwu.ac.za, c=US
Date: 2015.04.20 20:35:13 +02'00'

Prof Linda du Plessis
Chair NWU Research Ethics Regulatory Committee (RERC)

ADDENDUM C

EX VIVO TRANSPORT DATA OF RHODAMINE 123 ACROSS EXCISED PIG JEJUNUM AND APPARENT PERMEABILITY

Table C.1: Apical-to-basolateral cumulative percentage transport of Rhodamine 123 alone across excised pig jejunum

Time (min)	Percentage transport: chamber 1	Percentage transport: chamber 2	Percentage transport: chamber 3	Standard deviation	Mean percentage transport
0	0.000	0.000	0.000	0.000	0.000
20	0.051	0.023	0.047	0.012	0.040
40	0.098	0.044	0.092	0.024	0.078
60	0.136	0.110	0.126	0.011	0.124
80	0.209	0.213	0.172	0.019	0.198
100	0.243	0.304	0.207	0.040	0.251
120	0.307	0.394	0.315	0.040	0.339
P_{app} ($x10^{-7}$)	2.366	3.202	2.248	0.425	

Table C.2: Basolateral-to-apical cumulative percentage transport of Rhodamine 123 alone across excised pig jejunum

Time (min)	Percentage transport: chamber 1	Percentage transport: chamber 2	Percentage transport: chamber 3	Standard deviation	Mean percentage transport
0	0.000	0.000	0.000	0.000	0.000
20	0.283	0.429	0.051	0.156	0.254
40	0.440	0.660	0.296	0.150	0.465
60	0.496	0.688	0.550	0.081	0.578
80	0.546	0.783	0.601	0.101	0.643
100	0.566	0.774	0.684	0.085	0.675
120	0.575	0.794	1.048	0.193	0.806
P_{app} ($x10^{-7}$)	4.009	5.339	7.885	1.608	

Table C.3: Apical-to-basolateral cumulative percentage transport of Rhodamine 123 in the presence of 0.0005% (w/v) croscarmellose sodium (Ac-di-sol®) across excised pig jejunum

Time (min)	Percentage transport: chamber 1	Percentage transport: chamber 2	Percentage transport: chamber 3	Standard deviation	Mean percentage transport
0	0.000	0.000	0.000	0.000	0.000
20	0.104	0.059	0.092	0.019	0.085
40	0.217	0.185	0.197	0.013	0.200
60	0.388	0.359	0.341	0.020	0.363
80	0.459	0.465	0.358	0.049	0.427
100	0.513	0.532	0.420	0.049	0.489
120	0.538	0.662	0.507	0.067	0.569
P_{app} ($x10^{-7}$)	4.471	5.371	3.910	0.602	

Table C.4: Basolateral-to-apical cumulative percentage transport of Rhodamine 123 in the presence of 0.0005% (w/v) croscarmellose sodium (Ac-di-sol®) across excised pig jejunum

Time (min)	Percentage transport: chamber 1	Percentage transport: chamber 2	Percentage transport: chamber 3	Standard deviation	Mean percentage transport
0	0.000	0.000	0.000	0.000	0.000
20	0.668	0.627	0.511	0.066	0.602
40	0.970	0.744	0.687	0.122	0.800
60	1.004	1.068	0.949	0.049	1.007
80	1.352	1.076	0.930	0.175	1.119
100	1.184	0.967	0.995	0.097	1.049
120	1.356	1.029	1.118	0.138	1.168
P_{app} ($x10^{-7}$)	9.166	6.854	7.634	0.960	

Table C.5: Apical-to-basolateral cumulative percentage transport of Rhodamine 123 in the presence of 0.001% (w/v) croscarmellose sodium (Ac-di-sol®) across excised pig jejunum

Time (min)	Percentage transport: chamber 1	Percentage transport: chamber 2	Percentage transport: chamber 3	Standard deviation	Mean percentage transport
0	0.000	0.000	0.000	0.000	0.000
20	0.175	0.088	0.096	0.039	0.120
40	0.265	0.172	0.146	0.051	0.194
60	0.343	0.291	0.233	0.045	0.289
80	0.437	0.474	0.315	0.068	0.409
100	0.538	0.552	0.384	0.076	0.491
120	0.653	0.735	0.509	0.093	0.632
P_{app} ($x10^{-7}$)	4.777	5.743	3.799	0.794	

Table C.6: Basolateral-to-apical cumulative percentage transport of Rhodamine 123 in the presence of 0.001% (w/v) croscarmellose sodium (Ac-di-sol®) across excised pig jejunum

Time (min)	Percentage transport: chamber 1	Percentage transport: chamber 2	Percentage transport: chamber 3	Standard deviation	Mean percentage transport
0	0.000	0.000	0.000	0.000	0.000
20	0.407	0.386	0.494	0.047	0.429
40	0.388	0.355	0.540	0.081	0.428
60	0.550	0.611	0.777	0.096	0.646
80	0.661	0.785	0.934	0.111	0.794
100	0.737	0.809	0.730	0.036	0.759
120	0.780	0.902	0.992	0.087	0.892
P_{app} ($x10^{-7}$)	5.475	6.660	6.425	0.512	

Table C.7: Apical-to-basolateral cumulative percentage transport of Rhodamine 123 in the presence of 0.005% (w/v) croscarmellose sodium (Ac-di-sol®) across excised pig jejunum

Time (min)	Percentage transport: chamber 1	Percentage transport: chamber 2	Percentage transport: chamber 3	Standard deviation	Mean percentage transport
0	0.000	0.000	0.000	0.000	0.000
20	1.319	0.543	1.243	0.349	1.035
40	1.472	0.667	1.412	0.366	1.184
60	1.513	0.787	1.436	0.326	1.245
80	1.570	0.818	1.557	0.351	1.315
100	1.622	0.931	1.587	0.318	1.380
120	1.603	1.080	1.604	0.247	1.429
P_{app} ($x10^{-7}$)	9.214	6.964	9.439	1.118	

Table C.8: Basolateral-to-apical cumulative percentage transport of Rhodamine 123 in the presence of 0.005% (w/v) croscarmellose sodium (Ac-di-sol®) across excised pig jejunum

Time (min)	Percentage transport: chamber 1	Percentage transport: chamber 2	Percentage transport: chamber 3	Standard deviation	Mean percentage transport
0	0.000	0.000	0.000	0.000	0.000
20	0.326	0.538	0.384	0.090	0.416
40	0.423	0.641	0.470	0.094	0.512
60	0.475	0.783	0.506	0.138	0.588
80	0.517	0.801	0.558	0.125	0.625
100	0.574	0.834	0.625	0.112	0.678
120	0.651	0.881	0.650	0.109	0.728
P_{app} ($x10^{-7}$)	4.255	5.677	4.212	0.681	

Table C.9: Apical-to-basolateral cumulative percentage transport of Rhodamine 123 in the presence of 0.01% (w/v) croscarmellose sodium (Ac-di-sol®) across excised pig jejunum

Time (min)	Percentage transport: chamber 1	Percentage transport: chamber 2	Percentage transport: chamber 3	Standard deviation	Mean percentage transport
0	0.000	0.000	0.000	0.000	0.000
20	2.520	2.992	2.252	0.306	2.588
40	2.527	3.329	2.435	0.402	2.764
60	2.533	3.549	2.622	0.459	2.901
80	2.653	3.673	2.863	0.440	3.063
100	2.702	3.743	3.053	0.433	3.166
120	2.850	3.819	3.083	0.413	3.251
P_{app} ($x10^{-7}$)	15.113	22.243	18.857	2.912	

Table C.10: Basolateral-to-apical cumulative percentage transport of Rhodamine 123 in the presence of 0.01% (w/v) croscarmellose sodium (Ac-di-sol®) across excised pig jejunum

Time (min)	Percentage transport: chamber 1	Percentage transport: chamber 2	Percentage transport: chamber 3	Standard deviation	Mean percentage transport
0	0.000	0.000	0.000	0.000	0.000
20	0.133	0.105	0.192	0.036	0.144
40	0.194	0.186	0.228	0.018	0.203
60	0.251	0.202	0.265	0.027	0.239
80	0.327	0.239	0.313	0.039	0.293
100	0.320	0.271	0.394	0.051	0.328
120	0.378	0.359	0.447	0.038	0.395
P_{app} ($x10^{-7}$)	2.745	2.441	3.059	0.252	

Table C.11: Apical-to-basolateral cumulative percentage transport of Rhodamine 123 in the presence of 0.005% (w/v) microcrystalline cellulose (Avicel® PH-200) across excised pig jejunum

Time (min)	Percentage transport: chamber 1	Percentage transport: chamber 2	Percentage transport: chamber 3	Standard deviation	Mean percentage transport
0	0.000	0.000	0.000	0.000	0.000
20	0.084	0.096	0.075	0.009	0.085
40	0.149	0.253	0.164	0.046	0.189
60	0.254	0.444	0.270	0.086	0.323
80	0.438	0.585	0.418	0.075	0.480
100	0.535	0.696	0.490	0.089	0.574
120	0.686	0.790	0.598	0.078	0.691
P_{app} ($x10^{-7}$)	5.432	6.525	4.813	0.708	

Table C.12: Basolateral-to-apical cumulative percentage transport of Rhodamine 123 in the presence of 0.005% (w/v) microcrystalline cellulose (Avicel® PH-200) across excised pig jejunum

Time (min)	Percentage transport: chamber 1	Percentage transport: chamber 2	Percentage transport: chamber 3	Standard deviation	Mean percentage transport
0	0.000	0.000	0.000	0.000	0.000
20	0.644	0.626	0.380	0.120	0.550
40	0.784	0.738	0.496	0.126	0.673
60	0.883	0.833	0.597	0.125	0.771
80	0.891	0.899	0.683	0.100	0.824
100	0.818	0.857	0.692	0.071	0.789
120	0.847	0.833	0.687	0.072	0.789
P_{app} ($x10^{-7}$)	5.010	5.222	4.802	0.172	

Table C.13: Apical-to-basolateral cumulative percentage transport of Rhodamine 123 in the presence of 0.01% (w/v) microcrystalline cellulose (Avicel® PH-200) across excised pig jejunum

Time (min)	Percentage transport: chamber 1	Percentage transport: chamber 2	Percentage transport: chamber 3	Standard deviation	Mean percentage transport
0	0.000	0.000	0.000	0.000	0.000
20	0.044	0.002	0.034	0.018	0.027
40	0.086	0.029	0.119	0.037	0.078
60	0.165	0.148	0.280	0.059	0.198
80	0.228	0.212	0.339	0.057	0.260
100	0.333	0.314	0.442	0.056	0.363
120	0.418	0.455	0.701	0.126	0.524
P_{app} ($x10^{-7}$)	3.301	3.630	5.246	0.850	

Table C.14: Basolateral-to-apical cumulative percentage transport of Rhodamine 123 in the presence of 0.01% (w/v) microcrystalline cellulose (Avicel® PH-200) across excised pig jejunum

Time (min)	Percentage transport: chamber 1	Percentage transport: chamber 2	Percentage transport: chamber 3	Standard deviation	Mean percentage transport
0	0.000	0.000	0.000	0.000	0.000
20	0.409	0.132	0.408	0.130	0.316
40	0.491	0.207	0.533	0.145	0.410
60	0.597	0.432	0.633	0.087	0.554
80	0.641	0.505	0.702	0.083	0.616
100	0.671	0.557	0.718	0.067	0.649
120	0.694	0.596	0.742	0.061	0.677
P_{app} ($x10^{-7}$)	4.611	4.908	5.040	0.179	

Table C.15: Apical-to-basolateral cumulative percentage transport of Rhodamine 123 in the presence of 0.015% (w/v) microcrystalline cellulose (Avicel® PH-200) across excised pig jejunum

Time (min)	Percentage transport: chamber 1	Percentage transport: chamber 2	Percentage transport: chamber 3	Standard deviation	Mean percentage transport
0	0.000	0.000	0.000	0.000	0.000
20	0.129	0.166	0.118	0.020	0.138
40	0.177	0.237	0.158	0.034	0.191
60	0.217	0.275	0.214	0.028	0.235
80	0.252	0.360	0.253	0.051	0.288
100	0.286	0.399	0.313	0.048	0.333
120	0.347	0.424	0.356	0.035	0.375
P_{app} ($x10^{-7}$)	2.387	3.114	2.594	0.306	

Table C.16: Basolateral-to-apical cumulative percentage transport of Rhodamine 123 in the presence of 0.015% (w/v) microcrystalline cellulose (Avicel® PH-200) across excised pig jejunum

Time (min)	Percentage transport: chamber 1	Percentage transport: chamber 2	Percentage transport: chamber 3	Standard deviation	Mean percentage transport
0	0.000	0.000	0.000	0.000	0.000
20	0.168	0.185	0.145	0.016	0.166
40	0.202	0.251	0.219	0.020	0.224
60	0.260	0.286	0.292	0.014	0.279
80	0.342	0.368	0.394	0.021	0.368
100	0.455	0.435	0.400	0.023	0.430
120	0.487	0.538	0.438	0.041	0.488
P_{app} ($x10^{-7}$)	3.637	3.732	3.340	0.167	

Table C.17: Apical-to-basolateral cumulative percentage transport of Rhodamine 123 in the presence of 0.03% (w/v) microcrystalline cellulose (Avicel® PH-200) across excised pig jejunum

Time (min)	Percentage transport: chamber 1	Percentage transport: chamber 2	Percentage transport: chamber 3	Standard deviation	Mean percentage transport
0	0.000	0.000	0.000	0.000	0.000
20	0.088	0.044	0.152	0.044	0.094
40	0.135	0.091	0.194	0.042	0.140
60	0.239	0.139	0.229	0.045	0.202
80	0.283	0.175	0.288	0.052	0.249
100	0.332	0.227	0.330	0.049	0.296
120	0.379	0.284	0.350	0.040	0.338
P_{app} ($x10^{-7}$)	2.965	2.178	2.512	0.322	

Table C.18: Basolateral-to-apical cumulative percentage transport of Rhodamine 123 in the presence of 0.03% (w/v) microcrystalline cellulose (Avicel® PH-200) across excised pig jejunum

Time (min)	Percentage transport: chamber 1	Percentage transport: chamber 2	Percentage transport: chamber 3	Standard deviation	Mean percentage transport
0	0.000	0.000	0.000	0.000	0.000
20	0.096	0.091	0.119	0.012	0.102
40	0.132	0.145	0.142	0.006	0.140
60	0.173	0.189	0.172	0.008	0.178
80	0.210	0.208	0.246	0.017	0.221
100	0.228	0.239	0.263	0.015	0.243
120	0.252	0.268	0.307	0.023	0.276
P_{app} ($x10^{-7}$)	1.834	1.944	2.197	0.152	

Table C.19: Apical-to-basolateral cumulative percentage transport of Rhodamine 123 in the presence of 0.002% (w/v) sodium starch glycolate (Explotab®) across excised pig jejunum

Time (min)	Percentage transport: chamber 1	Percentage transport: chamber 2	Percentage transport: chamber 3	Standard deviation	Mean percentage transport
0	0.000	0.000	0.000	0.000	0.000
20	0.152	0.110	0.138	0.017	0.133
40	0.218	0.140	0.132	0.039	0.163
60	0.280	0.196	0.169	0.047	0.215
80	0.321	0.234	0.202	0.050	0.252
100	0.358	0.292	0.218	0.057	0.289
120	0.427	0.334	0.275	0.063	0.345
P_{app} ($x10^{-7}$)	3.005	2.438	1.763	0.508	

Table C.20: Basolateral-to-apical cumulative percentage transport of Rhodamine 123 in the presence of 0.002% (w/v) sodium starch glycolate (Explotab®) across excised pig jejunum

Time (min)	Percentage transport: chamber 1	Percentage transport: chamber 2	Percentage transport: chamber 3	Standard deviation	Mean percentage transport
0	0.000	0.000	0.000	0.000	0.000
20	0.094	0.049	0.164	0.047	0.102
40	0.116	0.118	0.187	0.033	0.140
60	0.155	0.191	0.243	0.036	0.196
80	0.201	0.270	0.307	0.044	0.259
100	0.263	0.332	0.353	0.039	0.316
120	0.292	0.371	0.385	0.041	0.349
P_{app} ($x10^{-7}$)	2.172	3.065	2.761	0.371	

Table C.21: Apical-to-basolateral cumulative percentage transport of Rhodamine 123 in the presence of 0.004% (w/v) sodium starch glycolate (Explotab®) across excised pig jejunum

Time (min)	Percentage transport: chamber 1	Percentage transport: chamber 2	Percentage transport: chamber 3	Standard deviation	Mean percentage transport
0	0.000	0.000	0.000	0.000	0.000
20	0.010	0.000	0.053	0.023	0.021
40	0.034	0.019	0.097	0.034	0.050
60	0.099	0.058	0.171	0.047	0.109
80	0.141	0.081	0.220	0.057	0.147
100	0.168	0.166	0.289	0.058	0.207
120	0.208	0.232	0.427	0.098	0.289
P_{app} ($x10^{-7}$)	1.751	1.822	3.135	0.637	

Table C.22: Basolateral-to-apical cumulative percentage transport of Rhodamine 123 in the presence of 0.004% (w/v) sodium starch glycolate (Explotab®) across excised pig jejunum

Time (min)	Percentage transport: chamber 1	Percentage transport: chamber 2	Percentage transport: chamber 3	Standard deviation	Mean percentage transport
0	0.000	0.000	0.000	0.000	0.000
20	0.187	0.076	0.163	0.048	0.142
40	0.241	0.110	0.208	0.056	0.186
60	0.287	0.115	0.229	0.071	0.210
80	0.294	0.154	0.304	0.068	0.251
100	0.330	0.213	0.395	0.075	0.313
120	0.375	0.236	0.413	0.076	0.341
P_{app} ($x10^{-7}$)	2.450	1.719	3.007	0.528	

Table C.23: Apical-to-basolateral cumulative percentage transport of Rhodamine 123 in the presence of 0.008% (w/v) sodium starch glycolate (Explotab®) across excised pig jejunum

Time (min)	Percentage transport: chamber 1	Percentage transport: chamber 2	Percentage transport: chamber 3	Standard deviation	Mean percentage transport
0	0.000	0.000	0.000	0.000	0.000
20	0.040	0.021	0.034	0.008	0.032
40	0.080	0.134	0.075	0.027	0.096
60	0.103	0.193	0.114	0.040	0.137
80	0.133	0.257	0.177	0.051	0.189
100	0.170	0.310	0.256	0.058	0.246
120	0.215	0.354	0.289	0.057	0.286
P_{app} ($x10^{-7}$)	1.603	2.948	2.363	0.551	

Table C.24: Basolateral-to-apical cumulative percentage transport of Rhodamine 123 in the presence of 0.008% (w/v) sodium starch glycolate (Explotab®) across excised pig jejunum

Time (min)	Percentage transport: chamber 1	Percentage transport: chamber 2	Percentage transport: chamber 3	Standard deviation	Mean percentage transport
0	0.000	0.000	0.000	0.000	0.000
20	0.133	0.135	0.127	0.003	0.132
40	0.244	0.165	0.151	0.041	0.187
60	0.258	0.192	0.181	0.034	0.211
80	0.275	0.200	0.262	0.033	0.246
100	0.303	0.238	0.336	0.041	0.293
120	0.332	0.294	0.404	0.046	0.344
P_{app} ($x10^{-7}$)	2.287	1.879	2.915	0.426	

Table C.25: Apical-to-basolateral cumulative percentage transport of Rhodamine 123 in the presence of 0.016% (w/v) sodium starch glycolate (Explotab®) across excised pig jejunum

Time (min)	Percentage transport: chamber 1	Percentage transport: chamber 2	Percentage transport: chamber 3	Standard deviation	Mean percentage transport
0	0.000	0.000	0.000	0.000	0.000
20	0.059	0.000	0.009	0.026	0.023
40	0.130	0.040	0.133	0.043	0.101
60	0.201	0.059	0.167	0.060	0.142
80	0.249	0.082	0.216	0.072	0.182
100	0.272	0.121	0.261	0.069	0.218
120	0.318	0.178	0.353	0.075	0.283
P_{app} ($x10^{-7}$)	2.505	1.369	2.753	0.603	

Table C.26: Basolateral-to-apical cumulative percentage transport of Rhodamine 123 in the presence of 0.016% (w/v) sodium starch glycolate (Explotab®) across excised pig jejunum

Time (min)	Percentage transport: chamber 1	Percentage transport: chamber 2	Percentage transport: chamber 3	Standard deviation	Mean percentage transport
0	0.000	0.000	0.000	0.000	0.000
20	0.051	0.025	0.082	0.023	0.053
40	0.112	0.063	0.167	0.043	0.114
60	0.159	0.130	0.244	0.048	0.178
80	0.202	0.187	0.286	0.043	0.225
100	0.264	0.240	0.358	0.051	0.287
120	0.300	0.292	0.417	0.057	0.337
P_{app} ($x10^{-7}$)	2.368	2.393	3.213	0.393	

Table C.27: Apical-to-basolateral cumulative percentage transport of Rhodamine 123 in the presence of 0.002% (w/v) crospovidone (Kollidon® CL-M) across excised pig jejunum

Time (min)	Percentage transport: chamber 1	Percentage transport: chamber 2	Percentage transport: chamber 3	Standard deviation	Mean percentage transport
0	0.000	0.000	0.000	0.000	0.000
20	0.103	0.090	0.189	0.044	0.127
40	0.247	0.215	0.268	0.022	0.243
60	0.318	0.288	0.318	0.014	0.308
80	0.374	0.353	0.357	0.009	0.361
100	0.432	0.405	0.415	0.011	0.417
120	0.469	0.453	0.448	0.009	0.456
P_{app} ($x10^{-7}$)	3.665	3.552	3.154	0.219	

Table C.28: Basolateral-to-apical cumulative percentage transport of Rhodamine 123 in the presence of 0.002% (w/v) crospovidone (Kollidon® CL-M) across excised pig jejunum

Time (min)	Percentage transport: chamber 1	Percentage transport: chamber 2	Percentage transport: chamber 3	Standard deviation	Mean percentage transport
0	0.000	0.000	0.000	0.000	0.000
20	0.343	0.318	0.364	0.019	0.342
40	0.413	0.368	0.387	0.018	0.389
60	0.420	0.403	0.413	0.007	0.412
80	0.434	0.531	0.506	0.041	0.490
100	0.485	0.515	0.520	0.016	0.507
120	0.493	0.546	0.529	0.022	0.522
P_{app} ($x10^{-7}$)	2.981	3.668	3.374	0.282	

Table C.29: Apical-to-basolateral cumulative percentage transport of Rhodamine 123 in the presence of 0.004% (w/v) crospovidone (Kollidon® CL-M) across excised pig jejunum

Time (min)	Percentage transport: chamber 1	Percentage transport: chamber 2	Percentage transport: chamber 3	Standard deviation	Mean percentage transport
0	0.000	0.000	0.000	0.000	0.000
20	0.174	0.044	0.070	0.056	0.096
40	0.344	0.204	0.197	0.068	0.249
60	0.474	0.378	0.355	0.051	0.403
80	0.539	0.393	0.495	0.061	0.476
100	0.570	0.442	0.571	0.060	0.528
120	0.622	0.525	0.658	0.056	0.602
P_{app} ($x10^{-7}$)	4.769	4.278	5.477	0.492	

Table C.30: Basolateral-to-apical cumulative percentage transport of Rhodamine 123 in the presence of 0.004% (w/v) crospovidone (Kollidon® CL-M) across excised pig jejunum

Time (min)	Percentage transport: chamber 1	Percentage transport: chamber 2	Percentage transport: chamber 3	Standard deviation	Mean percentage transport
0	0.000	0.000	0.000	0.000	0.000
20	0.032	0.264	0.097	0.098	0.131
40	0.150	0.300	0.190	0.064	0.213
60	0.290	0.326	0.313	0.015	0.309
80	0.376	0.337	0.408	0.029	0.374
100	0.371	0.342	0.434	0.038	0.382
120	0.410	0.429	0.450	0.016	0.430
P_{app} ($x10^{-7}$)	3.569	2.469	3.750	0.566	

Table C.31: Apical-to-basolateral cumulative percentage transport of Rhodamine 123 in the presence of 0.005% (w/v) crospovidone (Kollidon® CL-M) across excised pig jejunum

Time (min)	Percentage transport: chamber 1	Percentage transport: chamber 2	Percentage transport: chamber 3	Standard deviation	Mean percentage transport
0	0.000	0.000	0.000	0.000	0.000
20	0.307	0.057	0.088	0.111	0.150
40	0.354	0.161	0.182	0.086	0.232
60	0.377	0.268	0.303	0.045	0.316
80	0.417	0.551	0.429	0.060	0.465
100	0.456	0.637	0.540	0.074	0.544
120	0.514	0.770	0.742	0.115	0.675
P_{app} ($x10^{-7}$)	3.178	6.453	5.648	1.393	

Table C.32: Basolateral-to-apical cumulative percentage transport of Rhodamine 123 in the presence of 0.005% (w/v) crospovidone (Kollidon® CL-M) across excised pig jejunum

Time (min)	Percentage transport: chamber 1	Percentage transport: chamber 2	Percentage transport: chamber 3	Standard deviation	Mean percentage transport
0	0.000	0.000	0.000	0.000	0.000
20	0.279	0.263	0.234	0.019	0.258
40	0.345	0.336	0.287	0.026	0.322
60	0.369	0.358	0.363	0.004	0.363
80	0.392	0.385	0.405	0.008	0.394
100	0.411	0.394	0.425	0.013	0.410
120	0.437	0.398	0.454	0.024	0.430
P_{app} ($x10^{-7}$)	2.714	2.516	3.117	0.250	

Table C.33: Apical-to-basolateral cumulative percentage transport of Rhodamine 123 in the presence of 0.01% (w/v) crospovidone (Kollidon® CL-M) across excised pig jejunum

Time (min)	Percentage transport: chamber 1	Percentage transport: chamber 2	Percentage transport: chamber 3	Standard deviation	Mean percentage transport
0	0.000	0.000	0.000	0.000	0.000
20	0.013	0.077	0.038	0.026	0.043
40	0.412	0.351	0.347	0.029	0.370
60	0.632	0.551	0.596	0.033	0.593
80	0.783	0.687	0.649	0.057	0.706
100	0.841	0.890	0.683	0.089	0.805
120	0.863	0.990	0.830	0.069	0.894
P_{app} ($x10^{-7}$)	7.719	8.250	6.824	0.588	

Table C.34: Basolateral-to-apical cumulative percentage transport of Rhodamine 123 in the presence of 0.01% (w/v) crospovidone (Kollidon® CL-M) across excised pig jejunum

Time (min)	Percentage transport: chamber 1	Percentage transport: chamber 2	Percentage transport: chamber 3	Standard deviation	Mean percentage transport
0	0.000	0.000	0.000	0.000	0.000
20	0.065	0.020	0.022	0.021	0.036
40	0.112	0.047	0.064	0.027	0.074
60	0.120	0.081	0.070	0.022	0.091
80	0.134	0.141	0.101	0.017	0.126
100	0.153	0.160	0.147	0.005	0.153
120	0.188	0.170	0.164	0.010	0.174
P_{app} ($x10^{-7}$)	1.273	1.477	1.303	0.090	

Table C.35: Apical-to-basolateral cumulative percentage transport of Rhodamine 123 in the presence of 0.0025% (w/v) sodium alginate across excised pig jejunum

Time (min)	Percentage transport: chamber 1	Percentage transport: chamber 2	Percentage transport: chamber 3	Standard deviation	Mean percentage transport
0	0.000	0.000	0.000	0.000	0.000
20	0.255	0.078	0.148	0.073	0.160
40	0.299	0.138	0.249	0.067	0.229
60	0.317	0.187	0.323	0.063	0.276
80	0.369	0.318	0.402	0.035	0.363
100	0.450	0.355	0.537	0.074	0.447
120	0.510	0.474	0.654	0.077	0.546
P_{app} ($x10^{-7}$)	3.327	3.607	4.832	0.653	

Table C.36: Basolateral-to-apical cumulative percentage transport of Rhodamine 123 in the presence of 0.0025% (w/v) sodium alginate across excised pig jejunum

Time (min)	Percentage transport: chamber 1	Percentage transport: chamber 2	Percentage transport: chamber 3	Standard deviation	Mean percentage transport
0	0.000	0.000	0.000	0.000	0.000
20	0.138	0.139	0.049	0.042	0.109
40	0.179	0.173	0.076	0.047	0.143
60	0.198	0.194	0.094	0.048	0.162
80	0.218	0.205	0.122	0.042	0.181
100	0.241	0.226	0.191	0.021	0.219
120	0.260	0.231	0.222	0.016	0.237
P_{app} ($x10^{-7}$)	1.714	1.500	1.663	0.091	

Table C.37: Apical-to-basolateral cumulative percentage transport of Rhodamine 123 in the presence of 0.005% (w/v) sodium alginate across excised pig jejunum

Time (min)	Percentage transport: chamber 1	Percentage transport: chamber 2	Percentage transport: chamber 3	Standard deviation	Mean percentage transport
0	0.000	0.000	0.000	0.000	0.000
20	0.047	0.049	0.501	0.213	0.199
40	0.086	0.161	0.589	0.222	0.278
60	0.132	0.260	0.630	0.211	0.341
80	0.200	0.335	0.709	0.215	0.415
100	0.259	0.443	0.775	0.213	0.492
120	0.312	0.492	0.854	0.225	0.552
P_{app} ($x10^{-7}$)	2.463	4.077	5.401	1.201	

Table C.38: Basolateral-to-apical cumulative percentage transport of Rhodamine 123 in the presence of 0.005% (w/v) sodium alginate across excised pig jejunum

Time (min)	Percentage transport: chamber 1	Percentage transport: chamber 2	Percentage transport: chamber 3	Standard deviation	Mean percentage transport
0	0.000	0.000	0.000	0.000	0.000
20	0.104	0.094	0.093	0.005	0.097
40	0.158	0.136	0.150	0.009	0.148
60	0.195	0.162	0.183	0.014	0.180
80	0.244	0.193	0.199	0.023	0.212
100	0.295	0.221	0.244	0.031	0.253
120	0.375	0.281	0.257	0.051	0.304
P_{app} ($x10^{-7}$)	2.663	1.926	1.874	0.360	

Table C.39: Apical-to-basolateral cumulative percentage transport of Rhodamine 123 in the presence of 0.01% (w/v) sodium alginate across excised pig jejunum

Time (min)	Percentage transport: chamber 1	Percentage transport: chamber 2	Percentage transport: chamber 3	Standard deviation	Mean percentage transport
0	0.000	0.000	0.000	0.000	0.000
20	0.066	0.073	0.060	0.005	0.066
40	0.140	0.126	0.141	0.007	0.136
60	0.217	0.172	0.212	0.020	0.201
80	0.244	0.219	0.282	0.026	0.248
100	0.280	0.254	0.352	0.041	0.296
120	0.326	0.304	0.465	0.071	0.365
P_{app} ($x10^{-7}$)	2.525	2.287	3.546	0.546	

Table C.40: Basolateral-to-apical cumulative percentage transport of Rhodamine 123 in the presence of 0.01% (w/v) sodium alginate across excised pig jejunum

Time (min)	Percentage transport: chamber 1	Percentage transport: chamber 2	Percentage transport: chamber 3	Standard deviation	Mean percentage transport
0	0.000	0.000	0.000	0.000	0.000
20	0.117	0.080	0.078	0.018	0.092
40	0.155	0.133	0.187	0.022	0.158
60	0.176	0.195	0.330	0.068	0.234
80	0.212	0.324	0.395	0.075	0.310
100	0.259	0.418	0.468	0.089	0.382
120	0.293	0.464	0.522	0.097	0.426
P_{app} ($x10^{-7}$)	2.040	3.780	4.270	0.957	

Table C.41: Apical-to-basolateral cumulative percentage transport of Rhodamine 123 in the presence of 0.02% (w/v) sodium alginate across excised pig jejunum

Time (min)	Percentage transport: chamber 1	Percentage transport: chamber 2	Percentage transport: chamber 3	Standard deviation	Mean percentage transport
0	0.000	0.000	0.000	0.000	0.000
20	0.025	0.033	0.019	0.006	0.026
40	0.049	0.065	0.064	0.007	0.059
60	0.147	0.111	0.098	0.021	0.118
80	0.201	0.179	0.120	0.034	0.167
100	0.260	0.211	0.173	0.036	0.214
120	0.302	0.277	0.236	0.028	0.272
P_{app} ($x10^{-7}$)	2.556	2.178	1.789	0.313	

Table C.42: Basolateral-to-apical cumulative percentage transport of Rhodamine 123 in the presence of 0.02% (w/v) sodium alginate across excised pig jejunum

Time (min)	Percentage transport: chamber 1	Percentage transport: chamber 2	Percentage transport: chamber 3	Standard deviation	Mean percentage transport
0	0.000	0.000	0.000	0.000	0.000
20	0.085	0.174	0.155	0.038	0.138
40	0.135	0.297	0.221	0.066	0.218
60	0.237	0.410	0.308	0.071	0.318
80	0.270	0.425	0.335	0.064	0.343
100	0.311	0.484	0.377	0.071	0.391
120	0.363	0.513	0.399	0.064	0.425
P_{app} ($x10^{-7}$)	2.801	3.821	2.936	0.452	

ADDENDUM D

EFFLUX RATIOS

Table D.1: Apparent permeability (P_{app}) values and efflux ratios (ER) for croscarmellose sodium (Ac-di-sol®) at selected test concentrations

Concentration (% w/v)	Transport direction	P_{app} (x 10^{-7})	Average P_{app} (x 10^{-7})	Efflux ratio
0.0005	**Apical-to-basolateral**	4.471	4.584	1.720
		5.371		
		3.910		
	Basolateral-to-apical	9.166	7.885	
		6.854		
		7.634		
0.001	**Apical-to-basolateral**	4.777	4.773	1.296
		5.743		
		3.799		
	Basolateral-to-apical	5.475	6.187	
		6.660		
		6.425		
0.005	**Apical-to-basolateral**	9.214	8.539	0.552
		6.964		
		9.439		
	Basolateral-to-apical	4.255	4.714	
		5.677		
		4.212		
0.01	**Apical-to-basolateral**	1.511	1.874	0.147
		2.224		
		1.886		
	Basolateral-to-apical	2.745	2.748	
		2.441		
		3.059		

Table D.2: Apparent permeability (P_{app}) values and efflux ratios (ER) for microcrystalline cellulose (Avicel® PH-200) at selected test concentrations

Concentration (% w/v)	Transport direction	P_{app} (x 10^{-7})	Average P_{app} (x 10^{-7})	Efflux ratio
0.005	**Apical-to-basolateral**	5.432	5.590	0.897
		6.525		
		4.813		
	Basolateral-to-apical	5.010	5.011	
		5.222		
		4.802		
0.01	**Apical-to-basolateral**	3.301	4.059	1.196
		3.630		
		5.246		
	Basolateral-to-apical	4.611	4.853	
		4.908		
		5.040		
0.015	**Apical-to-basolateral**	2.387	2.698	1.323
		3.114		
		2.594		
	Basolateral-to-apical	3.637	3.569	
		3.732		
		3.340		
0.03	**Apical-to-basolateral**	2.965	2.552	0.780
		2.178		
		2.512		
	Basolateral-to-apical	1.834	1.991	
		1.944		
		2.197		

Table D.3: Apparent permeability (P_{app}) values and efflux ratios (ER) for sodium starch glycolate (Explotab®) at selected test concentrations

Concentration (% w/v)	Transport direction	P_{app} (x 10^{-7})	Average P_{app} (x 10^{-7})	Efflux ratio
0.002	**Apical-to-basolateral**	3.005	2.402	1.110
		2.438		
		1.763		
	Basolateral-to-apical	2.172	2.666	
		3.065		
		2.761		
0.004	**Apical-to-basolateral**	1.751	2.236	1.070
		1.822		
		3.135		
	Basolateral-to-apical	2.450	2.392	
		1.719		
		3.00		
0.008	**Apical-to-basolateral**	1.603	2.304	1.024
		2.948		
		2.363		
	Basolateral-to-apical	2.287	2.360	
		1.879		
		2.915		
0.016	**Apical-to-basolateral**	2.505	2.209	1.203
		1.369		
		2.753		
	Basolateral-to-apical	2.368	2.658	
		2.393		
		3.213		

Table D.4: Apparent permeability (P_{app}) values and efflux ratios (ER) for crospovidone (Kollidon® CL-M) at selected test concentrations

Concentration (% w/v)	Transport direction	P_{app} (x 10^{-7})	Average P_{app} (x 10^{-7})	Efflux ratio
0.002	**Apical-to-basolateral**	3.665	3.457	0.966
		3.552		
		3.154		
	Basolateral-to-apical	2.981	3.341	
		3.668		
		3.374		
0.004	**Apical-to-basolateral**	4.769	4.841	0.674
		4.278		
		5.477		
	Basolateral-to-apical	3.569	3.263	
		2.469		
		3.750		
0.005	**Apical-to-basolateral**	3.178	5.093	0.546
		6.453		
		5.648		
	Basolateral-to-apical	2.714	2.782	
		2.516		
		3.117		
0.01	**Apical-to-basolateral**	7.719	7.598	0.178
		8.250		
		6.824		
	Basolateral-to-apical	1.273	1.351	
		1.477		
		1.303		

Table D.5: Apparent permeability (P_{app}) values and efflux ratios (ER) for sodium alginate at selected test concentrations

Concentration (% w/v)	Transport direction	P_{app} (x 10^{-7})	Average P_{app} (x 10^{-7})	Efflux ratio
0.0025	**Apical-to-basolateral**	3.327	3.922	0.414
		3.607		
		4.832		
	Basolateral-to-apical	1.714	1.625	
		1.500		
		1.663		
0.005	**Apical-to-basolateral**	2.463	3.981	0.541
		4.077		
		5.401		
	Basolateral-to-apical	2.663	2.155	
		1.926		
		1.874		
0.01	**Apical-to-basolateral**	2.525	2.786	1.207
		2.287		
		3.546		
	Basolateral-to-apical	2.040	3.363	
		3.780		
		4.270		
0.02	**Apical-to-basolateral**	2.556	2.174	1.465
		2.178		
		1.789		
	Basolateral-to-apical	2.801	3.186	
		3.821		
		2.936		

ADDENDUM E

TRANS-EPITHELIAL ELECTRICAL RESISTANCE (TEER) MEASUREMENTS

Table E.1: Apical-to-basolateral TEER measurements across excised pig jejunum in the presence of Rhodamine 123 alone

	TEER			
Time (min)	**Chamber 1**	**Chamber 2**	**Chamber 3**	**Average**
0	24.00	23.00	24.00	23.67
20	23.00	21.00	18.00	20.67
40	21.00	20.00	27.00	22.67
60	21.00	23.00	23.00	22.33
80	18.00	15.00	25.00	19.33
100	19.00	19.00	20.00	19.33
120	23.00	19.00	23.00	21.67
Percentage change	95.83	82.61	95.83	91.43

Table E.2: Basolateral-to-apical TEER measurements across excised pig jejunum in the presence of Rhodamine 123 alone

	TEER			
Time (min)	**Chamber 1**	**Chamber 2**	**Chamber 3**	**Average**
0	43.00	52.00	48.00	47.67
20	64.00	88.00	86.00	79.33
40	47.00	123.00	126.00	98.67
60	52.00	98.00	80.00	76.67
80	53.00	84.00	81.00	72.67
100	50.00	78.00	108.00	78.67
120	39.00	85.00	104.00	76.00
Percentage change	90.70	163.46	216.67	156.94

Table E.3: Apical-to-basolateral TEER measurements across excised pig jejunum in the presence of 0.0005% (w/v) croscarmellose sodium (Ac-di-sol®)

	TEER			
Time (min)	**Chamber 1**	**Chamber 2**	**Chamber 3**	**Average**
0	55.00	40.00	86.00	60.33
20	48.00	110.00	105.00	87.67
40	111.00	48.00	66.00	75.00
60	43.00	36.00	44.00	41.00
80	39.00	37.00	39.00	38.33
100	38.00	36.00	32.00	35.33
120	26.00	32.00	25.00	27.67
Percentage change	47.27	80.00	29.07	52.11

Table E.4: Basolateral-to-apical TEER measurements across excised pig jejunum in the presence of 0.0005% (w/v) croscarmellose sodium (Ac-di-sol®)

	TEER			
Time (min)	**Chamber 1**	**Chamber 2**	**Chamber 3**	**Average**
0	22.00	27.00	18.00	22.33
20	21.00	26.00	14.00	20.33
40	29.00	36.00	35.00	33.33
60	16.00	21.00	12.00	16.33
80	28.00	27.00	33.00	29.33
100	16.00	23.00	18.00	19.00
120	12.00	17.00	10.00	13.00
Percentage change	54.55	62.96	55.56	57.69

Table E.5: Apical-to-basolateral TEER measurements across excised pig jejunum in the presence of 0.001% (w/v) croscarmellose sodium (Ac-di-sol®)

	TEER			
Time (min)	**Chamber 1**	**Chamber 2**	**Chamber 3**	**Average**
0	21.00	17.00	26.00	21.33
20	16.00	11.00	24.00	17.00
40	14.00	29.00	14.00	19.00
60	10.00	34.00	19.00	21.00
80	9.00	8.00	12.00	9.67
100	20.00	20.00	19.00	19.67
120	15.00	15.00	5.00	11.67
Percentage change	71.43	88.24	19.23	59.63

Table E.6: Basolateral-to-apical TEER measurements across excised pig jejunum in the presence of 0.001% (w/v) croscarmellose sodium (Ac-di-sol®)

	TEER			
Time (min)	**Chamber 1**	**Chamber 2**	**Chamber 3**	**Average**
0	22.00	25.00	18.00	21.67
20	28.00	22.00	24.00	24.67
40	40.00	45.00	48.00	44.33
60	19.00	32.00	27.00	26.00
80	21.00	23.00	23.00	22.33
100	10.00	18.00	20.00	16.00
120	8.00	5.00	14.00	9.00
Percentage change	36.36	20.00	77.78	44.71

Table E.7: Apical-to-basolateral TEER measurements across excised pig jejunum in the presence of 0.005% (w/v) croscarmellose sodium (Ac-di-sol®)

	TEER			
Time (min)	**Chamber 1**	**Chamber 2**	**Chamber 3**	**Average**
0	50.00	53.00	72.00	58.33
20	52.00	55.00	63.00	56.67
40	66.00	52.00	61.00	59.67
60	63.00	54.00	58.00	58.33
80	45.00	41.00	42.00	42.67
100	49.00	47.00	63.00	53.00
120	47.00	38.00	52.00	45.67
Percentage change	94.00	71.70	72.22	79.31

Table E.8: Basolateral-to-apical TEER measurements across excised pig jejunum in the presence of 0.005% (w/v) croscarmellose sodium (Ac-di-sol®)

	TEER			
Time (min)	**Chamber 1**	**Chamber 2**	**Chamber 3**	**Average**
0	41.00	38.00	42.00	40.33
20	38.00	37.00	41.00	38.67
40	46.00	47.00	49.00	47.33
60	38.00	38.00	49.00	41.67
80	22.00	34.00	71.00	42.33
100	64.00	52.00	52.00	56.00
120	30.00	29.00	36.00	31.67
Percentage change	73.17	76.32	85.71	78.40

Table E.9: Apical-to-basolateral TEER measurements across excised pig jejunum in the presence of 0.01% (w/v) croscarmellose sodium (Ac-di-sol®)

	TEER			
Time (min)	**Chamber 1**	**Chamber 2**	**Chamber 3**	**Average**
0	16.00	18.00	22.00	18.67
20	38.00	41.00	32.00	37.00
40	16.00	18.00	13.00	15.67
60	19.00	19.00	17.00	18.33
80	6.00	10.00	3.00	6.33
100	-*	-*	-*	-*
120	-*	-*	-*	-*
Percentage change	37.50	55.56	13.64	35.56

(*Inconclusive/Insufficient data)

Table E.10: Basolateral-to-apical TEER measurements across excised pig jejunum in the presence of 0.01% (w/v) croscarmellose sodium (Ac-di-sol®)

	TEER			
Time (min)	**Chamber 1**	**Chamber 2**	**Chamber 3**	**Average**
0	31.00	36.00	47.00	38.00
20	29.00	33.00	39.00	33.67
40	13.00	13.00	17.00	14.33
60	14.00	18.00	23.00	18.33
80	12.00	17.00	19.00	16.00
100	14.00	17.00	19.00	16.67
120	17.00	19.00	14.00	16.67
Percentage change	54.84	52.78	29.79	45.80

Table E.11: Apical-to-basolateral TEER measurements across excised pig jejunum in the presence of 0.005% (w/v) microcrystalline cellulose (Avicel® PH-200)

	TEER			
Time (min)	**Chamber 1**	**Chamber 2**	**Chamber 3**	**Average**
0	45.00	41.00	38.00	41.33
20	35.00	40.00	31.00	35.33
40	37.00	34.00	29.00	33.33
60	32.00	34.00	29.00	31.67
80	29.00	31.00	28.00	29.33
100	31.00	32.00	25.00	29.33
120	28.00	31.00	29.00	29.33
Percentage change	62.22	75.61	76.32	71.38

Table E.12: Basolateral-to-apical TEER measurements across excised pig jejunum in the presence of 0.005% (w/v) microcrystalline cellulose (Avicel® PH-200)

	TEER			
Time (min)	**Chamber 1**	**Chamber 2**	**Chamber 3**	**Average**
0	57.00	68.00	57.00	60.67
20	61.00	76.00	75.00	70.67
40	58.00	80.00	71.00	69.67
60	49.00	65.00	60.00	58.00
80	74.00	84.00	89.00	82.33
100	75.00	87.00	97.00	86.33
120	72.00	106.00	101.00	93.00
Percentage change	126.32	155.88	177.19	153.13

Table E.13: Apical-to-basolateral TEER measurements across excised pig jejunum in the presence of 0.01% (w/v) microcrystalline cellulose (Avicel® PH-200)

	TEER			
Time (min)	**Chamber 1**	**Chamber 2**	**Chamber 3**	**Average**
0	16.00	26.00	31.00	24.33
20	23.00	29.00	23.00	25.00
40	27.00	37.00	33.00	32.33
60	23.00	27.00	23.00	24.33
80	23.00	25.00	20.00	22.67
100	19.00	31.00	24.00	24.67
120	17.00	31.00	17.00	21.67
Percentage change	106.25	119.23	54.84	93.44

Table E.14: Basolateral-to-apical TEER measurements across excised pig jejunum in the presence of 0.01% (w/v) microcrystalline cellulose (Avicel® PH-200)

	TEER			
Time (min)	**Chamber 1**	**Chamber 2**	**Chamber 3**	**Average**
0	62.00	67.00	74.00	67.67
20	60.00	84.00	75.00	73.00
40	86.00	96.00	98.00	93.33
60	77.00	108.00	101.00	95.33
80	67.00	130.00	108.00	101.67
100	55.00	110.00	117.00	94.00
120	81.00	113.00	124.00	106.00
Percentage change	130.65	168.66	167.57	155.62

Table E.15: Apical-to-basolateral TEER measurements across excised pig jejunum in the presence of 0.015% (w/v) microcrystalline cellulose (Avicel® PH-200)

	TEER			
Time (min)	**Chamber 1**	**Chamber 2**	**Chamber 3**	**Average**
0	61.00	80.00	87.00	76.00
20	42.00	33.00	32.00	35.67
40	37.00	41.00	50.00	42.67
60	36.00	34.00	36.00	35.33
80	34.00	30.00	40.00	34.67
100	48.00	40.00	50.00	46.00
120	49.00	47.00	47.00	47.67
Percentage change	80.33	58.75	54.02	64.37

Table E.16: Basolateral-to-apical TEER measurements across excised pig jejunum in the presence of 0.015% (w/v) microcrystalline cellulose (Avicel® PH-200)

	TEER			
Time (min)	**Chamber 1**	**Chamber 2**	**Chamber 3**	**Average**
0	33.00	38.00	46.00	39.00
20	49.00	60.00	64.00	57.67
40	79.00	71.00	84.00	78.00
60	66.00	60.00	62.00	62.67
80	53.00	58.00	83.00	64.67
100	74.00	66.00	70.00	70.00
120	51.00	77.00	112.00	80.00
Percentage change	154.55	202.63	243.48	200.22

Table E.17: Apical-to-basolateral TEER measurements across excised pig jejunum in the presence of 0.03% (w/v) microcrystalline cellulose (Avicel® PH-200)

	TEER			
Time (min)	**Chamber 1**	**Chamber 2**	**Chamber 3**	**Average**
0	36.00	43.00	37.00	38.67
20	46.00	40.00	33.00	39.67
40	26.00	38.00	37.00	33.67
60	23.00	35.00	33.00	30.33
80	23.00	35.00	44.00	34.00
100	34.00	38.00	53.00	41.67
120	17.00	44.00	31.00	30.67
Percentage change	47.22	102.33	83.78	77.78

Table E.18: Basolateral-to-apical TEER measurements across excised pig jejunum in the presence of 0.03% (w/v) microcrystalline cellulose (Avicel® PH-200)

	TEER			
Time (min)	**Chamber 1**	**Chamber 2**	**Chamber 3**	**Average**
0	44.00	54.00	50.00	49.33
20	45.00	58.00	56.00	53.00
40	56.00	50.00	74.00	60.00
60	52.00	79.00	61.00	64.00
80	42.00	58.00	74.00	58.00
100	62.00	75.00	68.00	68.33
120	64.00	69.00	76.00	69.67
Percentage change	145.45	127.78	152.00	141.74

Table E.19: Apical-to-basolateral TEER measurements across excised pig jejunum in the presence of 0.002% (w/v) sodium starch glycolate (Explotab®)

	TEER			
Time (min)	**Chamber 1**	**Chamber 2**	**Chamber 3**	**Average**
0	58.00	51.00	45.00	51.33
20	51.00	44.00	36.00	43.67
40	48.00	63.00	57.00	56.00
60	45.00	44.00	34.00	41.00
80	48.00	55.00	45.00	49.33
100	47.00	41.00	47.00	45.00
120	49.00	46.00	45.00	46.67
Percentage change	84.48	90.20	100.00	91.56

Table E.20: Basolateral-to-apical TEER measurements across excised pig jejunum in the presence of 0.002% (w/v) sodium starch glycolate (Explotab®)

	TEER			
Time (min)	**Chamber 1**	**Chamber 2**	**Chamber 3**	**Average**
0	24.00	29.00	27.00	26.67
20	34.00	33.00	43.00	36.67
40	28.00	32.00	41.00	33.67
60	30.00	30.00	39.00	33.00
80	39.00	38.00	35.00	37.33
100	29.00	61.00	51.00	47.00
120	43.00	50.00	51.00	48.00
Percentage change	179.17	172.41	188.89	180.16

Table E.21: Apical-to-basolateral TEER measurements across excised pig jejunum in the presence of 0.004% (w/v) sodium starch glycolate (Explotab®)

	TEER			
Time (min)	**Chamber 1**	**Chamber 2**	**Chamber 3**	**Average**
0	37.00	22.00	27.00	28.67
20	50.00	34.00	33.00	39.00
40	47.00	58.00	42.00	49.00
60	37.00	26.00	32.00	31.67
80	35.00	34.00	27.00	32.00
100	46.00	40.00	49.00	45.00
120	45.00	37.00	25.00	35.67
Percentage change	121.62	168.18	92.59	127.47

Table E.22: Basolateral-to-apical TEER measurements across excised pig jejunum in the presence of 0.004% (w/v) sodium starch glycolate (Explotab®)

	TEER			
Time (min)	**Chamber 1**	**Chamber 2**	**Chamber 3**	**Average**
0	47.00	57.00	46.00	50.00
20	58.00	71.00	67.00	65.33
40	54.00	66.00	58.00	59.33
60	54.00	73.00	81.00	69.33
80	50.00	84.00	91.00	75.00
100	52.00	55.00	90.00	65.67
120	83.00	108.00	99.00	96.67
Percentage change	176.60	189.47	215.22	193.76

Table E.23: Apical-to-basolateral TEER measurements across excised pig jejunum in the presence of 0.008% (w/v) sodium starch glycolate (Explotab®)

	TEER			
Time (min)	**Chamber 1**	**Chamber 2**	**Chamber 3**	**Average**
0	32.00	30.00	24.00	28.67
20	71.00	52.00	55.00	59.33
40	42.00	43.00	46.00	43.67
60	42.00	39.00	41.00	40.67
80	30.00	39.00	43.00	37.33
100	38.00	37.00	39.00	38.00
120	35.00	34.00	31.00	33.33
Percentage change	109.38	113.33	129.17	117.29

Table E.24: Basolateral-to-apical TEER measurements across excised pig jejunum in the presence of 0.008% (w/v) sodium starch glycolate (Explotab®)

	TEER			
Time (min)	**Chamber 1**	**Chamber 2**	**Chamber 3**	**Average**
0	43.00	47.00	39.00	43.00
20	40.00	41.00	36.00	39.00
40	39.00	40.00	32.00	37.00
60	73.00	73.00	31.00	59.00
80	54.00	71.00	42.00	55.67
100	45.00	46.00	32.00	41.00
120	70.00	66.00	37.00	57.67
Percentage change	162.79	140.43	94.87	132.70

Table E.25: Apical-to-basolateral TEER measurements across excised pig jejunum in the presence of 0.016% (w/v) sodium starch glycolate (Explotab®)

	TEER			
Time (min)	**Chamber 1**	**Chamber 2**	**Chamber 3**	**Average**
0	32.00	45.00	49.00	42.00
20	65.00	78.00	63.00	68.67
40	73.00	45.00	38.00	52.00
60	25.00	29.00	26.00	26.67
80	23.00	20.00	35.00	26.00
100	21.00	24.00	22.00	22.33
120	20.00	20.00	27.00	22.33
Percentage change	62.50	44.44	55.10	54.02

Table E.26: Basolateral-to-apical TEER measurements across excised pig jejunum in the presence of 0.016% (w/v) sodium starch glycolate (Explotab®)

	TEER			
Time (min)	**Chamber 1**	**Chamber 2**	**Chamber 3**	**Average**
0	22.00	28.00	26.00	25.33
20	31.00	32.00	39.00	34.00
40	21.00	35.00	27.00	27.67
60	23.00	41.00	47.00	37.00
80	34.00	41.00	33.00	36.00
100	32.00	43.00	47.00	40.67
120	31.00	45.00	41.00	39.00
Percentage change	140.91	160.71	157.69	153.11

Table E.27: Apical-to-basolateral TEER measurements across excised pig jejunum in the presence of 0.002% (w/v) crospovidone (Kollidon® CL-M)

	TEER			
Time (min)	**Chamber 1**	**Chamber 2**	**Chamber 3**	**Average**
0	55.00	67.00	82.00	68.00
20	77.00	96.00	94.00	89.00
40	67.00	79.00	41.00	62.33
60	67.00	62.00	48.00	59.00
80	58.00	62.00	54.00	58.00
100	54.00	43.00	39.00	45.33
120	51.00	49.00	43.00	47.67
Percentage change	92.73	73.13	52.44	72.77

Table E.28: Basolateral-to-apical TEER measurements across excised pig jejunum in the presence of 0.002% (w/v) crospovidone (Kollidon® CL-M)

	TEER			
Time (min)	**Chamber 1**	**Chamber 2**	**Chamber 3**	**Average**
0	-*	-*	-*	-*
20	-*	-*	-*	-*
40	36.00	53.00	58.00	49.00
60	30.00	35.00	42.00	35.67
80	33.00	42.00	53.00	42.67
100	35.00	33.00	53.00	40.33
120	35.00	54.00	65.00	51.33
Percentage change	97.22	101.89	112.07	103.73

(*Inconclusive/Insufficient data)

Table E.29: Apical-to-basolateral TEER measurements across excised pig jejunum in the presence of 0.004% (w/v) crospovidone (Kollidon® CL-M)

	TEER			
Time (min)	**Chamber 1**	**Chamber 2**	**Chamber 3**	**Average**
0	43.00	51.00	43.00	45.67
20	34.00	53.00	43.00	43.33
40	38.00	71.00	80.00	63.00
60	58.00	82.00	60.00	66.67
80	35.00	57.00	59.00	50.33
100	36.00	62.00	62.00	53.33
120	45.00	64.00	51.00	53.33
Percentage change	104.65	125.49	118.60	116.25

Table E.30: Basolateral-to-apical TEER measurements across excised pig jejunum in the presence of 0.004% (w/v) crospovidone (Kollidon® CL-M)

	TEER			
Time (min)	**Chamber 1**	**Chamber 2**	**Chamber 3**	**Average**
0	66.00	51.00	75.00	64.00
20	55.00	80.00	79.00	71.33
40	58.00	96.00	63.00	72.33
60	64.00	116.00	53.00	77.67
80	60.00	123.00	64.00	82.33
100	66.00	123.00	86.00	91.67
120	70.00	61.00	80.00	70.33
Percentage change	106.06	119.61	106.67	110.78

Table E.31: Apical-to-basolateral TEER measurements across excised pig jejunum in the presence of 0.005% (w/v) crospovidone (Kollidon® CL-M)

	TEER			
Time (min)	**Chamber 1**	**Chamber 2**	**Chamber 3**	**Average**
0	33.00	51.00	52.00	45.33
20	39.00	38.00	34.00	37.00
40	32.00	31.00	51.00	38.00
60	28.00	28.00	38.00	31.33
80	31.00	32.00	35.00	32.67
100	41.00	44.00	56.00	47.00
120	47.00	53.00	61.00	53.67
Percentage change	142.42	103.92	117.31	121.22

Table E.32: Basolateral-to-apical TEER measurements across excised pig jejunum in the presence of 0.005% (w/v) crospovidone (Kollidon® CL-M)

	TEER			
Time (min)	**Chamber 1**	**Chamber 2**	**Chamber 3**	**Average**
0	41.00	78.00	77.00	65.33
20	51.00	116.00	93.00	86.67
40	62.00	96.00	94.00	84.00
60	56.00	84.00	79.00	73.00
80	46.00	93.00	131.00	90.00
100	54.00	116.00	102.00	90.67
120	52.00	123.00	108.00	94.33
Percentage change	126.83	157.69	140.26	141.59

Table E.33: Apical-to-basolateral TEER measurements across excised pig jejunum in the presence of 0.01% (w/v) crospovidone (Kollidon® CL-M)

	TEER			
Time (min)	**Chamber 1**	**Chamber 2**	**Chamber 3**	**Average**
0	42.00	43.00	51.00	45.33
20	41.00	58.00	57.00	52.00
40	59.00	51.00	74.00	61.33
60	47.00	47.00	62.00	52.00
80	39.00	46.00	44.00	43.00
100	43.00	46.00	47.00	45.33
120	35.00	43.00	44.00	40.67
Percentage change	83.33	100.00	86.27	89.87

Table E.34: Basolateral-to-apical TEER measurements across excised pig jejunum in the presence of 0.01% (w/v) crospovidone (Kollidon® CL-M)

	TEER			
Time (min)	**Chamber 1**	**Chamber 2**	**Chamber 3**	**Average**
0	35.00	47.00	35.00	39.00
20	38.00	53.00	33.00	41.33
40	29.00	50.00	37.00	38.67
60	33.00	44.00	39.00	38.67
80	38.00	45.00	40.00	41.00
100	31.00	55.00	90.00	58.67
120	32.00	47.00	45.00	41.33
Percentage change	91.43	100.00	128.57	106.67

Table E.35: Apical-to-basolateral TEER measurements across excised pig jejunum in the presence of 0.0025% (w/v) sodium alginate

	TEER			
Time (min)	**Chamber 1**	**Chamber 2**	**Chamber 3**	**Average**
0	39.00	47.00	59.00	48.33
20	41.00	39.00	47.00	42.33
40	42.00	44.00	65.00	50.33
60	39.00	51.00	65.00	51.67
80	44.00	54.00	42.00	46.67
100	41.00	50.00	39.00	43.33
120	42.00	35.00	37.00	38.00
Percentage change	107.69	74.47	62.71	81.62

Table E.36: Basolateral-to-apical TEER measurements across excised pig jejunum in the presence of 0.0025% (w/v) sodium alginate

	TEER			
Time (min)	**Chamber 1**	**Chamber 2**	**Chamber 3**	**Average**
0	138.00	116.00	150.00	134.67
20	72.00	85.00	82.00	79.67
40	81.00	85.00	75.00	80.33
60	54.00	60.00	66.00	60.00
80	66.00	75.00	97.00	79.33
100	58.00	84.00	117.00	86.33
120	54.00	87.00	93.00	78.00
Percentage change	39.13	75.00	62.00	58.71

Table E.37: Apical-to-basolateral TEER measurements across excised pig jejunum in the presence of 0.005% (w/v) sodium alginate

	TEER			
Time (min)	**Chamber 1**	**Chamber 2**	**Chamber 3**	**Average**
0	47.00	40.00	41.00	42.67
20	56.00	57.00	45.00	52.67
40	49.00	41.00	41.00	43.67
60	43.00	57.00	51.00	50.33
80	33.00	38.00	38.00	36.33
100	40.00	37.00	45.00	40.67
120	38.00	36.00	45.00	39.67
Percentage change	80.85	90.00	109.76	93.54

Table E.38: Basolateral-to-apical TEER measurements across excised pig jejunum in the presence of 0.005% (w/v) sodium alginate

	TEER			
Time (min)	**Chamber 1**	**Chamber 2**	**Chamber 3**	**Average**
0	39.00	33.00	40.00	37.33
20	29.00	44.00	45.00	39.33
40	25.00	33.00	48.00	35.33
60	26.00	44.00	61.00	43.67
80	29.00	57.00	61.00	49.00
100	26.00	33.00	72.00	43.67
120	27.00	29.00	40.00	32.00
Percentage change	69.23	87.88	100.00	85.70

Table E.39: Apical-to-basolateral TEER measurements across excised pig jejunum in the presence of 0.01% (w/v) sodium alginate

	TEER			
Time (min)	**Chamber 1**	**Chamber 2**	**Chamber 3**	**Average**
0	59.00	66.00	82.00	69.00
20	116.00	116.00	102.00	111.33
40	47.00	80.00	125.00	84.00
60	52.00	86.00	61.00	66.33
80	66.00	85.00	73.00	74.67
100	48.00	61.00	65.00	58.00
120	44.00	65.00	67.00	58.67
Percentage change	74.58	98.48	81.71	84.92

Table E.40: Basolateral-to-apical TEER measurements across excised pig jejunum in the presence of 0.01% (w/v) sodium alginate

	TEER			
Time (min)	**Chamber 1**	**Chamber 2**	**Chamber 3**	**Average**
0	49.00	46.00	42.00	45.67
20	47.00	50.00	52.00	49.67
40	50.00	64.00	46.00	53.33
60	46.00	79.00	47.00	57.33
80	43.00	75.00	53.00	57.00
100	43.00	71.00	46.00	53.33
120	52.00	72.00	47.00	57.00
Percentage change	106.12	156.52	111.90	124.85

Table E.41: Apical-to-basolateral TEER measurements across excised pig jejunum in the presence of 0.02% (w/v) sodium alginate

	TEER			
Time (min)	**Chamber 1**	**Chamber 2**	**Chamber 3**	**Average**
0	32.00	37.00	43.00	37.33
20	92.00	88.00	86.00	88.67
40	42.00	41.00	42.00	41.67
60	52.00	80.00	58.00	63.33
80	44.00	42.00	55.00	47.00
100	44.00	56.00	50.00	50.00
120	31.00	36.00	52.00	39.67
Percentage change	96.88	97.30	120.93	105.03

Table E.42: Basolateral-to-apical TEER measurements across excised pig jejunum in the presence of 0.02% (w/v) sodium alginate

	TEER			
Time (min)	**Chamber 1**	**Chamber 2**	**Chamber 3**	**Average**
0	47.00	43.00	47.00	45.67
20	75.00	52.00	66.00	64.33
40	70.00	77.00	94.00	80.33
60	45.00	59.00	79.00	61.00
80	51.00	64.00	79.00	64.67
100	45.00	65.00	76.00	62.00
120	50.00	62.00	67.00	59.67
Percentage change	106.38	144.19	142.55	131.04

ADDENDUM F

STATYSTICAL ANALYSIS

Table F.1: Apical-to-basolateral descriptive statistics for apparent permeability of Rhodamine 123 over excised pig jejunum

Disintegrant description	N	Mean	Standard deviation	Standard error	95% confidence interval for mean		Minimum	Maximum
					Lower bound	Upper Bound		
Rhodamine 123 alone	3	.000000261	.000000052	.000000030	.000000131	.000000390	.000000225	.000000320
Ac-di-sol® 0.0005% (w/v)	3	.000000458	.000000074	.000000043	.000000275	.000000641	.000000391	.000000537
Ac-di-sol® 0.001% (w/v)	3	.000000477	.000000097	.000000056	.000000236	.000000719	.000000380	.000000574
Ac-di-sol® 0.005% (w/v)	3	.000000854	.000000137	.000000079	.000000514	.000001194	.000000696	.000000944
Ac-di-sol® 0.01% (w/v)	3	.000001874	.000000357	.000000206	.000000988	.000002760	.000001511	.000002224
Avicel® PH-200 0.005% (w/v)	3	.000000559	.000000087	.000000050	.000000344	.000000774	.000000481	.000000652
Avicel® PH-200 0.01% (w/v)	3	.000000406	.000000104	.000000060	.000000147	.000000665	.000000330	.000000525
Avicel® PH-200 0.015% (w/v)	3	.000000270	.000000037	.000000022	.000000177	.000000363	.000000239	.000000311
Avicel® PH-200 0.03% (w/v)	3	.000000255	.000000039	.000000023	.000000157	.000000353	.000000218	.000000296
Explotab® 0.002% (w/v)	3	.000000240	.000000062	.000000036	.000000086	.000000395	.000000176	.000000300
Explotab® 0.004% (w/v)	3	.000000224	.000000078	.000000045	.000000030	.000000417	.000000175	.000000314
Explotab® 0.008% (w/v)	3	.000000230	.000000067	.000000039	.000000063	.000000398	.000000160	.000000295
Explotab® 0.016% (w/v)	3	.000000221	.000000074	.000000043	.000000037	.000000404	.000000137	.000000275
Kollidon® CL-M 0.002% (w/v)	3	.000000346	.000000027	.000000015	.000000279	.000000412	.000000315	.000000366
Kollidon® CL-M 0.004% (w/v)	3	.000000484	.000000060	.000000035	.000000334	.000000634	.000000428	.000000548
Kollidon® CL-M 0.005% (w/v)	3	.000000509	.000000171	.000000099	.000000085	.000000933	.000000318	.000000645
Kollidon® CL-M 0.01% (w/v)	3	.000000760	.000000072	.000000042	.000000581	.000000939	.000000682	.000000825
Sodium alginate 0.0025% (w/v)	3	.000000392	.000000080	.000000046	.000000193	.000000591	.000000333	.000000483
Sodium alginate 0.005% (w/v)	3	.000000398	.000000147	.000000085	.000000033	.000000764	.000000246	.000000540
Sodium alginate 0.01% (w/v)	3	.000000279	.000000067	.000000039	.000000112	.000000445	.000000229	.000000355
Sodium alginate 0.02% (w/v)	3	.000000217	.000000038	.000000022	.000000122	.000000313	.000000179	.000000256
Total	63	.000000463	.000000374	.000000047	.000000368	.000000557	.000000137	.000002224

Table F.2: Basolateral-to-apical descriptive statistics for apparent permeability of Rhodamine 123 over excised pig jejunum

Disintegrant description	N	Mean	Standard deviation	Standard error	95% confidence interval for mean		Minimum	Maximum
					Lower bound	Upper Bound		
Rhodamine 123 alone	3	.000000574	.000000197	.000000114	.000000085	.000001064	.000000401	.000000788
Ac-di-sol® 0.0005% (w/v)	3	.000000788	.000000118	.000000068	.000000496	.000001081	.000000685	.000000917
Ac-di-sol® 0.001% (w/v)	3	.000000619	.000000063	.000000036	.000000463	.000000774	.000000548	.000000666
Ac-di-sol® 0.005% (w/v)	3	.000000471	.000000083	.000000048	.000000264	.000000679	.000000421	.000000568
Ac-di-sol® 0.01% (w/v)	3	.000000275	.000000031	.000000018	.000000198	.000000352	.000000244	.000000306
Avicel® PH-200 0.005% (w/v)	3	.000000501	.000000021	.000000012	.000000449	.000000553	.000000480	.000000522
Avicel® PH-200 0.01% (w/v)	3	.000000485	.000000022	.000000013	.000000431	.000000540	.000000461	.000000504
Avicel® PH-200 0.015% (w/v)	3	.000000357	.000000020	.000000012	.000000306	.000000408	.000000334	.000000373
Avicel® PH-200 0.03% (w/v)	3	.000000199	.000000019	.000000011	.000000153	.000000245	.000000183	.000000220
Explotab® 0.002% (w/v)	3	.000000267	.000000045	.000000026	.000000154	.000000379	.000000217	.000000307
Explotab® 0.004% (w/v)	3	.000000239	.000000065	.000000037	.000000079	.000000400	.000000172	.000000301
Explotab® 0.008% (w/v)	3	.000000236	.000000052	.000000030	.000000106	.000000366	.000000188	.000000291
Explotab® 0.016% (w/v)	3	.000000266	.000000048	.000000028	.000000146	.000000385	.000000237	.000000321
Kollidon® CL-M 0.002% (w/v)	3	.000000334	.000000034	.000000020	.000000248	.000000420	.000000298	.000000367
Kollidon® CL-M 0.004% (w/v)	3	.000000326	.000000069	.000000040	.000000154	.000000499	.000000247	.000000375
Kollidon® CL-M 0.005% (w/v)	3	.000000278	.000000031	.000000018	.000000202	.000000354	.000000252	.000000312
Kollidon® CL-M 0.01% (w/v)	3	.000000135	.000000011	.000000006	.000000108	.000000163	.000000127	.000000148
Sodium alginate 0.0025% (w/v)	3	.000000163	.000000011	.000000006	.000000135	.000000190	.000000150	.000000171
Sodium alginate 0.005% (w/v)	3	.000000215	.000000044	.000000025	.000000106	.000000325	.000000187	.000000266
Sodium alginate 0.01% (w/v)	3	.000000336	.000000117	.000000068	.000000045	.000000628	.000000204	.000000427
Sodium alginate 0.02% (w/v)	3	.000000319	.000000055	.000000032	.000000181	.000000456	.000000280	.000000382
Total	63	.000000352	.000000172	.000000022	.000000308	.000000395	.000000127	.000000917

Table F.3: ANOVA analysis of apical-to-basolateral transport studies across excised pig jejunum (*statistically significant differences compared to the control, $p \leq 0.05$)

	Sum of squares ($\times 10^{-12}$)	**df**	**Mean square ($\times 10^{-14}$)**	**F**	**Sigificance ($\times 10^{-19}$)**
Between groups	8.115	20	0.406	30.713	6.902*
Within groups	0.555	42	1.321		
Total	8.669	62			

Table F.4: ANOVA analysis of basolateral-to-apical transport studies across excised pig jejunum (*statistically significant differences compared to the control, $p \leq 0.05$)

	Sum of squares ($\times 10^{-12}$)	**df**	**Mean square ($\times 10^{-14}$)**	**F**	**Sigificance ($\times 10^{-14}$)**
Between groups	1.635	20	8.175	16.612	5.824*
Within groups	0.207	42	0.492		
Total	1.842	62			

Table F.5: Dunnett's t-test for post hoc multiple comparison of apical-to-basolateral transport of Rhodamine 123 in the presence of selected disintegrants over excised pig jejunum (*statistically significant differences when compared to the control, $p \leq 0.05$)

Disintegrant description	Mean difference	Standard error	Significance	95% confidence interval	
				Lower bound	Upper bound
Ac-di-sol® 0.0005% (w/v)	.000000198	.000000094	.347467946	-.000000088	.000000484
Ac-di-sol® 0.001% (w/v)	.000000217	.000000094	.243753629	-.000000069	.000000503
Ac-di-sol® 0.005% (w/v)	.000000593	.000000094	.000002553*	.000000307	.000000879
Ac-di-sol® 0.01% (w/v)	.000001613	.000000094	.000000016*	.000001327	.000001899
Avicel® PH-200 0.005% (w/v)	.000000298	.000000094	.036130806*	.000000012	.000000584
Avicel® PH-200 0.01% (w/v)	.000000145	.000000094	.738033626	-.000000141	.000000431
Avicel® PH-200 0.015% (w/v)	.000000009	.000000094	1.000000000	-.000000277	.000000295
Avicel® PH-200 0.03% (w/v)	-.000000005	.000000094	1.000000000	-.000000291	.000000281
Explotab® 0.002% (w/v)	-.000000020	.000000094	1.000000000	-.000000306	.000000266
Explotab® 0.004% (w/v)	-.000000037	.000000094	.999999992	-.000000323	.000000249
Explotab® 0.008% (w/v)	-.000000030	.000000094	1.000000000	-.000000316	.000000256
Explotab® 0.016% (w/v)	-.000000040	.000000094	.999999973	-.000000326	.000000246
Kollidon® CL-M 0.002% (w/v)	.000000085	.000000094	.994493737	-.000000201	.000000371
Kollidon® CL-M 0.004% (w/v)	.000000224	.000000094	.212383938	-.000000062	.000000510
Kollidon® CL-M 0.005% (w/v)	.000000249	.000000094	.123334817	-.000000037	.000000535
Kollidon® CL-M 0.01% (w/v)	.000000499	.000000094	.000066867*	.000000213	.000000785
Sodium alginate 0.0025% (w/v)	.000000132	.000000094	.836072150	-.000000154	.000000418
Sodium alginate 0.005% (w/v)	.000000138	.000000094	.796080102	-.000000148	.000000424
Sodium alginate 0.01% (w/v)	.000000018	.000000094	1.000000000	-.000000268	.000000304
Sodium alginate 0.02% (w/v)	-.000000043	.000000094	.999999879	-.000000329	.000000243

Table F.6: Dunnett's t-test for post hoc multiple comparison of basolateral-to-apical transport of Rhodamine 123 in the presence of selected disintegrants over excised pig jejunum (*statistically significant differences when compared to the control, $p \leq 0.05$)

Disintegrant description	Mean difference	Standard error	Significance	95% confidence interval	
				Lower bound	Upper bound
Ac-di-sol® 0.0005% (w/v)	.000000214	.000000057	.008269417*	.000000039	.000000389
Ac-di-sol® 0.001% (w/v)	.000000044	.000000057	.999113933	-.000000130	.000000219
Ac-di-sol® 0.005% (w/v)	-.000000103	.000000057	.553587908	-.000000278	.000000072
Ac-di-sol® 0.01% (w/v)	-.000000300	.000000057	.000088996*	-.000000474	-.000000125
Avicel® PH-200 0.005% (w/v)	-.000000073	.000000057	.903749999	-.000000248	.000000101
Avicel® PH-200 0.01% (w/v)	-.000000089	.000000057	.733097898	-.000000264	.000000085
Avicel® PH-200 0.015% (w/v)	-.000000217	.000000057	.006993654*	-.000000392	-.000000043
Avicel® PH-200 0.03% (w/v)	-.000000375	.000000057	.000001213*	-.000000550	-.000000201
Explotab® 0.002% (w/v)	-.000000308	.000000057	.000056144*	-.000000482	-.000000133
Explotab® 0.004% (w/v)	-.000000335	.000000057	.000011879*	-.000000510	-.000000161
Explotab® 0.008% (w/v)	-.000000338	.000000057	.000009889*	-.000000513	-.000000164
Explotab® 0.016% (w/v)	-.000000309	.000000057	.000053497*	-.000000483	-.000000134
Kollidon® CL-M 0.002% (w/v)	-.000000240	.000000057	.002208945*	-.000000415	-.000000066
Kollidon® CL-M 0.004% (w/v)	-.000000248	.000000057	.001467246*	-.000000423	-.000000074
Kollidon® CL-M 0.005% (w/v)	-.000000296	.000000057	.000107683*	-.000000471	-.000000122
Kollidon® CL-M 0.01% (w/v)	-.000000439	.000000057	.000000047*	-.000000614	-.000000265
Sodium alginate 0.0025% (w/v)	-.000000412	.000000057	.000000163*	-.000000586	-.000000237
Sodium alginate 0.005% (w/v)	-.000000359	.000000057	.000003064*	-.000000534	-.000000184
Sodium alginate 0.01% (w/v)	-.000000238	.000000057	.002475938*	-.000000413	-.000000064
Sodium alginate 0.02% (w/v)	-.000000256	.000000057	.000977124*	-.000000430	-.000000081

Table F.7: Kruskal-Wallis test for non-parametric comparison of apical-to-basolateral transport of Rhodamine 123 in presence of selected disintegrants across excised pig jejunum (*statistically significant differences when compared to other samples, $p \leq 0.05$)

	ADS0 .0005	ADS0 .001	ADS0 .005	ADS0 .01	AVC0 .005	AVC0 .01	AVC0 .015	AVC0 .03	XPT0 .002	XPT0 .004	XPT0 .008	XPT0 .016	SAL0 .0025	SAL0 .005	SAL0 .01	SAL0 .02	CLM0 .002	CLM0 .004	CLM0 .005	CLM0 .01	PC5
ADS0 .0005		1.000	1.000	1.000	1.000	1.000	1.000	1.000	1.000	1.000	1.000	1.000	1.000	1.000	1.000	1.000	1.000	1.000	1.000	1.000	1.000
ADS0 .001	1.000		1.000	1.000	1.000	1.000	1.000	1.000	1.000	1.000	1.000	1.000	1.000	1.000	1.000	1.000	1.000	1.000	1.000	1.000	1.000
ADS0 .005	1.000	1.000		1.000	1.000	1.000	1.000	0.982	0.642	0.382	0.382	0.479	1.000	1.000	1.000	0.282	1.000	1.000	1.000	1.000	1.000
ADS0 .01	1.000	1.000	1.000		1.000	1.000	0.916	0.444	0.282	0.162	0.162	0.206	1.000	1.000	1.000	0.117	1.000	1.000	1.000	1.000	0.515
AVC0 .005	1.000	1.000	1.000	1.000		1.000	1.000	1.000	1.000	1.000	1.000	1.000	1.000	1.000	1.000	1.000	1.000	1.000	1.000	1.000	1.000
AVC0 .01	1.000	1.000	1.000	1.000	1.000		1.000	1.000	1.000	1.000	1.000	1.000	1.000	1.000	1.000	1.000	1.000	1.000	1.000	1.000	1.000
AVC0 .015	1.000	1.000	1.000	0.916	1.000	1.000		1.000	1.000	1.000	1.000	1.000	1.000	1.000	1.000	1.000	1.000	1.000	1.000	1.000	1.000
AVC0 .03	1.000	1.000	0.982	0.444	1.000	1.000	1.000		1.000	1.000	1.000	1.000	1.000	1.000	1.000	1.000	1.000	1.000	1.000	1.000	1.000
XPT0 .002	1.000	1.000	0.642	0.282	1.000	1.000	1.000	1.000		1.000	1.000	1.000	1.000	1.000	1.000	1.000	1.000	1.000	1.000	0.916	1.000
XPT0 .004	1.000	1.000	0.382	0.162	1.000	1.000	1.000	1.000	1.000		1.000	1.000	1.000	1.000	1.000	1.000	1.000	1.000	1.000	0.555	1.000
XPT0 .008	1.000	1.000	0.382	0.162	1.000	1.000	1.000	1.000	1.000	1.000		1.000	1.000	1.000	1.000	1.000	1.000	1.000	1.000	0.555	1.000
XPT0 .016	1.000	1.000	0.479	0.206	1.000	1.000	1.000	1.000	1.000	1.000	1.000		1.000	1.000	1.000	1.000	1.000	1.000	1.000	0.690	1.000
SAL0 .0025	1.000	1.000	1.000	1.000	1.000	1.000	1.000	1.000	1.000	1.000	1.000	1.000		1.000	1.000	1.000	1.000	1.000	1.000	1.000	1.000
SAL0 .005	1.000	1.000	1.000	1.000	1.000	1.000	1.000	1.000	1.000	1.000	1.000	1.000	1.000		1.000	1.000	1.000	1.000	1.000	1.000	1.000
SAL0 .01	1.000	1.000	1.000	1.000	1.000	1.000	1.000	1.000	1.000	1.000	1.000	1.000	1.000	1.000		1.000	1.000	1.000	1.000	1.000	1.000
SAL0 .02	1.000	1.000	0.282	0.117	1.000	1.000	1.000	1.000	1.000	1.000	1.000	1.000	1.000	1.000	1.000		1.000	1.000	1.000	0.412	1.000
CLM0 .002	1.000	1.000	1.000	1.000	1.000	1.000	1.000	1.000	1.000	1.000	1.000	1.000	1.000	1.000	1.000	1.000		1.000	1.000	1.000	1.000
CLM0 .004	1.000	1.000	1.000	1.000	1.000	1.000	1.000	1.000	1.000	1.000	1.000	1.000	1.000	1.000	1.000	1.000	1.000		1.000	1.000	1.000
CLM0 .005	1.000	1.000	1.000	1.000	1.000	1.000	1.000	1.000	1.000	1.000	1.000	1.000	1.000	1.000	1.000	1.000	1.000	1.000		1.000	1.000
CLM0 .01	1.000	1.000	1.000	1.000	1.000	1.000	1.000	1.000	0.916	0.555	0.555	0.690	1.000	1.000	1.000	0.412	1.000	1.000	1.000		1.000
PC5	1.000	1.000	1.000	0.515	1.000	1.000	1.000	1.000	1.000	1.000	1.000	1.000	1.000	1.000	1.000	1.000	1.000	1.000	1.000	1.000	

Table F.8: Kruskal-Wallis test for non-parametric comparison of basolateral-to-apical transport of Rhodamine 123 in presence of selected disintegrants across excised pig jejunum (*statistically significant differences when compared to other samples, $p \leq 0.05$)

	ADS0 .0005	ADS0 .001	ADS0 .005	ADS0 .01	AVC0 .005	AVC0 .01	AVC0 .015	AVC0 .03	XPT0 .002	XPT0 .004	XPT0 .008	XPT0 .016	SAL0 .0025	SAL0 .005	SAL0 .01	SAL0 .02	CLM0 .002	CLM0 .004	CLM0 .005	CLM0 .01	PC5
ADS0 .0005		1.000	1.000	1.000	1.000	1.000	1.000	0.190	1.000	1.000	0.795	1.000	0.035 *	0.354	1.000	1.000	1.000	1.000	1.000	0.015 *	1.000
ADS0 .001	1.000		1.000	1.000	1.000	1.000	1.000	0.444	1.000	1.000	1.000	1.000	0.091	0.795	1.000	1.000	1.000	1.000	1.000	0.042 *	1.000
ADS0 .005	1.000	1.000		1.000	1.000	1.000	1.000	1.000	1.000	1.000	1.000	1.000	0.555	1.000	1.000	1.000	1.000	1.000	1.000	0.282	1.000
ADS0 .01	1.000	1.000	1.000		1.000	1.000	1.000	1.000	1.000	1.000	1.000	1.000	1.000	1.000	1.000	1.000	1.000	1.000	1.000	1.000	1.000
AVC0 .005	1.000	1.000	1.000	1.000		1.000	1.000	1.000	1.000	1.000	1.000	1.000	0.354	1.000	1.000	1.000	1.000	1.000	1.000	0.175	1.000
AVC0 .01	1.000	1.000	1.000	1.000	1.000		1.000	1.000	1.000	1.000	1.000	1.000	0.444	1.000	1.000	1.000	1.000	1.000	1.000	0.223	1.000
AVC0 .015	1.000	1.000	1.000	1.000	1.000	1.000		1.000	1.000	1.000	1.000	1.000	1.000	1.000	1.000	1.000	1.000	1.000	1.000	1.000	1.000
AVC0 .03	0.190	0.444	1.000	1.000	1.000	1.000	1.000		1.000	1.000	1.000	1.000	1.000	1.000	1.000	1.000	1.000	1.000	1.000	1.000	0.982
XPT0 .002	1.000	1.000	1.000	1.000	1.000	1.000	1.000	1.000		1.000	1.000	1.000	1.000	1.000	1.000	1.000	1.000	1.000	1.000	1.000	1.000
XPT0 .004	1.000	1.000	1.000	1.000	1.000	1.000	1.000	1.000	1.000		1.000	1.000	1.000	1.000	1.000	1.000	1.000	1.000	1.000	1.000	1.000
XPT0 .008	0.795	1.000	1.000	1.000	1.000	1.000	1.000	1.000	1.000	1.000		1.000	1.000	1.000	1.000	1.000	1.000	1.000	1.000	1.000	1.000
XPT0 .016	1.000	1.000	1.000	1.000	1.000	1.000	1.000	1.000	1.000	1.000	1.000		1.000	1.000	1.000	1.000	1.000	1.000	1.000	1.000	1.000
SAL0 .0025	0.035 *	0.091	0.555	1.000	0.354	0.444	1.000	1.000	1.000	1.000	1.000	1.000		1.000	1.000	1.000	1.000	1.000	1.000	1.000	0.223
SAL0 .005	0.354	0.795	1.000	1.000	1.000	1.000	1.000	1.000	1.000	1.000	1.000	1.000	1.000		1.000	1.000	1.000	1.000	1.000	1.000	1.000
SAL0 .01	1.000	1.000	1.000	1.000	1.000	1.000	1.000	1.000	1.000	1.000	1.000	1.000	1.000	1.000		1.000	1.000	1.000	1.000	1.000	1.000
SAL0 .02	1.000	1.000	1.000	1.000	1.000	1.000	1.000	1.000	1.000	1.000	1.000	1.000	1.000	1.000	1.000		1.000	1.000	1.000	1.000	1.000
CLM0 .002	1.000	1.000	1.000	1.000	1.000	1.000	1.000	1.000	1.000	1.000	1.000	1.000	1.000	1.000	1.000	1.000		1.000	1.000	1.000	1.000
CLM0 .004	1.000	1.000	1.000	1.000	1.000	1.000	1.000	1.000	1.000	1.000	1.000	1.000	1.000	1.000	1.000	1.000	1.000		1.000	1.000	1.000
CLM0 .005	1.000	1.000	1.000	1.000	1.000	1.000	1.000	1.000	1.000	1.000	1.000	1.000	1.000	1.000	1.000	1.000	1.000	1.000		1.000	1.000
CLM0 .01	0.015 *	0.042 *	0.282	1.000	0.175	0.223	1.000	1.000	1.000	1.000	1.000	1.000	1.000	1.000	1.000	1.000	1.000	1.000	1.000		0.108
PC5	1.000	1.000	1.000	1.000	1.000	1.000	1.000	0.982	1.000	1.000	1.000	1.000	0.223	1.000	1.000	1.000	1.000	1.000	1.000	0.108	